This is to certify that the
dissertation entitled

FUNCTIONS OF *RAD52* IN DNA DAMAGE REPAIR AND TELOMERE MAINTENANCE IN *SACCHAROMYCES CEREVISIAE*

presented by

LIANJIE LI

has been accepted towards fulfillment
of the requirements for the

Ph.D. degree in MICROBIOLOGY AND MOLECULAR GENETICS

Walter J Esselman
Major Professor's Signature

12/09/04
Date

FUNCTIONS OF *RAD52* IN DNA DAMAGE REPAIR AND TELOMERE MAINTENANCE IN *SACCHAROMYCES CEREVISIAE*

BY

LIANJIE LI

A DISSERTATION

Submitted to
Michigan State University
in partial fulfillment of the requirements
for the degree of

DOCTOR OF PHILOSOPHY

Department of Microbiology and Molecular Genetics

2004

ABSTRACT

FUNCTIONS OF *RAD52* IN DNA DAMAGE REPAIR AND TELOMERE MAINTENANCE IN *SACCHAROMYCES CEREVISIAE*

By

Lianjie Li

Homologous recombination is the major and the most efficient pathway to repair double-strand breaks in *Saccharomyces cerevisiae*. This pathway depends on the *RAD52* epistasis group, including *RAD50, RAD51, RAD52, RAD54, RAD55, RAD57, RAD59, RDH54, MRE11* and *XRS2*. Among these genes, *RAD52* plays a central role as it is required in virtually all forms of homologous recombination. Homologous recombination also plays important roles in telomere maintenance in telomerase-negative yeast cells. Two distinct homologous recombination pathways operate in telomerase-negative yeast cells. The type I pathway, which generates type I survivors, depends on *RAD52, RAD51, RAD54, RAD55* and *RAD57*; the type II pathway, which generates type II survivors, requires *RAD50, RAD52, RAD59, MRE11* and *XRS2*.

In this thesis, I have examined the effects of *RAD52* overexpression on DNA damage repair. I demonstrated that overexpression of Rad52 has a strong negative effect on DNA damage repair induced by the DNA-damaging agent methylmethanesulfonate. This effect is mediated by sequestration of Rad51 by excess amounts of Rad52. I found

that Rad52 overexpression also has a negative effect on a *RAD51*-independent DNA damage repair pathway(s). However, this additional effect appears to be nonspecific. In addition, I found that among the five in-frame 5'-terminal ATGs in the *RAD52* gene, the third, fifth, and possibly the fourth, can be used as a translation initiation codon *in vivo*. Rad52 translated from the fifth ATG is as competent as that translated from the third ATG in DNA damage repair induced by methylmethanesulfonate.

I have also studied how Rad52 differentially participates in the two homologous recombination pathways that generate survivors in telomerase-negative yeast cells. I screened a library of randomly mutagenized *rad52* and identified fifty-seven *rad52* alleles that have negative effects on survivor pathways. I studied four alleles for their functions in telomerase-independent telomere maintenance and homologous recombination. I found that *rad52R70G, rad52K159E, rad52R171S* have defects in the type II pathway, and they seem to be able to carry out the type I pathway normally. In contrast, *rad52D164G* has defects in both type I and type II pathways. I also demonstrated a correlation between the two survivor pathways and different homologous recombination events: a mutant defective in the type I pathway also has defects in interchromosomal recombination; a mutant defective in the type II pathway also has defects in direct-repeat recombination. This correlation supports the proposed model of interchromosomal recombination for type I survivors. The results also argue that telomeres in type II survivors are most likely maintained by telomere looping back to copy telomere repeats intrachromosomally.

To my husband, Xiaoyu, and my daughter, Evelyn

ACKNOWLEDGEMENTS

I would like to thank my guidance committee, Dr. Susan Conrad, Dr. Walter Esselman, Dr. Michele Fluck and Dr. Min-Hao Kuo for their understanding, support, collective thoughts and invaluable expertise. Especially, I give my sincere thanks to Dr. Walter Esselman and Dr. Min-Hao Kuo who have taken the responsibility to be my mentors and made my education during graduate school a success. I would like to thank my former mentor Dr. He Wang for his guidance and help. I would also like to thank all my friends in the Department of Microbiology and Molecular Genetics, who have offered me enormous friendship and support. I would like to thank Xiaoyu, my husband, for his understanding and support through these years. Finally, I would like to thank Evelyn, my daughter, who gives me so much joy and happiness.

TABLE OF CONTENTS

LIST OF TABLES

LIST OF FIGURES

CHAPTER 1

LITERATURE REVIEW

INTRODUCTION

Homologous recombination refers to the exchange or transfer of information between homologous partners. The primary function of homologous recombination in mitotic cells is to repair double-strand breaks resulting from replication fork collapse, from spontaneous damage, and from exposure to DNA-damaging agents (reviewed in [1]). In *Saccharomyces cerevisiae*, homologous recombination depends on the *RAD52* epistasis group, including *RAD50, RAD51, RAD52, RAD54, RDH54, RAD55, RAD57, RAD59, MRE11*, and *XRS2* (reviewed in [1, 2]). *RAD52* is the central component (reviewed in [1, 2]). It is required in virtually all homologous recombination pathways. Mutations of *RAD52* lead to the most severe defects in homologous recombination and highest sensitivity to DNA-damaging agents.

Telomeres are specialized protein-DNA structures at the ends of eukaryotic chromosomes. Their specialized structure caps chromosome ends to provide protection against degradation and end-to-end fusion, as well as to prevent chromosome ends from being recognized as double-strand breaks [3]. In most cases, telomeres are replenished by telomerase, the reverse transcriptase which adds telomere repeats to chromosome ends [3]. In the absence of telomerase, telomeres continue to shorten with each cell division until eventually, they lose their capping function. The chromosome ends are then recognized as double-strand breaks and induce cell cycle arrest at G_2/M phase [4]. Most

telomerase-negative *S. cerevisiae* cells cease division in 50-100 generations. However, a small population of cells can survive and proliferate at a rate similar to telomerase-positive cells [5]. In these survivors, telomeres are maintained by homologous recombination between telomere repeats or subtelomeric regions [5-7]. Since *RAD52* is the central player in homologous recombination, it is not surprising that it also plays key roles in telomere maintenance in telomerase-negative cells. Double knockout mutants of telomerase and *RAD52* can not generate any survivors [5].

This thesis will focus on the functions of Rad52 in DNA damage repair and telomerase-independent telomere maintenance. Therefore, this literature review will address the following topics: (1) homologous recombination pathways for double-strand breaks repair; (2) recombination proteins in *S. cerevisiae*, with an emphasis on Rad52 and Rad51; and (3) structure, function and maintenance of *S. cerevisiae* telomeres

HOMOLOGOUS RECOMBINATION PATHWAYS FOR DOUBLE-STRAND BREAKS REPAIR

Double-strand breaks (DSB) are generally considered the most severe DNA damage in mitotic cells. Homologous recombination is the major and the most efficient repair pathway in *S. cerevisiae*. This pathway utilizes a sequence homologous to the damaged DNA for repair. There are several mechanisms of homologous recombination by which yeast cells repair DSB, including gene conversion, single-strand annealing, and break-induced replication (reviewed in [1, 2]).

Gene conversion

Gene conversion is defined as a nonreciprocal transfer of genetic information between two homologous partners. Two models proposed for gene conversion have been widely accepted: double-strand break repair and synthesis-dependent strand annealing.

Double-strand break repair model (DSBR)

In DSBR model (Figure 1-1), the 5' ends of a DSB are resected to form 3' single-stranded tails that can invade an intact homologous template. Following strand invasion, the 3' end acts as a primer for new DNA synthesis. The noninvading 3' single-stranded tail on the other side of the DSB will pair with the D-loop formed by strand invasion, and initiate DNA synthesis. This process leads to the formation of a double-Holiday-junction. Alternate resolution of the two Holiday junctions will yield crossover or noncrossover products. If the resolution is random, an equal number of crossover or noncrossover products should be expected. However, only 10-20% of mitotic gene conversion events are associated with crossing over (reviewed in [2]).

Synthesis-dependent strand annealing (SDSA)

SDSA model was proposed to account for the low frequency of gene conversion associated with crossing over. In this model, one or both resected 3' ends invades the homologous duplex and initiates DNA synthesis. For a two-ended invasion, both newly synthesized strands will be unwound from their templates and anneal to each other (Figure 1-2A) [1, 2]. For a one-end invasion, three possible subsequent events have been proposed [2]. The newly synthesized strand is displaced and annealed to the other side of the DSB (Figure 1-2B). Alternatively, the second 3' end anneals with the D-loop (Figure

1-2C). In the third scenario, which is termed repair replication fork capture, the invasion of one 3' end establishes a modified replication fork. DNA synthesis will continue until the repair replication fork is "captured" by the other side of the DSB (Figure 1-2D). It should be pointed out that the annealing with D-loop and replication fork capture mechanisms can produce crossover products.

Single-strand annealing (SSA)

SSA is an efficient repair pathway when a DSB occurs between direct repeats [2]. In SSA model, 5' to 3' resection of a DSB produces 3' single-stranded tails. The resection will continue until homologous sequences are revealed. The homologous single-stranded DNA then anneals, and the nonhomologous tails are removed, resulting in deletion of the intervening sequence and one of the repeats [1, 2, 8](Figure 1-3).

Break-induced replication (BIR)

Double-stranded breaks sometimes produce only one end. Collapsed replication forks generate only one end. The chromosome ends will also be recognized as one-ended double-strand breaks when telomeres are uncapped and eroded. These damages can not be repaired by gene conversion, which requires a second end. Instead, these DSBs are repaired by break-induced replication, in which the broken ends invade homologous sequences and initiate DNA synthesis to copy all the donor sequences to the chromosome ends (Figure 1-4) [1, 2]. This process is thought to act to maintain telomeres in telomerase-negative cells [7, 9].

RECOMBINATION PROTEINS IN *S. CEREVISIAE*

In *S. cerevisiae*, homologous recombination depends on the *RAD52* epistasis group, including *RAD52, RAD51, RAD54, RAD55, RAD57, RAD59, RDH54, RAD50, MRE11* and *XRS2* (Table 1-1). Most of these genes were identified by their increased sensitivity to DNA-damaging agents, such as ionizing radiation (reviewed in [1]). These genes can be further grouped into two subgroups. One consists of *RAD50, MRE11* and *XRS2* and the other consists of *RAD52, RAD51, RAD54, RAD55, RAD57, RAD59* and *RDH54*. Within the RAD52 subgroup, *RAD52* stands alone as it is essential for all forms of homologous recombination during mitotic growth. *RAD51, RAD54, RAD55* and *RAD57* are required for gene conversion and break-induced replication, whereas *RAD59* is involved in break-induced replication and single-strand annealing.

RAD50, *MRE11* and *XRS2* function at the early stage of DSB repair. They are involved in processing DSBs to form 3' single-stranded DNA tails that can invade homologous donor and initiate DNA synthesis (Figure 1-5) (reviewed in [10]). The 3' single-stranded tails are bound by Rad51, the recombinase that catalyzes homologous pairing and strand exchange [11]. The functions of Rad51 are stimulated by Rad52, Rad54, Rdh54, Rad55 and Rad57 at different phases during recombination (Figure 1-5 and see below).

Rad50/Mre11/Xrs2

Rad50, Mre11 and Xrs2 form a complex (MRX) which probably contains two molecules of Rad50, two molecules of Mre11 and one molecule of Xrs2 [12, 13]. Mre11 (~80 kDa) has manganese-dependent nuclease activities [14-16], including a 3' to 5' exonulease activity on both double- and single-stranded DNA, an endonulcease activity

on single-stranded DNA, and a structure-specific endonulease activity that cleaves the 3' single-stranded overhangs at the single-/double-stranded junction. The exonuclease activity and the structure-specific endonuclease activity of Mre11 is enhanced by interacting with Rad50 [15, 16] and Xrs2 [17]. Xrs2 (~96 kDa) binds to both single- and double-stranded DNA. However, its preferred substrate is tailed duplexes, indicating that Xrs2 recognizes the junction between the double- and the single-stranded regions of DNA molecules [17]. Rad50 (~150 kDa) has an ATP-dependent double-stranded DNA binding activity [18]. The conserved nucleotide-binding motifs Walker A and Walker B are located at the N-terminus and the C-terminus, respectively. The ATP-binding motifs are indispensable for Rad50 functions [19].

MRX complexes are involved in processing DSBs into 3' single-stranded tails that initiate strand invasion [10, 20]. However, Mre11 is a 3' to 5' exonuclease. Several models have been proposed to solve the directionality conflict (review in [10]). MRX may cooperate with a helicase to unwind DNA duplex, Mre11 could then process the ends by its endonuclease activity. Alternatively, MRX is responsible for the initial processing of DSBs using its structure-specific endonuclease activity, after which other nucleases further process the ends to generate the 3' single-stranded tail. Indeed, a DNA unwinding activity has been observed for MRX [17].

Rad51

RAD51 encodes a 400-amino acid protein (43 kDa) with significant homology to RecA [21, 22]. The highest homology is located at the central portion of the two proteins, including the Walker A and Walker B motifs for nucleotide binding and/or hydrolysis. Like RecA, Rad51 catalyzes homologous pairing and strand exchange [11]. The strand

exchange reaction catalyzed by Rad51 occurs from 3' to 5' relative to the single strand [23, 24]. This polarity is opposite to that observed for RecA. However, it has been shown that Rad51 can catalyze strand exchange bidirectionally when the ends of a double-stranded DNA exist as overhanging structures [25].

Rad51 binds to both ssDNA and dsDNA to form right-handed helical filaments similar to that formed by RecA [23, 26]. However, dsDNA with single-stranded tails is the preferred binding substrates of Rad51 [27].While ssDNA binding is greatly enhanced by the presence of ATP, dsDNA binding completely depends on ATP [21]. ssDNA-Rad51 filaments are active in strand exchange, whereas dsDNA-Rad51 filaments in fact inhibit the reaction [23].

Rad51 has a DNA-dependent ATPase activity [11]. ssDNA is more effective in activating ATP hydrolysis. When a conserved lysine residue (K191) in the Walker A-box is mutated to arginine, the ATPase activity is abolished [24]. However, the mutant protein can still bind to DNA in a ATP-dependent manner, and catalyze homologous pairing and strand exchange. Consistent with this result, wild type Rad51 is able to catalyze homologous pairing and strand exchange in the presence of nonhydrolizable ATP analogs [24]. Furthermore, *rad51K191R* can complement the MMS sensitivity of *rad51Δ* strains [24]. These results argue that nucleotide binding is sufficient for Rad51 biological functions.

Rad51 self-associates through its N-terminal domain [28]. The importance of this interaction is demonstrated by the dominant negative phenotype of *rad51K191A*. *rad51K159A* is inactive in strand exchange [24]. When expressed from a high copy plasmid, *rad51K159A* negatively affects DNA repair in wild type cells, but it has no

additional effect in *rad51Δ* strains, suggesting that *rad51K191A* exerts its negative effect by associating with wild type Rad51 [28]. In addition, the crystal structure of Rad51 nucleoprotein filaments suggests that the functional unit of Rad51 is a dimer [29].

Since dsDNA-Rad51 nucleoprotein filaments inhibit strand exchange [23], secondary structures within single stranded DNA substrates must be eliminated. This function is fulfilled by replication protein A (RPA) [30], a heterotrimeric single-stranded DNA binding protein (Figure 1-5). However, the stimulatory effect of RPA on strand exchange can only be observed when it is incorporated into reactions after Rad51 has bound to ssDNA [31-33]. If RPA is introduced in the nucleation phase of Rad51, it inhibits the subsequent reaction by competing for ssDNA binding [31, 34]. RPA is abundant and present during ssDNA-Rad51 filament formation *in vivo*. Cells overcome the inhibitory effect of RPA by employing a set of mediator proteins, including Rad52 and Rad55/Rad57 heterodimer (discussed below).

Rad54 and Rdh54

RAD54 encodes a 898-amino acid protein (102 kDa) with a dsDNA-dependent ATPase activity [35]. Rad54 topologically unwinds dsDNA [36, 37]. It directly interacts with Rad51 as demonstrated by two-hybrid and co-immunoprecipitation experiments [38, 39]. In vitro, Rad54 stimulates Rad51-mediated strand exchange reactions [35, 36, 40-42]. This stimulatory effect is not due to Rad54 facilitating Rad51 nucleoprotein filament formation, but rather is mediated by direct interactions of Rad54 with preassembled filaments [37]. This interaction also enhances the ATPase and DNA unwinding activity of Rad54 [37], which in turn promotes Rad51-catalyzed homologous pairing [36]. In addition, Rad54 can stabilize Rad51 nucleoprotein filaments [43], as well as stimulate

heteroduplex extension of joint molecules [40]. Therefore, Rad54 functions in both synaptic and postsynaptic phases during strand exchange (Figure 1-5). Rad54 has also been shown to displace Rad51 from dsDNA, which may be important for Rad51 turnover [10, 41].

Rdh54 is a Rad54 homologue. Like Rad54, it possesses a dsDNA-dependent ATPase activity and promotes a conformational change of circular dsDNA [44]. It also displays a similar stimulatory effect on Rad51-catalyzed strand exchange reactions [44].

Rad55/Rad57

Rad55 (406 aa, 46 kDa) and Rad57 (460aa, 52 kDa) are referred to as Rad51 paralogs since they share sequence similarity with Rad51, especially at the putative nucleotide binding motifs [45, 46]. Mutation of the conserved lysine residue within the Walker A-type box to arginine or alanine in Rad55 (Lys49) results in a severe defect in DNA damage repair induced by γ radiation. However, an analogous mutation in Rad57 (Lys131) has no effect on γ-ray resistance [47]. Unlike Rad51, neither Rad55 nor Rad57 exhibits self-interaction [47]. Instead, Rad55 and Rad57 form a stable heterodimer [34, 47, 48]. Rad55 also interacts with Rad51 in two-hybrid systems [34, 47, 48]. Rad55/Rad57 promotes Rad51-catalyzed strand exchange by facilitating the displacement of RPA from ssDNA (Figure 1-5) [34]. Consistent with this observation, a set of *rad51* alleles with an increased DNA binding activity can partially bypass the requirement of Rad55/Rad57 [49]. Rad55/Rad57 only interacts with Rad51, but not with RPA [47, 48], suggesting that the mediator function of Rad55/Rad57 is different from that of Rad52, which interacts with both Rad51 and RPA (see below).

Rad52

RAD52 encodes a protein of 471 amino acids with a molecular weight of 52.4 kDa. Rad52 has multiple functional domains. The partially overlapping DNA binding and self-association regions are located at its N-terminus [50-52]. These regions are highly conserved throughout eukaryotes. The C-terminal two-thirds of the protein interacts with RPA and Rad51 [50, 53-55]. This region is less conserved. In fact, the Rad52-Rad51 interaction is species-specific [54].

Rad52 is expressed constitutively throughout the cell cycle [56]. It forms discrete foci during S phase [57]. Rad52 expression is induced by 9-fold early in meiosis [58]. Surprisingly, DNA damaging agents only have a moderate effect at very high dosage [56]. Consistent with this observation, Rad52 forms multiple foci (~15/nucleus) in meiotic cells, whereas only 1-2 foci per cell when cells are treated with γ-rays [57].

Rad52 performs multiple functions essential for homologous recombination. Rad52 can bind to both ssDNA and dsDNA with a slight preference for ssDNA [50]. Human Rad52 has also been shown to specifically bind to ssDNA termini and tailed duplex DNA [59]. Both yeast and human Rad52 form multimeric ring structures [51, 60, 61]. Human Rad52 rings have been shown to further assemble into higher order multimers [51]. While the ring formation between monomers is mediated by the conserved N-terminal self-association domain, the assembly of the higher structures requires the C-terminus. Rad52 by itself can efficiently promote annealing between short oligonucleotides [50, 60]. However, it needs RPA to efficiently anneal longer ssDNA. Since RPA has little effect on the annealing of longer DNA free of secondary structures, such as poly(dT), its primary role is to eliminate secondary structures in DNA molecules

[62]. Rad52 also interacts with Rad59, which has been suggested to augment Rad52's activity in strand annealing [63]. Rad52 acts as a mediator between RPA and Rad51 to stimulate Rad51-meidated DNA strand exchange by facilitating Rad51 nucleating on ssDNA substrates (Figure 1-5) [31, 33, 64, 65]. The physical interaction between Rad52 and Rad51 is required for this activity since a *rad52* mutant unable to interact with Rad51 also fails to perform its mediator function [55]. The C-terminal one-third of Rad52 is both necessary and sufficient for the Rad52-Rad51 interaction [54, 55]. The relative ratio of Rad52 to Rad51 is important for Rad52's mediator function [32]. A maximal mediator function is achieved when Rad52 is about one-tenth of the amount of Rad51. The physical interaction between Rad52 and RPA has been demonstrated in a yeast two-hybrid system as well as in co-immunoprecipitation experiments [53, 60], and is suggested to be important for Rad52's mediator function [53, 64]. Rad52 exhibits a different stimulatory function probably by stabilizing Rad51 presynaptic filament through its interaction with Rad51when RPA is present at subsaturating level[66]. However, unlike its mediator role, the physical interaction of Rad52-RPA is not required in this case.

Rad59

RAD59 encodes a 238 amino acid protein (26 kDa) with a significant homology to the N-terminal half of Rad52 [67]. Rad59 shares several biochemical activities with Rad52. It binds to DNA, with a higher affinity for ssDNA. It self-associates to form multimers [68]. Rad59 also anneals complementary ssDNA *in vitro* [63, 69]. However, unlike Rad52, Rad59's single strand annealing activity is not promoted by RPA [69]. In fact, Rad59 can not displace RPA from ssDNA [63]. The physical interaction between

Rad52 and Rad59 has been demonstrated using a two-hybrid system and by co-immunoprecipitation experiments [63]. A complex containing Rad52, Rad51 and Rad59 can be immunoprecipitated, but Rad51 and Rad59 fail to interact in the absence of Rad52 [1], suggesting that Rad59 and Rad51 bind to different interaction interfaces on Rad52.

STRUCTURE, FUNCTION AND MAINTENANCE OF *S. CEREVISIAE* TELOMERES

Telomere biology began with the pioneering work done by Herman Muller and Barbara McClintock back in the 1930s. Muller analyzed chromosome rearrangement following X-irridiation in Drosophila [70]. He never recovered a chromosome with terminal deletion. McClintock discovered that broken chromosome ends in maize could fuse with each other to form an unstable dicentric chromosome [71]. These pioneering studies suggest that telomeres are essential parts of eukaryotic chromosomes, and that they have special structures and functions to prevent chromosome fusion.

Telomeric DNA and telomere-associated sequences

Telomeres are specialized DNA and protein structures at the ends of eukaryotic chromosomes. Telomeric DNA consists of tandem arrays of short repeats. These repeats are polarized with G-rich repeats oriented from 5' to 3' (centromere to telomere), therefore called G-strand for convenience (and the complementary strand C-strand). However, the two strands do not contain significantly more G or C residues in some species [72]. Some organisms, such as tetrahymena and some fungi, have homogenous arrays of repeat sequences, while others have heterogeneous repeats (reviewed in [73,

74]). The sequence of telomeric DNA in *S. cerevisiae* is $(TG)_{1\text{-}6}TG_{2\text{-}3}$ [75]. The length of yeast telomeric DNA at individual telomeres varies with an average length of 300±75 base pairs [76]. Telomeres do not terminate with blunt ends ([77] and reviewed in [73]). The G strand extends to form a 3' overhang. Long single-stranded G-tails (~50-100 bases) can be detected at late S phase in yeast [78-80].

In addition to the simple repeats, many organisms also have middle repetitive DNA sequences located immediately internal to the short repeats (reviewed in [73, 81]). These sequences are referred to as telomere-associated sequences (TAS). Yeast has two classes of TAS, X and Y' [82]. X, ranging from 0.3 to 3.75 kb, consists of at least five species of ~45-~560 bp in size, not all of which are present in every X [83]. However, the longest species, also called core X (~560 bp), is present at most telomeres [83]. Y' has two major variants, the 6.7 kb Y' long and the 5.2 kb Y' short. Y' is found on only a subset of chromosomes [84]. Some chromosomes have up to 4 copies of Y' elements [82]. If both X and Y' are present on the same chromosome, X is located internal to Y' [83].

Telomere chromatin structure

Depending on the type of telomeres examined, telomeres may assume different chromatin structures (reviewed in [73]). In yeast, the entire terminal $C_{1\text{-}3}A/TG_{1\text{-}3}$ duplex is packed in a nonnucleosomal chromatin structure called telosome [76]. The telosomes do not seem to build around the nucleosomal cores since the stability of protein-DNA interactions in telosomes is different from those in nucleosomes [85], and deletions or duplications of histone genes which lead to changes in histone stoichiometry do not disrupt telomere chromatin structures [86]. Furthermore, the telosome contains twice as

much DNA as a nucleosome because the entire telomere duplex is protected by telosome [76].

Both X and Y' elements are assembled in nucleosomes. However, subtelomeric nucleosomes are less accessible to *dam* methylase [87]. In addition, the amino terminal tails of histones H3 and H4 are hypoacetylated [88]. These results suggest that subtelomeric regions are more compact than elsewhere in the genome.

Functions of Telomeres and TAS

Early work of B. McClintock suggested that telomeres are important for chromosome stability [71]. Indeed, yeast cells with defects in *EST1*, which lead to progressive shortening of telomeres, exhibit increased chromosome loss and cell death [89]. Greider group examined the mutation rate of the *CAN1* locus as telomeres progressively shorten in *est1* strains [90]. Early passages of *est1* cells exhibit a mutation rate similar to that of wild type strain. The mutation rate increases about 10 -fold at the peak of senescence when telomeres are critically short, then drops to wild type level as survivors emerge (survivors are discussed in detail in the section of Telomere Maintenance in Yeast). By monitoring the fate of *CAN1* and the *ADE2* gene which was placed telomeric to *CAN1*, Greider and co-worker also showed that telomere shortening leads to terminal deletions. Therefore, the increased mutation rate is caused by gross chromosomal rearrangements, rather than small deletions or point mutations. In another study, the fate of a nonessential test chromosome in which the entire telomere tract can be eliminated in a controlled manner was monitored [91]. The loss rate of this chromosome increases ~10 -fold after cleavage of the telomere tract. In cells that the test chromosome is maintained, the telomere-less chromosome is frequently (~70%) healed by *RAD52*-

mediated homologous recombination or de novo telomere addition. However, unhealed chromosomes can be replicated and segregated for four to ten cell divisions before being lost. These results suggest that while telomeres are essential for stable maintenance of yeast chromosomes, they are probably not required for cells to maintain a chromosome for a given cell cycle [91].

Telomeres help to distinguish chromosome ends from DNA breaks. Double-strand DNA breaks induce *RAD9*-dependent G_2/M arrest. The loss of a single telomere on a nonessential chromosome leads to temperate *RAD9*-mediated G_2/M arrest [91]. The G_2/M arrest is more permanent if multiple dysfunctional telomeres are present [92].

Telomeres also serve as substrates for telomerase, the specialized reverse transcriptase that elongates telomeres. Conventional DNA polymerases need RNA primers to synthesize DNA. Removal of the most distal RNA primer leads to incomplete replication of the lagging strand. Without a mechanism to compensate for the sequence loss, telomeres will continuously shorten with each cell division. Telomerase allows the complete replication of the ends of the chromosomes by utilizing its RNA subunit as the template for telomere replication (Also discussed in the section of Telomere Maintenance in Yeast).

In addition, telomeres affect the transcription of adjacent genes. The transcription of a gene is repressed when it is placed near a telomere [93]. This phenomenon is referred to as telomere position effect (TPE). In general, TPE is reversely proportional to the distance from telomeres [94]. Longer telomeres have greater silencing effect [95]. However, if telomere lengthening is accompanied by the loss of certain telomere binding proteins, TPE could be reduced [96].

One possible function of TAS is to act as a buffer zone to prevent TPE from repressing essential genes located near telomeres [3]. It should be noted that not every natural telomere displays TPE [97], and the density of ORFs near telomeres is lower than elsewhere in the genome (reviewed in [3]). In telomerase-negative yeast cells, TAS is also important for telomere maintenance. This function will be discussed in the section of Telomere Maintenance in Yeast.

Telomere binding proteins

Telomeres provide binding sites for proteins that are important for maintenance of telomere length and structures. These proteins can be divided into four groups based on the sites they bind to: proteins that bind to the single-stranded tails of G strands, including Cdc13, Stn1, Ten1 and Est1; proteins that bind to the border between the double-stranded and the single-stranded region of telomeres, including yKu70 and yKu80; proteins that bind to the double-stranded region of telomeres, including Rap1, Rif1, Rif2, and Sir proteins; and proteins that bind to subtelomeric regions, such as Tbf1p [98-100].

CDC13 encodes an essential protein (924 aa, 104 kDa) that specifically binds to single-stranded telomeric DNA [101-104]. It contributes to telomere maintenance in two ways: by protecting telomere ends and by controlling the access of telomerase [105]. Cdc13, along with Stn1 and Ten1, forms a complex to "cap" telomeres. Single-stranded G-tails generated at late S phase are normal intermediates of telomere replication [78]. They are generated by degradation of C-strands [78, 80]. A temperature sensitive mutant, *cdc13-1*, accumulates single-stranded DNA at chromosome ends and arrests at G_2 in a *RAD9*-dependent manner when grown at restrictive temperature (37°C) [103, 106]. The single-stranded DNA, could be as long as 30 kb, contains TAS and telomeres

corresponding to the G strands [103]. These data suggest that Cdc13 limits C-strand degradation at the late S phase and helps to shield chromosome ends from DNA damage checkpoint. Cdc13 regulates telomerase activity both positively and negatively. Cdc13 is responsible for recruiting telomerase through the interaction between Cdc13 and Est1, a subunit of telomerase holoenzyme [107]. The length of telomere repeats is increased about 0.9 kb in *cdc13-1* mutant, suggesting that Cdc13 also serves as a negative regulator of telomere replication [108].

STN1 was isolated in a screen looking for suppressors for *cdc13-1*. Like *cdc13-1*, a temperature sensitive mutant *stn1-13* accumulates single-stranded DNA at the chromosome ends and displays elongated telomeres [108]. Physical interaction between Cdc13 and Stn1 has been demonstrated by a two-hybrid system [108]. A fusion protein consists of the DNA-binding domain of Cdc13 and Stn1 is able to rescue the lethality of *cdc13Δ* strain, indicating that Stn1 is the primary participant in chromosome end protection, and Cdc13 serves as a delivery vehicle [107]. *TNE1* (160 aa) was isolated as a suppressor of temperature sensitive *stn1* mutants [109]. It interacts with both Cdc13 and Stn1 [109]. Like *cdc13-1* and *stn1-13*, *ten1* mutants also accumulate long ssDNA at telomeric region which induces a *RAD9*-dependent G_2 arrest [109]. While overexpression of Ten1 can not complement *cdc13-1*, rescue of *cdc13-1* by Stn1 can be improved by co-overexpression of Stn1 and Ten1 [109]. In addition, Ten1-Stn1 fusion protein rescues inviability of *stn1Δ* cells and *ten1 Δ* cells. These data suggest that Ten1 participates in chromosome end protection and telomere length regulation in association with Stn1 and Cdc13, and together these proteins form a protective cap to shield telomeres [110].

Est1 is a subunit of telomerase holoenzyme. It will be discussed in the section of Telomere Maintenance in Yeast.

yKu70/Hdf1 and yKu80/Hdf2 form a heterodimer to bind to the junction between the single- and double-stranded regions of telomeres. They play key roles in telomere structures. Mutations in either protein result in the increase in the single-stranded G tails throughout cell cycle [111, 112]. yKu70/yKu80 also positively regulates telomerase activity. A Cdc13-yKu70 fusion protein results in longer than wild type length telomeres [113]. Although yKu70/yKu80 functionally interacts with Cdc13, they show no association *in vivo*. It appears that yK70/yKu80 fulfill their function in telomerase regulation by interacting with *TLC1* RNA, a subunit of telomerase [114].

Rap1 (827 aa, 120 kDa) binds to the double-stranded region of telomeres to regulate telomere length and TPE [3, 100, 115]. Rap1 interacts with Rif1 [116] and Rif2 [117] to form a negative regulator for telomere addition. Deletion mutations of *RIF1* and *RIF2*, as well as a C-terminal truncation mutation of Rap1 result in dramatic telomere elongation [116, 117]. It has been proposed that telomere length is regulated by a negative feedback mechanism in which the number of Rap1 molecules bound to telomeres is counted [118]. Rap1 also acts as a positive regulator for telomere elongation [119, 120]. It appears that Rap1 helps to recruit telomerase and increase the activity of telomerase [119]. It has been suggested that the balance between internal Rap1 promoting telomerase activity and Rap1 binding to the more terminal region of telomeres controlling telomerase access maintain telomeres at a constant length [119]. Rap1 interacts with Sir3 and Sir4 to form complexes to organize heterochromatin formation at telomeres and other

transcription silencing loci [100, 121-124]. Sir2 is involved in those complexes through the interaction with Sir4 [125].

Telomere maintenance in yeast

Telomere maintenance by telomerase

In wild type yeast, telomere replication occurs in late S phase [126]. There are three activities participating in telomere replication in yeast. The bulk of telomeric DNA is replicated by conventional DNA polymerases. Telomerase binds to the single-stranded tails of G-strands and elongates telomeres. C-strands can then be replicated by conventional DNA polymerase using G-strands as the templates.

Telomerase holoenzyme consists of four subunits: a RNA subunit encoded by *TLC1* and a catalytic protein subunit encoded by *EST2* form a catalytic core; two accessory subunits encoded by *EST1* and *EST3* regulate *in vivo* telomerase activity [127-130]. In vitro, *TLC1* RNA and Est2 alone can catalyze telomere addition, since cell extracts from *est1Δ* or *est3Δ* strains display telomerase activity [131]. However, both Est1 and Est3 are necessary *in vivo*. Deletion of either gene leads to progressive telomere shortening and senescence, the same phenotype shown by *tlc1Δ* or *est2Δ* mutants [127, 128].

The 1.3 kb *TLC1* RNA contains a sequence of 5'-CACCACACCCACACAC-3' serving as the template for telomere replication [132]. It also serves as a scaffold for the assembly of telomerase holoenzyme [133-135]. Binding of Est2 to *TLC1* RNA requires nt. 101-138, and nt. 728-864, binding of Est1 to *TLC1* RNA needs nt. 553-707 [136].

Est2 is a 804-amino acid, 103 kDa protein with a reverse transcriptase activity [127, 137, 138]. The reverse transcriptase domain lies between amino acids 420-740

[137]. There are three invariant aspartic acid residues within that motif among different reverse transcriptases. Point mutations of these residues in Est2 (Asp530Ala or Asp530Glu; Asp670Ala; Asp671Ala) abolish its reverse transcriptase activity and lead to telomere shortening and senescence [137] [138].

EST1 encodes a 82 kDa single-stranded telomere binding protein [89, 128, 139]. Efficient binding of Est1 to chromosome ends requires Cdc13-Est1 interaction [129]. Est1 directly interacts with *TLC1* RNA as demonstrated by co-immunoprecipitation experiments [140, 141]. It has been proposed that Est1recruits telomerase to the single-stranded chromosome termini as an adaptor between Cdc13 and the catalytic core of telomerase [107, 130]. Indeed, fusion protein of Est2-Cdc13 rescues the senescence phenotype of *est1Δ* cells [130]. However, recent studies reveal that Est1 and Est2 telomeric binding is uncoupled [142], and Est2 associates with telomeres in the G1 phase of the cell cycle when telomeres are not replicated [143]. These findings lead to a second model of Est1 action in which Est2/*TLC1* RNA associates with telomeres nonproductively by binding to the more internal regions of telomeres, and Cdc13-Est1 will translocate Est2/*TLC1* RNA to telomere termini [129]. Indeed, telomeric binding of Est1 requires a free 3' terminus [139].

Est3 is a stable component of telomerase since it is co-immunoprecipitated with *TLC1* RNA and telomerase activity [144]. Its association with telomerase complex requires an intact catalytic core [144]. A recent study suggests that the N-terminal domain of Est2 is required for Est3 binding [145]. The precise function of Est3 is still unknown.

Telomere maintenance in telomerase-negative survivors

Survival through senescence

Yeast cells with *TLC1* or any of the *EST* genes deleted display gradual telomere shortening accompanied by a progressive decline in growth potential, termed cellular senescence [5, 89, 127, 132]. Most cells cease division after 50-100 generations. However, a subpopulation outgrow senescence and become survivors [5, 6]. Survivor generation in a telomerase-deficient strain is not an isolated event. In fact, it occurs with a high frequency as demonstrated by the appearance of survivors in all of the more than 100 *est1Δ* strains examined in one study [5].

Survivors display dramatic changes in subtelomeric and telomeric regions [5, 6]. Based on those changes, the survivors are grouped into two types. Type I survivors have amplified Y' elements (70-fold on average) followed by short tracts of telomeric repeats. Type II survivors maintain long and heterogeneous telomeric repeats with little Y' amplification. These two types of survivors can be distinguished by the pattern of telomeric *Xho*I fragments using Southern blot analysis (Figure 1-6) [5, 6]. There is a single *Xho*I site located at ~900 bp from the 3' end of Y' elements. Type I survivors yield three major *Xho*I fragments detected by a 3' Y' probe or a poly(dG-dT) probe (Figure 1-6A & B). The sizes of these bands are ~1.3 kb, 5.2 kb and 6.7 kb. The ~1.3 kb fragment is the terminal fragment consisting of the distal portion of the terminal Y' and telomeric repeats. The strong signals at 5.2 and 6.7 kb are due to amplified Y'-short and Y'-long, respectively. In contrast, type II survivors have many *Xho*I fragments with different sizes, which hybridize to a 3' Y' probe and a poly(dG-dT) probe (Figure 1-6A & B). These fragments can not be detected by probes that hybridize to other portions of Y' (Figure 1-6A), indicating that they are terminal fragments that contain telomere repeats.

Although survivors are healthy cells that have recovered from senescence, continued streakouts for single colonies reveal variable growth patterns in both types of survivors [5]. Some survivors display stable growth rates that are comparable to wild type cells for extended periods, while others show a gradual decline in growth rate and senesce again. For the latter group, survivors can reappear readily. It appears that all type I survivors undergo senescence repeatedly, whereas only a subset of type II survivors display similar re-senescence phenotype. In addition, type II survivors grow faster than type I survivors [6]. Amplification of Y' results in about 10% increase in genome size. The burden of replicating such increased genome might contribute to the growth disadvantage of type I survivors [146].

Type I survivors are not stable. They can convert to type II during outgrowth [6]. In contrast, type II survivors are stable. The type II pattern of telomeric *Xho*I fragments can be maintained for at least 250 generations [6]. However, the individual *Xho*I fragment shortens overtime. When a single telomere was marked, the rate of telomere shortening was measured at ~3bp/cell division [6].

Survivors and homologous recombination

The appearance of survivors from telomerase-deficient strains is mediated by homologous recombination since no survivor can be recovered from strains lacking both telomerase and Rad52, which is essential in virtually all forms of homologous recombination [5, 7, 147]. The roles of the *RAD52* epistasis group in telomerase-independent telomere maintenance have been studied in detail. While *RAD52* is indispensable for both type I and type II survivors, *RAD51*, *RAD54*, *Rad55* and presumably *RAD57* are essential to generate type I survivors [7, 9], and *RAD50*, *Mre11*,

Xrs2 and RAD59 are required to generate type II survivors [7, 9]. Double mutants of *tlc1Δ* and genes involved in the generation of either type I or type II survivors (but not both) do not affect survivor generation, whereas triple mutants of *tlc1Δ rad51Δ rad50Δ* and *tlc1Δ rad51Δ rad59Δ* completely block survivor generation [7, 147].

The genetic requirements of the two survivor pathways and the structures of survivor telomeres have led to the proposal of two distinct genetic pathways that function in telomerase-deficient yeast cells to maintenance telomeres (Figure 1-7) [7]. The type I pathway, which generates type I survivors, is mediated by recombination between Y' elements on different chromosomes. The type II pathway, which generates type II survivors, is mediated by recombination between telomere repeats on the same or different chromosomes.

Although telomere shortening results in senescence, senescence is not strictly correlated with telomere length. Double mutants of *tlc1Δ rad52Δ*, *tlc1Δ rad51Δ*, *tlc1Δ rad54Δ* and *tlc1Δ rad57Δ* display an accelerated decline in growth potential compared to *tlc1Δ* single mutants [5, 147]. However, single mutants with deletion mutations of these recombination genes have telomere length similar to that in wild type cells [147]. In addition, the rate of telomere shortening in *tlc1Δ rad52Δ* mutants is similar to that in *tlc1Δ* mutants [7]. These observations also suggest that recombination starts to contribute to telomere functions in the initial phase of telomere shortening.

It might be expected that rare survivors arising from telomerase-deficient strains are hyper-recombination mutants. In fact, recombination rates in survivors and wild type cells are statistically indistinguishable [5]. However, when a recombination reporter is placed in the subtelomeric region of one telomere, it is found that recombination rate is

increased by up to1000-fold in telomerase-deficient strains [148]. Therefore, survivors display hyper-recombination phenotype in a telomere-specific manner.

Four homologous recombination-based mechanisms have been proposed for telomere maintenance in telomerase-deficient cells [146]: (1) break-induced replication, (2) integration of extrachromosomal DNA, (3) rolling circle replication, and (4) elongation via t-loop.

Break-induced replication (BIR): is a one-ended nonreciprocal recombination process in which a broken chromosome end invades into homologous sequences on an intact chromosome and copy the donor sequence all the way to telomeres. There are a *RAD51*-dependent BIR pathway, as well as a *RAD51*-independent, *RAD50/RAD59*-dependent BIR pathway [149-153]. This suggests that type I survivors are generated via *RAD51*-dependent BIR, whereas type II survivors arise through *RAD51*-independent BIR. It seems that the degree of homology between Y' elements or that between telomere repeats could be one of the factors that determine which pathway to employ. Rad51 is very sensitive to the mismatches in the homologous region during strand exchange [154]. The efficiency of strand exchange is only 20% of the wild type level when a 6 bp nonhomologous insertion exists in a duplex substrate [155]. Indeed, Y' elements are highly conserved with about 1% divergence within a strain [156]. Furthermore, although Y' long and Y' short share more than 5 kb homology, most Y'-Y' recombination occurs between elements of the same size [157]. In addition, the *RAD51*-dependent pathway needs at least ~100 bp of homology to initiate strand invasion, whereas the *RAD51*-independent pathway requires only ~30 bp [150].

Integration of extrachromosomal DNA and rolling circle replication: These two models provide alternative mechanisms to explain the sudden changes in the size of telomeric and subtelomeric repeats that can not be readily explained by BIR. Telomeres in type II survivors continue to shorten at a rate of ~3 bp/cell division. This gradual shortening is interspersed with episodes of sudden telomere elongation, increasing the size of telomeres by 1 to 2 kb [9]. This one-step of telomere elongation has been proposed to be mediated by integration of multiple extrachromosomal telomeric DNA [146]. Alternatively, the 3' tail of a G-strand could invade an extrachromosomal telomeric circle and prime DNA synthesis [9, 146].

Elongation of t-loop: This model provides an alternative to the rolling circle replication model. Instead of invading an extrachromosomal telomeric circle, the 3' tail of a G-strand invades the internal duplex telomeric region and forms an intramolecular loop. This structure, called t-loop, has been observed in evolutionarily unrelated organisms [158, 159], suggesting they are a conserved feature of eukaryotic telomeres. Although t-loops have not been observed in yeast telomeres, similar structures have been proposed to mediate telomere length regulation and transcriptional regulation of genes placed in subtelomeric region [122, 160-162]. In addition, the telomere binding protein Rap1 can promote association of single-stranded telomeric sequence with its homologous duplex sequence [163].

Telomerase-independent telomere maintenance in human cells: ALT

Most of human tumor samples and immortalized human cell lines exhibit telomerase activity. However, a subset of tumor cells and cell lines maintain telomeres in the absence of telomerase ([164] reviewed in [165]). These telomeres are maintained by

so-called Alternative Lengthening of Telomere (ALT) pathway. Rapid elongation of telomeres following gradual shortening has been observed in human telomerase-negative cells [166]. The long and heterogeneous telomeres observed in ALT cells are similar to that in type II yeast survivors, suggesting that human ALT is mediated by a recombination process similar to that occurs in type II yeast survivors [6, 146]. Indeed, DNA sequences can be copied from telomere to telomere [167]. ALT human cells contain ALT-associated PML bodies (APB), which are novel promyelocytic leukemia (PML) bodies [168]. APBs contain extrachromosomal telomeric DNA, telomere-specific binding proteins, and proteins involved in DNA replication and recombination. Noticeably, the appearance of APB coincides with the activation of ALT.

The existence of ALT poses a new question for tumor therapy. For ALT tumors, treatment with telomerase inhibitors will not be effective. For telomerase-positive tumors, telomerase inhibition can induce apoptosis and senescence [169-171]. However, such treatment may provide a selective advantage to cells that activate ALT. It may be important to develop inhibitors of ALT. It seems that normal cells and some telomerase-positive immortal cells contain repressors for the ALT telomere phenotype [172].

SUMMARY

This literature review focuses on homologous recombination repair of DSBs and mechanisms that contribute to telomere maintenance in *Saccharomyces cerevisiae*, including telomerase-dependent pathway and telomerase-independent, homologous recombination-mediated survivor pathway. Although the functions of *RAD52* in homologous recombination and telomere maintenance have been studied in great detail, it remains controversial as to how cells respond to changes in Rad52 concentration. In

addition, it is still unknown whether and how Rad52 differentially participates in telomere maintenance in different types of survivors. This study investigates the effects of Rad52 overexpression on DNA damage repair and demonstrates that the Rad52 cellular level needs to be tightly controlled to fulfill its functions. This study also investigates the functions of Rad52 in the two survivor pathways by charactering four novel *RAD52* alleles identified in a genetic screen.

APPENDIX 1: TABLES AND FIGURES FOR CHAPTER 1

Table 1-1 Homologous recombination proteins and their functions

In S. cerevisiae, homologous recombination depends on the RAD52 epistasis group, including RAD52, RAD51, RAD54, RAD55, RAD57, RAD59, RDH54, RAD50, MRE11 and XRS2. These genes can be further grouped into two subgroups. One group consists of RAD50, MRE11 and XRS2. These genes are required for processing DNA ends. The other group consists of RAD52, RAD51, RAD54, RAD55, RAD57, RAD59 and RDH54. Within the RAD52 subgroup, RAD52 stands alone as it is essential for all forms of homologous recombination during mitotic growth. RAD51, RAD54, RAD55 and RAD57 are required for gene conversion and break-induced replication. RAD59 is involved in Rad51-independent break-induced replication and single-strand annealing.

Table 1-1 Homologous recombination proteins and their functions

Recombination protein	Functions in homologous recombination	Homologous recombination pathways
Rad52	Promoting annealing between complementary single-stranded DNA ; Stimulating Rad51-mediated homologous pairing and strand exchange [31, 66]	Single strand annealing; Gene conversion; Break-induced replication [2]
Rad51	Catalyzing homologous pairing and strand exchange [11]	Gene conversion; Break-induced replication [2, 153]
Rad54	Stimulating Rad51-mediated strand exchange [36, 40-42]	Gene conversion; Break-induced replication [2, 153]
Rdh54	Stimulating Rad51-mediated strand exchange [44]	Gene conversion; Break-induced replication [2, 153]
Rad55/Rad57	Stimulating Rad51-mediated strand exchange [34]	Gene conversion; Break-induced replication [2, 153]
Rad59	Promoting annealing between complementary single-stranded DNA [63, 69]	Single strand annealing; Break-induced replication [2, 153]
Rad50/Mre11/Xrs2	Processing DSB ends [10, 20]	

Figure 1-1 Double-strand break repair model

After a DSB is created, 5' to 3' resection generates 3' single-stranded tails. The resulting 3' ends invade a homologous template to initiate DNA synthesis. Two Holiday junctions formed are resolved independently to generate crossover or noncrossover products.

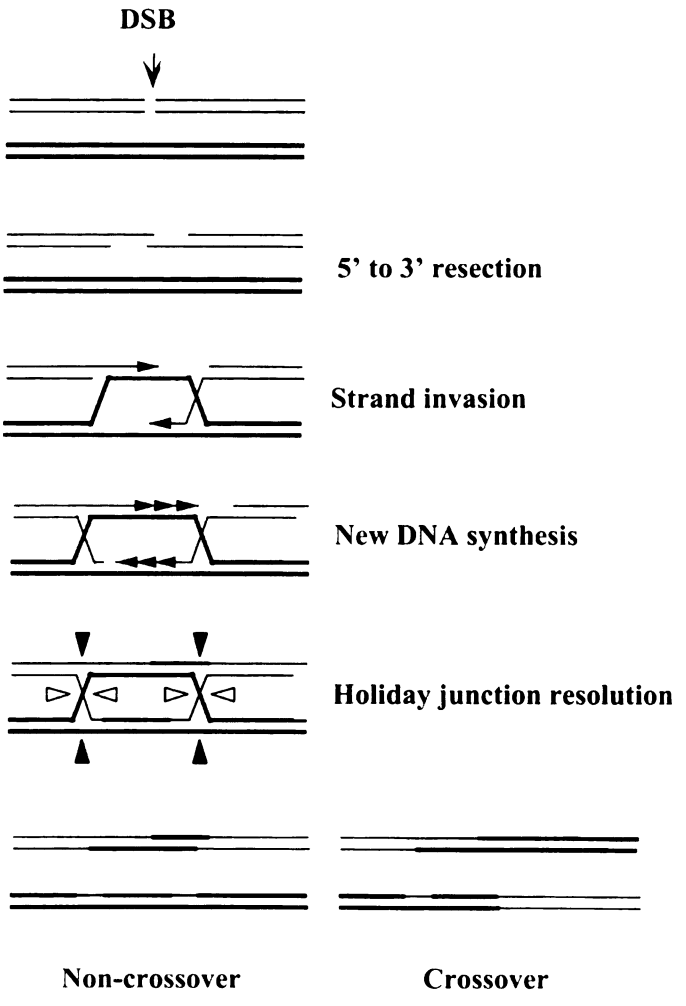

Figure 1-1

Taken from PÂQUES, F and J. E. HABER
Microbiol Mol Biol Rev 63(2): 394-404

Figure 1-2 Synthesis-dependent strand annealing

After a DSB is created, 5' to 3' resection generates 3' single-stranded tails. Both (A) or one (B, C & D) of the resulting 3' ends invade a homologous template to initiate DNA synthesis. For a two-ended invasion, both newly synthesized strands are displayed and annealed to each other (A). For a one-end invasion, the noninvading 3' end anneals with the displayed newly synthesized stand (B) or the D-loop (C). Alternatively, a repair replication fork can be established following strand invasion (D).

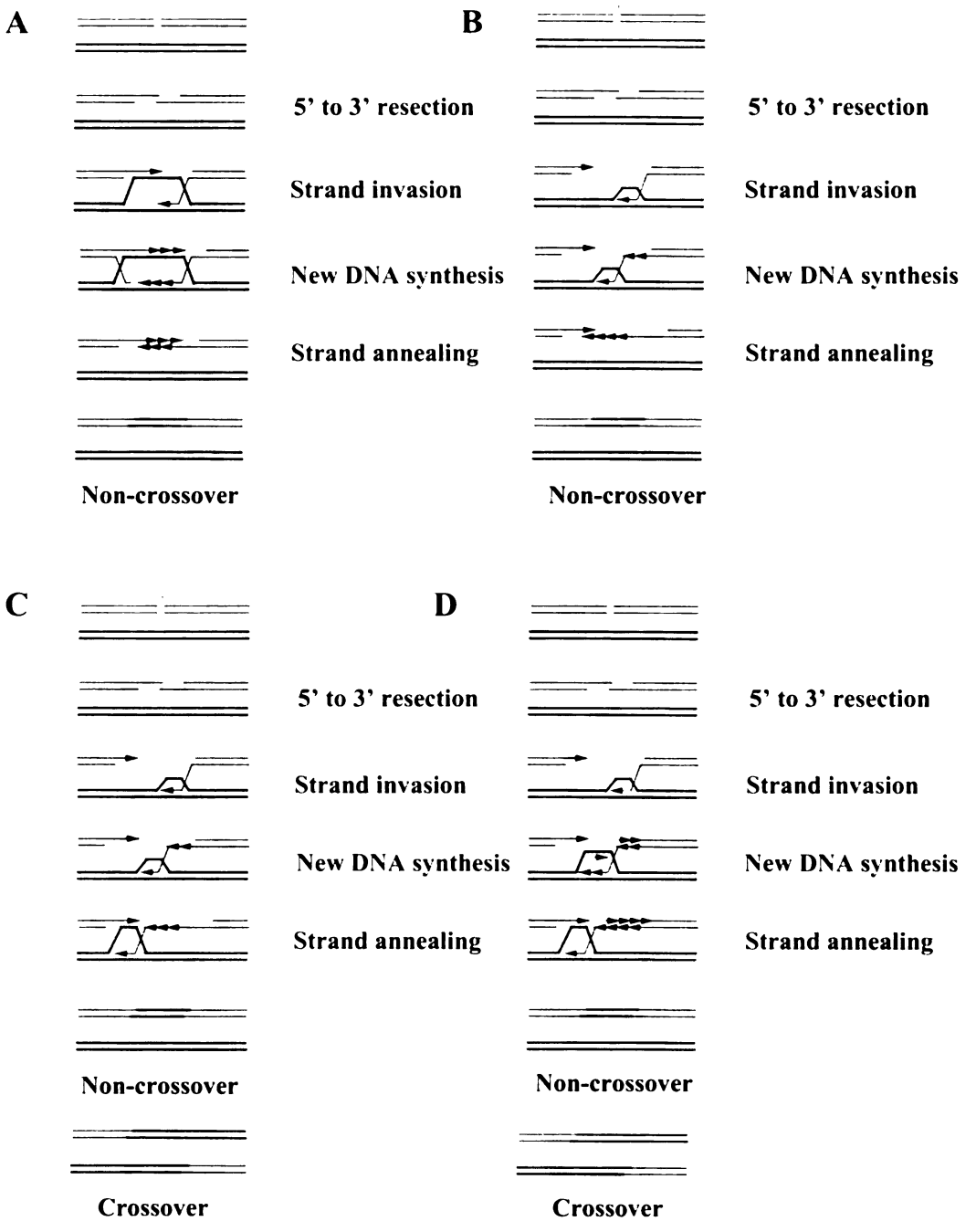

Figure 1-2

Taken from PÂQUES, F and J. E. HABER
Microbiol Mol Biol Rev 63(2): 394-404

Figure 1-3 Single-strand annealing

A DSB made between direct repeats is subjected to 5`to 3`resection. When complementary sequences are revealed, the single-stranded DNA anneals resulting in deletion of the intervening sequence and one of the repeats.

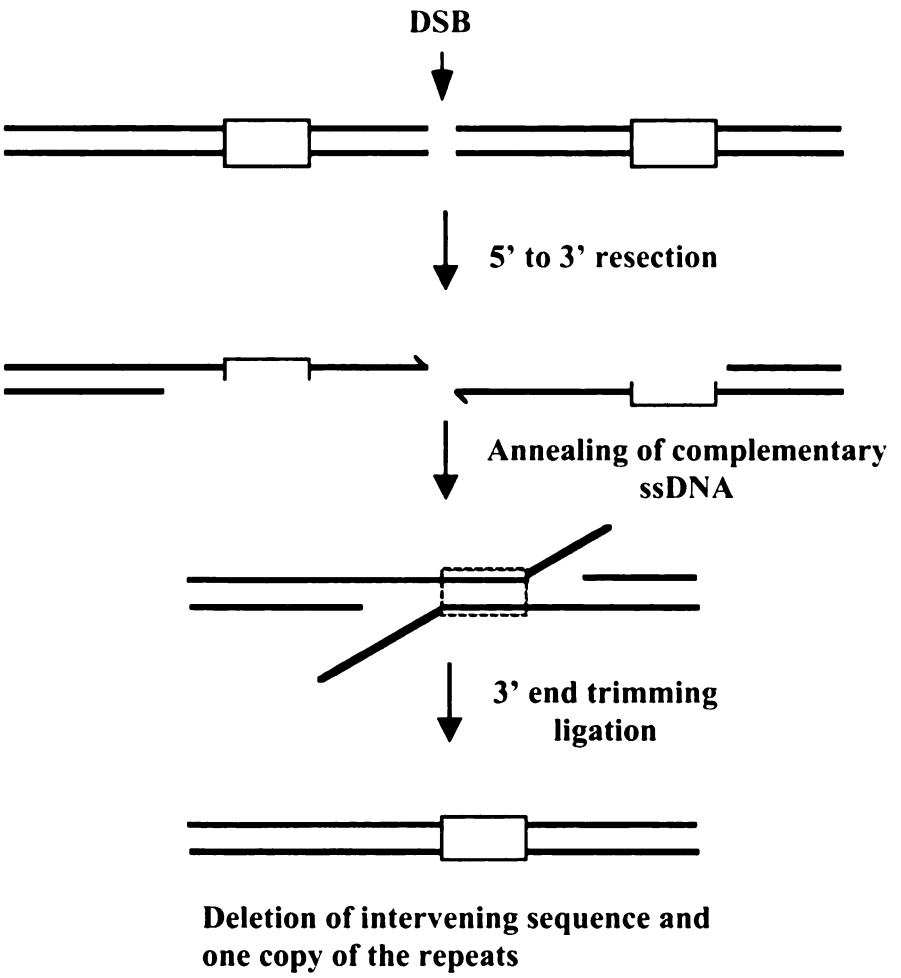

Figure 1-3

Taken from PÂQUES, F and J. E. HABER
Microbiol Mol Biol Rev 63(2): 394-404

Figure 1-4 Break-induced replication

When only one end of a DSB is available for homologous recombination, or a telomere becomes uncapped, the broken end can invades a homologous sequence and initiate DNA synthesis. Replication will proceed to the end of the chromosome.

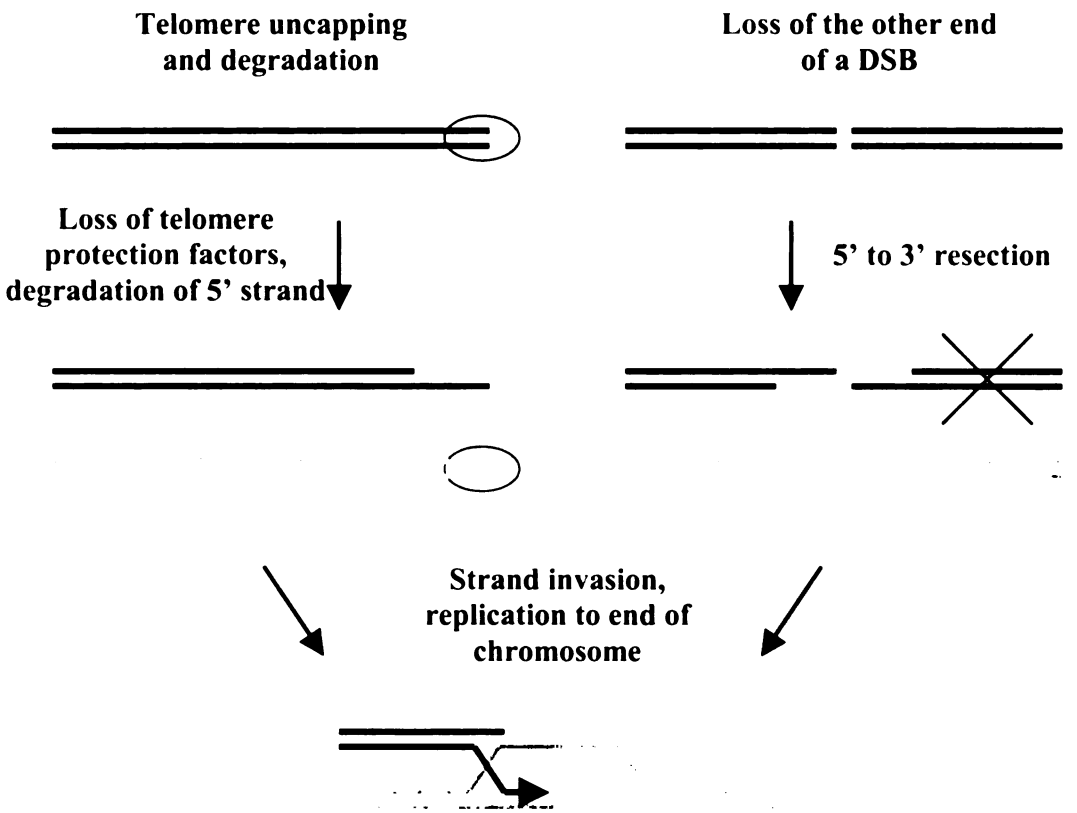

Figure 1-4

Taken from Krogh, B. O. and L. S. Symington
Annu Rev Genet 38: 233-271

Figure 1-5 Model for *RAD51*-catalyzed homologous pairing and strand exchange

When a DSB is created (only one side of the DSB is shown), (1) MRX and/or other exonucleases process the ends to generate 3' single-stranded tails. (2) RPA binds to the single-stranded tails to remove secondary structures. (3) Rad52 recruits Rad51 to the RPA-bound single-stranded DNA and facilitates the initial displacement of RPA. (4) Rad55/Rad57 facilitates Rad51 nucleoprotein filament extension. (5) The Rad51 nucleoprotein filament searches and locates homologous sequence. (6) Rad54 promotes DNA unwinding and strand annealing.

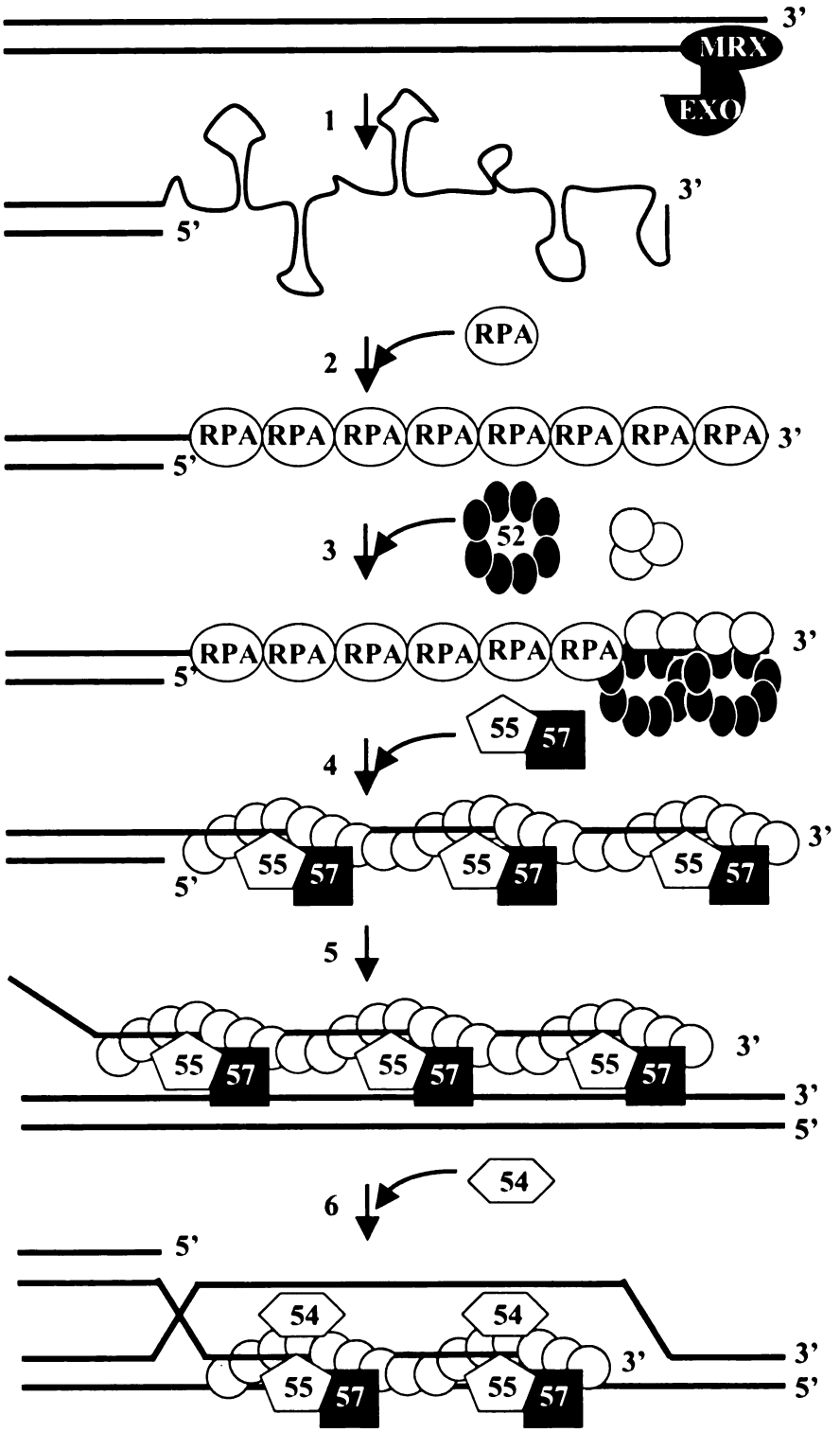

Figure 1-5

Taken from Krogh, B. O. and L. S. Symington
Annu Rev Genet 38: 233-271

Figure 1-6 Detection of telomeres in type I and type II survivors by Southern blotting analysis

A. Telomeric and subtelomeric region of *S. cerevisiae*. The $C_{1-3}A$/ TG_{1-3} DNA is shown in black. The open rectangle and the striped rectangle represent the Y' and X element, respectively. The solid lines indicate probes that can be used to detect telomeres for Southern blotting analysis. *Xho*I restriction site is also indicated.

B. Telomeres in wild type and telomerase-negative survivor yeast cells. Genomic DNA from wild type cells, type I survivors and type II survivors was digested with *Xho*I, resolved in 1% agarose gel. The southern blot was hybridized to a poly(dG-dT) probe.

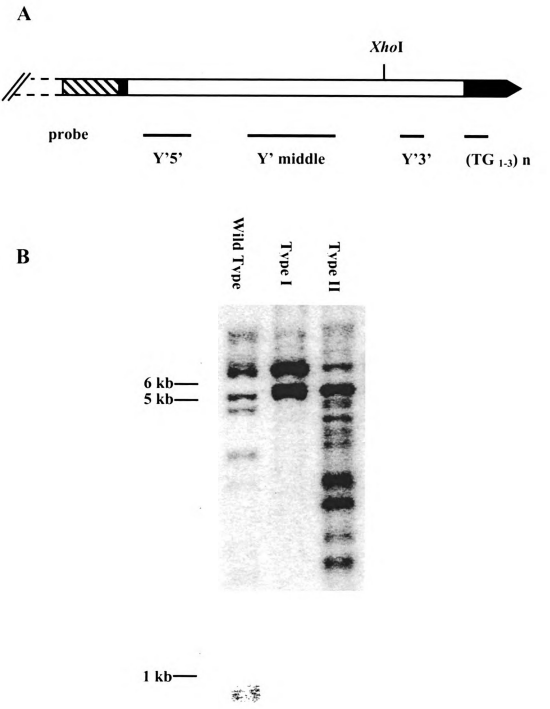
A
XhoI
probe
Y'5'
Y' middle
Y'3'
(TG 1-3) n
B
Wild Type
Type I
Type II
6 kb
5 kb
1 kb

Figure 1-6

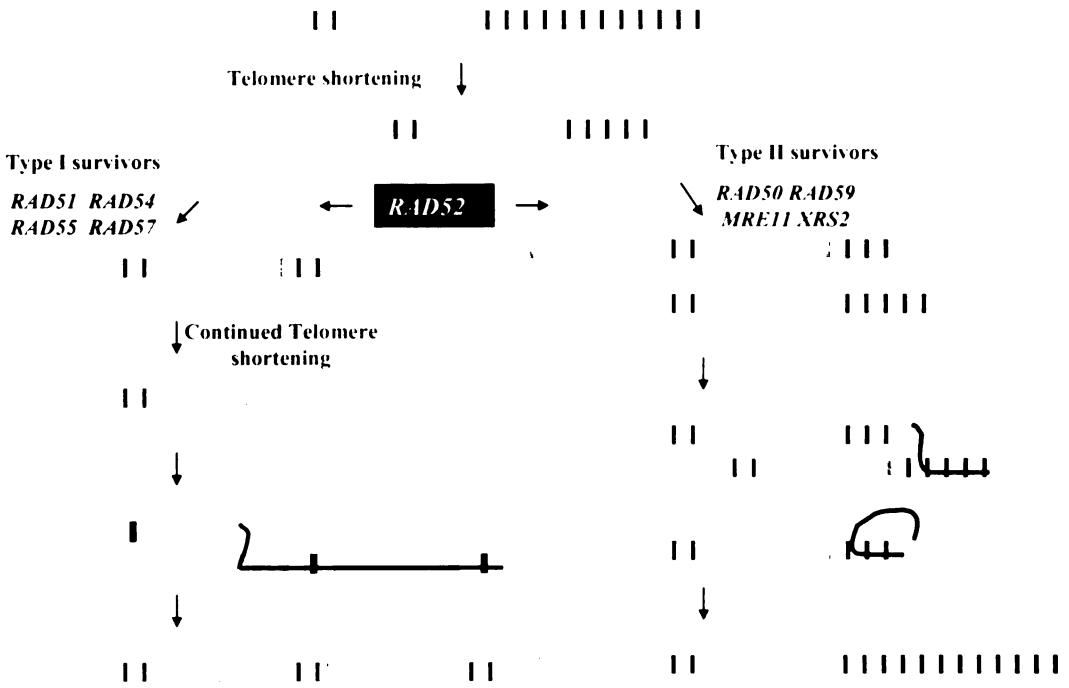

Figure 1-7

Modification of the model proposed by Greider and colleagues, MCB 21(5)1819-1827

Figure 1-7 Two survivor pathways that maintain telomeres in the absence of telomerase

A telomere containing two copies of Y' (gray boxes) and TG_{1-3} repeats (small white boxes) is shown at the top. Telomere shortening occurs in the absence of telomerase. Survivors can be generated via two pathways, both of which require *RAD52*. ***A.*** The type I survivor pathway also depends on *RAD51, RAD54, RAD55* and *RAD57*. Telomere shortening exposes Y'. 3' single-stranded tail initiate recombination between Y' on different chromosomes.

B. The type II survivor pathway also depends on *RAD50, MRE11, XRS2* and *RAD59*. Recombination is initiated between telomere repeats on different chromosomes, or the 3' single-stranded tail pairs with the duplex region of the telomere and primes DNA synthesis.

REFERENCE

1. Symington, L.S., *Role of RAD52 epistasis group genes in homologous recombination and double-strand break repair.* Microbiol Mol Biol Rev, 2002. **66**(4): p. 630-70, table of contents.

2. Paques, F. and J.E. Haber, *Multiple pathways of recombination induced by double-strand breaks in Saccharomyces cerevisiae.* Microbiol Mol Biol Rev, 1999. **63**(2): p. 349-404.

3. Zakian, V.A., *Structure, function, and replication of Saccharomyces cerevisiae telomeres.* Annu Rev Genet, 1996. **30**: p. 141-72.

4. Johnson, F.B., et al., *The Saccharomyces cerevisiae WRN homolog Sgs1p participates in telomere maintenance in cells lacking telomerase.* Embo J, 2001. **20**(4): p. 905-13.

5. Lundblad, V. and E.H. Blackburn, *An alternative pathway for yeast telomere maintenance rescues est1- senescence.* Cell, 1993. **73**(2): p. 347-60.

6. Teng, S.C. and V.A. Zakian, *Telomere-telomere recombination is an efficient bypass pathway for telomere maintenance in Saccharomyces cerevisiae.* Mol Cell Biol, 1999. **19**(12): p. 8083-93.

7. Chen, Q., A. Ijpma, and C.W. Greider, *Two survivor pathways that allow growth in the absence of telomerase are generated by distinct telomere recombination events.* Mol Cell Biol, 2001. **21**(5): p. 1819-27.

8. Sugawara, N. and J.E. Haber, *Characterization of double-strand break-induced recombination: homology requirements and single-stranded DNA formation.* Mol Cell Biol, 1992. **12**(2): p. 563-75.

9. Teng, S.C., et al., *Telomerase-independent lengthening of yeast telomeres occurs by an abrupt Rad50p-dependent, Rif-inhibited recombinational process.* Mol Cell, 2000. **6**(4): p. 947-52.

10. Krogh, B.O. and L.S. Symington, *Recombination Proteins in Yeast.* Annu Rev Genet, 2004.

11. Sung, P., *Catalysis of ATP-dependent homologous DNA pairing and strand exchange by yeast RAD51 protein.* Science, 1994. **265**(5176): p. 1241-3.

12. Anderson, D.E., et al., *Structure of the Rad50 x Mre11 DNA repair complex from Saccharomyces cerevisiae by electron microscopy.* J Biol Chem, 2001. **276**(40): p. 37027-33.

13. Chen, L., et al., *Promotion of Dnl4-catalyzed DNA end-joining by the Rad50/Mre11/Xrs2 and Hdf1/Hdf2 complexes.* Mol Cell, 2001. **8**(5): p. 1105-15.

14. Usui, T., et al., *Complex formation and functional versatility of Mre11 of budding yeast in recombination.* Cell, 1998. **95**(5): p. 705-16.

15. Trujillo, K.M. and P. Sung, *DNA structure-specific nuclease activities in the Saccharomyces cerevisiae Rad50*Mre11 complex.* J Biol Chem, 2001. **276**(38): p. 35458-64.

16. Paull, T.T. and M. Gellert, *The 3' to 5' exonuclease activity of Mre 11 facilitates repair of DNA double-strand breaks.* Mol Cell, 1998. **1**(7): p. 969-79.

17. Trujillo, K.M., et al., *Yeast xrs2 binds DNA and helps target rad50 and mre11 to DNA ends.* J Biol Chem, 2003. **278**(49): p. 48957-64.

18. Raymond, W.E. and N. Kleckner, *RAD50 protein of S.cerevisiae exhibits ATP-dependent DNA binding.* Nucleic Acids Res, 1993. **21**(16): p. 3851-6.

19. Alani, E., R. Padmore, and N. Kleckner, *Analysis of wild-type and rad50 mutants of yeast suggests an intimate relationship between meiotic chromosome synapsis and recombination.* Cell, 1990. **61**(3): p. 419-36.

20. Haber, J.E., *The many interfaces of Mre11.* Cell, 1998. **95**(5): p. 583-6.

21. Shinohara, A., H. Ogawa, and T. Ogawa, *Rad51 protein involved in repair and recombination in S. cerevisiae is a RecA-like protein.* Cell, 1992. **69**(3): p. 457-70.

22. Aboussekhra, A., et al., *Semidominant suppressors of Srs2 helicase mutations of Saccharomyces cerevisiae map in the RAD51 gene, whose sequence predicts a*

protein with similarities to procaryotic RecA proteins. Mol Cell Biol, 1992. **12**(7): p. 3224-34.

23. Sung, P. and D.L. Robberson, *DNA strand exchange mediated by a RAD51-ssDNA nucleoprotein filament with polarity opposite to that of RecA.* Cell, 1995. **82**(3): p. 453-61.

24. Sung, P. and S.A. Stratton, *Yeast Rad51 recombinase mediates polar DNA strand exchange in the absence of ATP hydrolysis.* J Biol Chem, 1996. **271**(45): p. 27983-6.

25. Namsaraev, E. and P. Berg, *Characterization of strand exchange activity of yeast Rad51 protein.* Mol Cell Biol, 1997. **17**(9): p. 5359-68.

26. Ogawa, T., et al., *Similarity of the yeast RAD51 filament to the bacterial RecA filament.* Science, 1993. **259**(5103): p. 1896-9.

27. Mazin, A.V., et al., *Tailed duplex DNA is the preferred substrate for Rad51 protein-mediated homologous pairing.* Embo J, 2000. **19**(5): p. 1148-56.

28. Donovan, J.W., G.T. Milne, and D.T. Weaver, *Homotypic and heterotypic protein associations control Rad51 function in double-strand break repair.* Genes Dev, 1994. **8**(21): p. 2552-62.

29. Conway, A.B., et al., *Crystal structure of a Rad51 filament.* Nat Struct Mol Biol, 2004. **11**(8): p. 791-6.

30. Sugiyama, T., E.M. Zaitseva, and S.C. Kowalczykowski, *A single-stranded DNA-binding protein is needed for efficient presynaptic complex formation by the Saccharomyces cerevisiae Rad51 protein.* J Biol Chem, 1997. **272**(12): p. 7940-5.

31. Sugiyama, T. and S.C. Kowalczykowski, *Rad52 protein associates with replication protein A (RPA)-single-stranded DNA to accelerate Rad51-mediated displacement of RPA and presynaptic complex formation.* J Biol Chem, 2002. **277**(35): p. 31663-72.

32. Song, B. and P. Sung, *Functional interactions among yeast Rad51 recombinase, Rad52 mediator, and replication protein A in DNA strand exchange.* J Biol Chem, 2000. **275**(21): p. 15895-904.

33. Shinohara, A. and T. Ogawa, *Stimulation by Rad52 of yeast Rad51-mediated recombination.* Nature, 1998. **391**(6665): p. 404-7.

34. Sung, P., *Yeast Rad55 and Rad57 proteins form a heterodimer that functions with replication protein A to promote DNA strand exchange by Rad51 recombinase.* Genes Dev, 1997. **11**(9): p. 1111-21.

35. Petukhova, G., S. Stratton, and P. Sung, *Catalysis of homologous DNA pairing by yeast Rad51 and Rad54 proteins.* Nature, 1998. **393**(6680): p. 91-4.

36. Petukhova, G., et al., *Yeast Rad54 promotes Rad51-dependent homologous DNA pairing via ATP hydrolysis-driven change in DNA double helix conformation.* J Biol Chem, 1999. **274**(41): p. 29453-62.

37. Mazin, A.V., et al., *Rad54 protein is targeted to pairing loci by the Rad51 nucleoprotein filament.* Mol Cell, 2000. **6**(3): p. 583-92.

38. Clever, B., et al., *Recombinational repair in yeast: functional interactions between Rad51 and Rad54 proteins.* Embo J, 1997. **16**(9): p. 2535-44.

39. Jiang, H., et al., *Direct association between the yeast Rad51 and Rad54 recombination proteins.* J Biol Chem, 1996. **271**(52): p. 33181-6.

40. Solinger, J.A., et al., *Rad54 protein stimulates heteroduplex DNA formation in the synaptic phase of DNA strand exchange via specific interactions with the presynaptic Rad51 nucleoprotein filament.* J Mol Biol, 2001. **307**(5): p. 1207-21.

41. Solinger, J.A., K. Kiianitsa, and W.D. Heyer, *Rad54, a Swi2/Snf2-like recombinational repair protein, disassembles Rad51:dsDNA filaments.* Mol Cell, 2002. **10**(5): p. 1175-88.

42. Solinger, J.A. and W.D. Heyer, *Rad54 protein stimulates the postsynaptic phase of Rad51 protein-mediated DNA strand exchange.* Proc Natl Acad Sci U S A, 2001. **98**(15): p. 8447-53.

43. Mazin, A.V., A.A. Alexeev, and S.C. Kowalczykowski, *A novel function of Rad54 protein. Stabilization of the Rad51 nucleoprotein filament.* J Biol Chem, 2003. **278**(16): p. 14029-36.

44. Petukhova, G., P. Sung, and H. Klein, *Promotion of Rad51-dependent D-loop formation by yeast recombination factor Rdh54/Tid1.* Genes Dev, 2000. **14**(17): p. 2206-15.

45. Lovett, S.T., *Sequence of the RAD55 gene of Saccharomyces cerevisiae: similarity of RAD55 to prokaryotic RecA and other RecA-like proteins.* Gene, 1994. **142**(1): p. 103-6.

46. Kans, J.A. and R.K. Mortimer, *Nucleotide sequence of the RAD57 gene of Saccharomyces cerevisiae.* Gene, 1991. **105**(1): p. 139-40.

47. Johnson, R.D. and L.S. Symington, *Functional differences and interactions among the putative RecA homologs Rad51, Rad55, and Rad57.* Mol Cell Biol, 1995. **15**(9): p. 4843-50.

48. Hays, S.L., A.A. Firmenich, and P. Berg, *Complex formation in yeast double-strand break repair: participation of Rad51, Rad52, Rad55, and Rad57 proteins.* Proc Natl Acad Sci U S A, 1995. **92**(15): p. 6925-9.

49. Fortin, G.S. and L.S. Symington, *Mutations in yeast Rad51 that partially bypass the requirement for Rad55 and Rad57 in DNA repair by increasing the stability of Rad51-DNA complexes.* Embo J, 2002. **21**(12): p. 3160-70.

50. Mortensen, U.H., et al., *DNA strand annealing is promoted by the yeast Rad52 protein.* Proc Natl Acad Sci U S A, 1996. **93**(20): p. 10729-34.

51. Ranatunga, W., et al., *Human RAD52 exhibits two modes of self-association.* J Biol Chem, 2001. **276**(19): p. 15876-80.

52. Kagawa, W., et al., *Crystal structure of the homologous-pairing domain from the human Rad52 recombinase in the undecameric form.* Mol Cell, 2002. **10**(2): p. 359-71.

53. Hays, S.L., et al., *Studies of the interaction between Rad52 protein and the yeast single-stranded DNA binding protein RPA.* Mol Cell Biol, 1998. **18**(7): p. 4400-6.

54. Milne, G.T. and D.T. Weaver, *Dominant negative alleles of RAD52 reveal a DNA repair/recombination complex including Rad51 and Rad52.* Genes Dev, 1993. **7**(9): p. 1755-65.

55. Krejci, L., et al., *Interaction with Rad51 is indispensable for recombination mediator function of Rad52.* J Biol Chem, 2002. **277**(42): p. 40132-41.

56. Cole, G.M., et al., *Regulation of RAD54- and RAD52-lacZ gene fusions in Saccharomyces cerevisiae in response to DNA damage.* Mol Cell Biol, 1987. 7(3): p. 1078-84.

57. Lisby, M., R. Rothstein, and U.H. Mortensen, *Rad52 forms DNA repair and recombination centers during S phase.* Proc Natl Acad Sci U S A, 2001. **98**(15): p. 8276-82.

58. Cole, G.M., D. Schild, and R.K. Mortimer, *Two DNA repair and recombination genes in Saccharomyces cerevisiae, RAD52 and RAD54, are induced during meiosis.* Mol Cell Biol, 1989. **9**(7): p. 3101-4.

59. Parsons, C.A., et al., *Precise binding of single-stranded DNA termini by human RAD52 protein.* Embo J, 2000. **19**(15): p. 4175-81.

60. Shinohara, A., et al., *Rad52 forms ring structures and co-operates with RPA in single-strand DNA annealing.* Genes Cells, 1998. **3**(3): p. 145-56.

61. Stasiak, A.Z., et al., *The human Rad52 protein exists as a heptameric ring.* Curr Biol, 2000. **10**(6): p. 337-40.

62. Sugiyama, T., J.H. New, and S.C. Kowalczykowski, *DNA annealing by RAD52 protein is stimulated by specific interaction with the complex of replication protein A and single-stranded DNA.* Proc Natl Acad Sci U S A, 1998. **95**(11): p. 6049-54.

63. Davis, A.P. and L.S. Symington, *The yeast recombinational repair protein Rad59 interacts with Rad52 and stimulates single-strand annealing.* Genetics, 2001. **159**(2): p. 515-25.

64. New, J.H., et al., *Rad52 protein stimulates DNA strand exchange by Rad51 and replication protein A.* Nature, 1998. **391**(6665): p. 407-10.

65. Sung, P., *Function of yeast Rad52 protein as a mediator between replication protein A and the Rad51 recombinase.* J Biol Chem, 1997. **272**(45): p. 28194-7.

66. New, J.H. and S.C. Kowalczykowski, *Rad52 protein has a second stimulatory role in DNA strand exchange that complements replication protein-A function.* J Biol Chem, 2002. **277**(29): p. 26171-6.

67. Bai, Y. and L.S. Symington, *A Rad52 homolog is required for RAD51-independent mitotic recombination in Saccharomyces cerevisiae.* Genes Dev, 1996. **10**(16): p. 2025-37.

68. Davis, A.P. and L.S. Symington, *The Rad52-Rad59 complex interacts with Rad51 and replication protein A.* DNA Repair (Amst), 2003. **2**(10): p. 1127-34.

69. Petukhova, G., S.A. Stratton, and P. Sung, *Single strand DNA binding and annealing activities in the yeast recombination factor Rad59.* J Biol Chem, 1999. **274**(48): p. 33839-42.

70. Muller, H.J., *The remarking of chromosomes.* The Collecting Net, 1938. **13**: p. 181-195, 198.

71. McClintock, B., *The behavior in successive nuclear divisions of a chromosome broken at meiosis.* Proc. Natl. Acad. Sci., 1939. **25**: p. 405-416.

72. McEachern, M.J. and E.H. Blackburn, *A conserved sequence motif within the exceptionally diverse telomeric sequences of budding yeasts.* Proc Natl Acad Sci U S A, 1994. **91**(8): p. 3453-7.

73. Henderson, E., *Telomere DNA structure.* Cold Spring Harbor monograph series, 1995. **29**: p. 11-34.

74. McEachern, M.J., A. Krauskopf, and E.H. Blackburn, *Telomeres and their control.* Annu Rev Genet, 2000. **34**: p. 331-358.

75. Shampay, J., J.W. Szostak, and E.H. Blackburn, *DNA sequences of telomeres maintained in yeast.* Nature, 1984. **310**(5973): p. 154-7.

76. Wright, J.H., D.E. Gottschling, and V.A. Zakian, *Saccharomyces telomeres assume a non-nucleosomal chromatin structure.* Genes Dev, 1992. **6**(2): p. 197-210.

77. Henderson, E.R. and E.H. Blackburn, *An overhanging 3' terminus is a conserved feature of telomeres.* Mol Cell Biol, 1989. **9**(1): p. 345-8.

78. Wellinger, R.J., et al., *Evidence for a new step in telomere maintenance.* Cell, 1996. **85**(3): p. 423-33.

79. Wellinger, R.J., A.J. Wolf, and V.A. Zakian, *Saccharomyces telomeres acquire single-strand TG1-3 tails late in S phase.* Cell, 1993. **72**(1): p. 51-60.

80. Dionne, I. and R.J. Wellinger, *Cell cycle-regulated generation of single-stranded G-rich DNA in the absence of telomerase.* Proc Natl Acad Sci U S A, 1996. **93**(24): p. 13902-7.

81. Louis, E.J., *The chromosome ends of Saccharomyces cerevisiae.* Yeast, 1995. **11**(16): p. 1553-73.

82. Chan, C.S. and B.K. Tye, *Organization of DNA sequences and replication origins at yeast telomeres.* Cell, 1983. **33**(2): p. 563-73.

83. Louis, E.J., et al., *The chromosome end in yeast: its mosaic nature and influence on recombinational dynamics.* Genetics, 1994. **136**(3): p. 789-802.

84. Zakian, V.A. and H.M. Blanton, *Distribution of telomere-associated sequences on natural chromosomes in Saccharomyces cerevisiae.* Mol Cell Biol, 1988. **8**(5): p. 2257-60.

85. Wright, J.H. and V.A. Zakian, *Protein-DNA interactions in soluble telosomes from Saccharomyces cerevisiae.* Nucleic Acids Res, 1995. **23**(9): p. 1454-60.

86. Norris, D., B. Dunn, and M.A. Osley, *The effect of histone gene deletions on chromatin structure in Saccharomyces cerevisiae.* Science, 1988. **242**(4879): p. 759-61.

87. Gottschling, D.E., *Telomere-proximal DNA in Saccharomyces cerevisiae is refractory to methyltransferase activity in vivo.* Proc Natl Acad Sci U S A, 1992. **89**(9): p. 4062-5.

88. Braunstein, M., et al., *Transcriptional silencing in yeast is associated with reduced nucleosome acetylation.* Genes Dev, 1993. **7**(4): p. 592-604.

89. Lundblad, V. and J.W. Szostak, *A mutant with a defect in telomere elongation leads to senescence in yeast.* Cell, 1989. **57**(4): p. 633-43.

90. Hackett, J.A., D.M. Feldser, and C.W. Greider, *Telomere dysfunction increases mutation rate and genomic instability.* Cell, 2001. **106**(3): p. 275-86.

91. Sandell, L.L. and V.A. Zakian, *Loss of a yeast telomere: arrest, recovery, and chromosome loss.* Cell, 1993. **75**(4): p. 729-39.

92. AS, I.J. and C.W. Greider, *Short telomeres induce a DNA damage response in Saccharomyces cerevisiae.* Mol Biol Cell, 2003. **14**(3): p. 987-1001.

93. Gottschling, D.E., et al., *Position effect at S. cerevisiae telomeres: reversible repression of Pol II transcription.* Cell, 1990. **63**(4): p. 751-62.

94. Renauld, H., et al., *Silent domains are assembled continuously from the telomere and are defined by promoter distance and strength, and by SIR3 dosage.* Genes Dev, 1993. **7**(7A): p. 1133-45.

95. Kyrion, G., et al., *RAP1 and telomere structure regulate telomere position effects in Saccharomyces cerevisiae.* Genes Dev, 1993. **7**(7A): p. 1146-59.

96. Wiley, E.A. and V.A. Zakian, *Extra telomeres, but not internal tracts of telomeric DNA, reduce transcriptional repression at Saccharomyces telomeres.* Genetics, 1995. **139**(1): p. 67-79.

97. Pryde, F.E. and E.J. Louis, *Limitations of silencing at native yeast telomeres.* Embo J, 1999. **18**(9): p. 2538-50.

98. Koering, C.E., et al., *Identification of high affinity Tbf1p-binding sites within the budding yeast genome.* Nucleic Acids Res, 2000. **28**(13): p. 2519-26.

99. Bilaud, T., et al., *The telobox, a Myb-related telomeric DNA binding motif found in proteins from yeast, plants and human.* Nucleic Acids Res, 1996. **24**(7): p. 1294-303.

100. Dmitriev, P.V., A.V. Petrov, and O.A. Dontsova, *Yeast telosome complex: components and their functions.* Biochemistry (Mosc), 2003. **68**(7): p. 718-34.

101. Lin, J.J. and V.A. Zakian, *The Saccharomyces CDC13 protein is a single-strand TG1-3 telomeric DNA-binding protein in vitro that affects telomere behavior in vivo.* Proc Natl Acad Sci U S A, 1996. **93**(24): p. 13760-5.

102. Lin, Y.C., et al., *Specific binding of single-stranded telomeric DNA by Cdc13p of Saccharomyces cerevisiae.* J Biol Chem, 2001. **276**(27): p. 24588-93.

103. Garvik, B., M. Carson, and L. Hartwell, *Single-stranded DNA arising at telomeres in cdc13 mutants may constitute a specific signal for the RAD9 checkpoint.* Mol Cell Biol, 1995. **15**(11): p. 6128-38.

104. Bourns, B.D., et al., *Sir proteins, Rif proteins, and Cdc13p bind Saccharomyces telomeres in vivo.* Mol Cell Biol, 1998. **18**(9): p. 5600-8.

105. Lustig, A.J., *Cdc13 subcomplexes regulate multiple telomere functions.* Nat Struct Biol, 2001. **8**(4): p. 297-9.

106. Weinert, T.A. and L.H. Hartwell, *Cell cycle arrest of cdc mutants and specificity of the RAD9 checkpoint.* Genetics, 1993. **134**(1): p. 63-80.

107. Pennock, E., K. Buckley, and V. Lundblad, *Cdc13 delivers separate complexes to the telomere for end protection and replication.* Cell, 2001. **104**(3): p. 387-96.

108. Grandin, N., S.I. Reed, and M. Charbonneau, *Stn1, a new Saccharomyces cerevisiae protein, is implicated in telomere size regulation in association with Cdc13.* Genes Dev, 1997. **11**(4): p. 512-27.

109. Grandin, N., C. Damon, and M. Charbonneau, *Ten1 functions in telomere end protection and length regulation in association with Stn1 and Cdc13.* Embo J, 2001. **20**(5): p. 1173-83.

110. Enomoto, S., et al., *Telomere cap components influence the rate of senescence in telomerase-deficient yeast cells.* Mol Cell Biol, 2004. **24**(2): p. 837-45.

111. Polotnianka, R.M., J. Li, and A.J. Lustig, *The yeast Ku heterodimer is essential for protection of the telomere against nucleolytic and recombinational activities.* Curr Biol, 1998. **8**(14): p. 831-4.

112. Gravel, S., et al., *Yeast Ku as a regulator of chromosomal DNA end structure.* Science, 1998. **280**(5364): p. 741-4.

113. Grandin, N., C. Damon, and M. Charbonneau, *Cdc13 cooperates with the yeast Ku proteins and Stn1 to regulate telomerase recruitment.* Mol Cell Biol, 2000. **20**(22): p. 8397-408.

114. Peterson, S.E., et al., *The function of a stem-loop in telomerase RNA is linked to the DNA repair protein Ku.* Nat Genet, 2001. **27**(1): p. 64-7.

115. Gilson, E., et al., *Distortion of the DNA double helix by RAP1 at silencers and multiple telomeric binding sites.* J Mol Biol, 1993. **231**(2): p. 293-310.

116. Hardy, C.F., L. Sussel, and D. Shore, *A RAP1-interacting protein involved in transcriptional silencing and telomere length regulation.* Genes Dev, 1992. **6**(5): p. 801-14.

117. Wotton, D. and D. Shore, *A novel Rap1p-interacting factor, Rif2p, cooperates with Rif1p to regulate telomere length in Saccharomyces cerevisiae.* Genes Dev, 1997. **11**(6): p. 748-60.

118. Marcand, S., et al., *Rap1p and telomere length regulation in yeast.* Ciba Found Symp, 1997. **211**: p. 76-93; discussion 93-103.

119. Ray, A. and K.W. Runge, *The C terminus of the major yeast telomere binding protein Rap1p enhances telomere formation.* Mol Cell Biol, 1998. **18**(3): p. 1284-95.

120. Krauskopf, A. and E.H. Blackburn, *Control of telomere growth by interactions of RAP1 with the most distal telomeric repeats.* Nature, 1996. **383**(6598): p. 354-7.

121. Cockell, M., et al., *The carboxy termini of Sir4 and Rap1 affect Sir3 localization: evidence for a multicomponent complex required for yeast telomeric silencing.* J Cell Biol, 1995. **129**(4): p. 909-24.

122. Grunstein, M., *Molecular model for telomeric heterochromatin in yeast.* Curr Opin Cell Biol, 1997. **9**(3): p. 383-7.

123. Moretti, P., et al., *Evidence that a complex of SIR proteins interacts with the silencer and telomere-binding protein RAP1.* Genes Dev, 1994. **8**(19): p. 2257-69.

124. Pina, B., et al., *The different (sur)faces of Rap1p.* Mol Genet Genomics, 2003. **268**(6): p. 791-8.

125. Strahl-Bolsinger, S., et al., *SIR2 and SIR4 interactions differ in core and extended telomeric heterochromatin in yeast.* Genes Dev, 1997. **11**(1): p. 83-93.

126. Wellinger, R.J., A.J. Wolf, and V.A. Zakian, *Origin activation and formation of single-strand TG1-3 tails occur sequentially in late S phase on a yeast linear plasmid.* Mol Cell Biol, 1993. **13**(7): p. 4057-65.

127. Lendvay, T.S., et al., *Senescence mutants of Saccharomyces cerevisiae with a defect in telomere replication identify three additional EST genes.* Genetics, 1996. **144**(4): p. 1399-412.

128. Hughes, T.R., et al., *The role of the EST genes in yeast telomere replication.* Ciba Found Symp, 1997. **211**: p. 41-7; discussion 47-52, 71-5.

129. Bianchi, A., S. Negrini, and D. Shore, *Delivery of yeast telomerase to a DNA break depends on the recruitment functions of Cdc13 and Est1.* Mol Cell, 2004. **16**(1): p. 139-46.

130. Evans, S.K. and V. Lundblad, *Est1 and Cdc13 as comediators of telomerase access.* Science, 1999. **286**(5437): p. 117-20.

131. Lingner, J., et al., *Three Ever Shorter Telomere (EST) genes are dispensable for in vitro yeast telomerase activity.* Proc Natl Acad Sci U S A, 1997. **94**(21): p. 11190-5.

132. Singer, M.S. and D.E. Gottschling, *TLC1: template RNA component of Saccharomyces cerevisiae telomerase.* Science, 1994. **266**(5184): p. 404-9.

133. Zappulla, D.C. and T.R. Cech, *Yeast telomerase RNA: a flexible scaffold for protein subunits.* Proc Natl Acad Sci U S A, 2004. **101**(27): p. 10024-9.

134. Lin, J., et al., *A universal telomerase RNA core structure includes structured motifs required for binding the telomerase reverse transcriptase protein.* Proc Natl Acad Sci U S A, 2004. **101**(41): p. 14713-8.

135. Chappell, A.S. and V. Lundblad, *Structural elements required for association of the Saccharomyces cerevisiae telomerase RNA with the Est2 reverse transcriptase.* Mol Cell Biol, 2004. **24**(17): p. 7720-36.

136. Livengood, A.J., A.J. Zaug, and T.R. Cech, *Essential regions of Saccharomyces cerevisiae telomerase RNA: separate elements for Est1p and Est2p interaction.* Mol Cell Biol, 2002. **22**(7): p. 2366-74.

137. Lingner, J., et al., *Reverse transcriptase motifs in the catalytic subunit of telomerase.* Science, 1997. **276**(5312): p. 561-7.

138. Counter, C.M., et al., *The catalytic subunit of yeast telomerase.* Proc Natl Acad Sci U S A, 1997. **94**(17): p. 9202-7.

139. Virta-Pearlman, V., D.K. Morris, and V. Lundblad, *Est1 has the properties of a single-stranded telomere end-binding protein.* Genes Dev, 1996. **10**(24): p. 3094-104.

140. Steiner, B.R., K. Hidaka, and B. Futcher, *Association of the Est1 protein with telomerase activity in yeast.* Proc Natl Acad Sci U S A, 1996. **93**(7): p. 2817-21.

141. Zhou, J., K. Hidaka, and B. Futcher, *The Est1 subunit of yeast telomerase binds the Tlc1 telomerase RNA.* Mol Cell Biol, 2000. **20**(6): p. 1947-55.

142. Taggart, A.K., S.C. Teng, and V.A. Zakian, *Est1p as a cell cycle-regulated activator of telomere-bound telomerase.* Science, 2002. **297**(5583): p. 1023-6.

143. Marcand, S., et al., *Cell cycle restriction of telomere elongation.* Curr Biol, 2000. **10**(8): p. 487-90.

144. Hughes, T.R., et al., *The Est3 protein is a subunit of yeast telomerase.* Curr Biol, 2000. **10**(13): p. 809-12.

145. Friedman, K.L., et al., *N-terminal domain of yeast telomerase reverse transcriptase: recruitment of Est3p to the telomerase complex.* Mol Biol Cell, 2003. **14**(1): p. 1-13.

146. Lundblad, V., *Telomere maintenance without telomerase.* Oncogene, 2002. **21**(4): p. 522-31.

147. Le, S., et al., *RAD50 and RAD51 define two pathways that collaborate to maintain telomeres in the absence of telomerase.* Genetics, 1999. **152**(1): p. 143-52.

148. McEachern, M.J. and S. Iyer, *Short telomeres in yeast are highly recombinogenic.* Mol Cell, 2001. **7**(4): p. 695-704.

149. Signon, L., et al., *Genetic requirements for RAD51- and RAD54-independent break-induced replication repair of a chromosomal double-strand break.* Mol Cell Biol, 2001. **21**(6): p. 2048-56.

150. Ira, G. and J.E. Haber, *Characterization of RAD51-independent break-induced replication that acts preferentially with short homologous sequences.* Mol Cell Biol, 2002. **22**(18): p. 6384-92.

151. Malkova, A., E.L. Ivanov, and J.E. Haber, *Double-strand break repair in the absence of RAD51 in yeast: a possible role for break-induced DNA replication.* Proc Natl Acad Sci U S A, 1996. **93**(14): p. 7131-6.

152. Davis, A.P. and L.S. Symington, *RAD51-dependent break-induced replication in yeast.* Mol Cell Biol, 2004. **24**(6): p. 2344-51.

153. Kraus, E., W.Y. Leung, and J.E. Haber, *Break-induced replication: a review and an example in budding yeast.* Proc Natl Acad Sci U S A, 2001. **98**(15): p. 8255-62.

154. Chen, W. and S. Jinks-Robertson, *The role of the mismatch repair machinery in regulating mitotic and meiotic recombination between diverged sequences in yeast.* Genetics, 1999. **151**(4): p. 1299-313.

155. Holmes, V.F., et al., *Bypass of heterology during strand transfer by Saccharomyces cerevisiae Rad51 protein.* Nucleic Acids Res, 2001. **29**(24): p. 5052-7.

156. Louis, E.J. and J.E. Haber, *The structure and evolution of subtelomeric Y' repeats in Saccharomyces cerevisiae.* Genetics, 1992. **131**(3): p. 559-74.

157. Louis, E.J. and J.E. Haber, *Mitotic recombination among subtelomeric Y' repeats in Saccharomyces cerevisiae.* Genetics, 1990. **124**(3): p. 547-59.

158. Munoz-Jordan, J.L., et al., *t-loops at trypanosome telomeres.* Embo J, 2001. **20**(3): p. 579-88.

159. Griffith, J.D., et al., *Mammalian telomeres end in a large duplex loop.* Cell, 1999. **97**(4): p. 503-14.

160. Li, B. and A.J. Lustig, *A novel mechanism for telomere size control in Saccharomyces cerevisiae.* Genes Dev, 1996. **10**(11): p. 1310-26.

161. de Bruin, D., et al., *Telomere looping permits gene activation by a downstream UAS in yeast.* Nature, 2001. **409**(6816): p. 109-13.

162. de Bruin, D., et al., *Telomere folding is required for the stable maintenance of telomere position effects in yeast.* Mol Cell Biol, 2000. **20**(21): p. 7991-8000.

163. Gilson, E., et al., *RAP1 stimulates single- to double-strand association of yeast telomeric DNA: implications for telomere-telomere interactions.* Nucleic Acids Res, 1994. **22**(24): p. 5310-20.

164. Bryan, T.M., et al., *Evidence for an alternative mechanism for maintaining telomere length in human tumors and tumor-derived cell lines.* Nat Med, 1997. **3**(11): p. 1271-4.

165. Henson, J.D., et al., *Alternative lengthening of telomeres in mammalian cells.* Oncogene, 2002. **21**(4): p. 598-610.

166. Reddel, R.R., T.M. Bryan, and J.P. Murnane, *Immortalized cells with no detectable telomerase activity. A review.* Biochemistry (Mosc), 1997. **62**(11): p. 1254-62.

167. Dunham, M.A., et al., *Telomere maintenance by recombination in human cells.* Nat Genet, 2000. **26**(4): p. 447-50.

168. Yeager, T.R., et al., *Telomerase-negative immortalized human cells contain a novel type of promyelocytic leukemia (PML) body.* Cancer Res, 1999. **59**(17): p. 4175-9.

169. Saretzki, G., et al., *Ribozyme-mediated telomerase inhibition induces immediate cell loss but not telomere shortening in ovarian cancer cells.* Cancer Gene Ther, 2001. **8**(10): p. 827-34.

170. Zhang, X., et al., *Telomere shortening and apoptosis in telomerase-inhibited human tumor cells.* Genes Dev, 1999. **13**(18): p. 2388-99.

171. Hahn, W.C., et al., *Inhibition of telomerase limits the growth of human cancer cells.* Nat Med, 1999. **5**(10): p. 1164-70.

172. Perrem, K., et al., *Repression of an alternative mechanism for lengthening of telomeres in somatic cell hybrids.* Oncogene, 1999. **18**(22): p. 3383-90.

CHAPTER 2

STRONG NEGATIVE EFFECTS OF *RAD52* OVEREXPRESSION ON DNA DAMAGE REPAIR IN *S. CEREVIAISE*

ABSTACT

Rad52 is an essential multifunctional component of the homologous recombination machinery in *S. cerevisiae*. In this work, I examined the effect of *RAD52* overexpression on DNA damage repair. I demonstrated that among the five 5' ATG triplets, the third, fourth and fifth can be used as translation initiation codons. Rad52 protein translated from the fifth ATG is as competent as that translated from the third ATG in DNA damage repair. The 99 bp sequence between the first ATG and the third initiation ATG has a strong influence on the level of Rad52 expression controlled by a heterologous *GAL1* promoter. When overexpressed, Rad52 has a strong negative effect on DNA damage repair. Overexpression of Rad51 completely suppresses the negative effect of Rad52 overexpression. Overexpression of a mutant Rad52, which is defective in the Rad51 interaction, has a greatly reduced negative effect on DNA damage repair. These data suggest that the negative effect of Rad52 overexpression results mainly from the sequestration of Rad51 from other essential functions.

INTRODUCTION

Homologous recombination is an essential pathway for DNA damage repair in eukaryotic cells. In *S. cerevisiae*, the major components of the homologous recombination machinery are the protein products of the *RAD52* epistasis gene group, including *RAD52, RAD51, RAD54, RAD55, RAD57, RAD59, RDH54/TID1, MRE11, RAD50,* and *XRS2*. Rad52, Rad51, Rad54, Rad55, and Rad57 are required for gene conversion and break-induced replication [1-3]. Rad52 and Rad59 are required for additional types of homologous recombination, including *RAD51*-independent break-induced replication and single-strand annealing [2, 3]. Consistent with the essential roles of Rad52 in all types of homologous recombination, *rad52* null mutants have the most severe defect in mitotic recombination and are most sensitive to DNA damaging agents, such as γ-rays and methylmethanesulfonate (MMS) [4, 5].

In vitro studies suggest that Rad52 is required at a level substoichiometric to Rad51 to achieve an optimal recombination activity [7]. Consistent with this observation, Rad52 is of lower cellular abundance than Rad51 [7, 8]. While both genetic and biochemical studies suggest that cells are sensitive to the changes in Rad52 cellular level, especially under DNA damaging conditions [6-8], previous studies found no appreciable effect of Rad52 overexpression on DNA damage repair [9, 10]. However, the exact levels of Rad52 protein in those studies are unknown. There are five in-frame ATG triplets at the 5' end of the *RAD52* genomic sequence. In the previous studies on the effect of Rad52 overexpression, the entire ORF starting from the first ATG was placed downstream of a heterologous promoter (*ENO1*, *GAL1*, *ADH*) for the purpose of overexpressing Rad52 [9, 10]. Here I demonstrate that the third and fifth, possibly the

fourth ATG, but not the first and the second ATG can initiate protein translation *in vivo*. The sequence between the first ATG and the third ATG has a great negative influence on Rad52 protein expression controlled by the *GAL1* promoter. Removal of this sequence leads to a 40-fold increase in Rad52 protein level. Overexpression of *RAD52* has a strong negative effect on DNA damage repair. This effect is specific for DNA damage repair since cells overexpressing Rad52 show no apparent growth defect in the absence of a DNA damaging agent. Furthermore, overexpression of Rad51 completely suppresses the negative effect of Rad52 overexpression.

MATERIALS AND METHODS

Strains

Yeast strains used in this study are listed in table 2-1. JP166 was generously provided by Dr. John Prescott (University of California, San Francisco). BY4735 (ATCC200897) was obtained from ATCC. All other strains were derived from these two strains. Disruption of specific genes was carried out as previously described [11, 12].

S. cerevisiae strains were propagated at 30°C in dropout media lacking the amino acids required for plasmid selection. Yeast transformation was performed according to Agatep, R. *et al.* [13].

Plasmids and site-directed mutagenesis

To create pRS415RAD52, the *Sal*I genomic fragment containing the *RAD52* coding sequence and its promoter [14] was cloned into pRS415, a *CEN* vector with a *LEU2* marker [15]. To create mutant *rad52* containing a single ATG initiation codon, all

other ATGs were mutated to ATC by site-directed mutagenesis in the pRS415RAD52 construct. Site directed mutagenesis was performed following the Quick-Change protocol using Pfu-Turbo polymerase (Stratagene).

Vector pRSG415 (generously provided by Dr. John Prescott, University of California, San Francisco) for galactose-inducible overexpression contains the *GAL1* promoter and the *CYC1* terminator on a *Hind*III-*Sac*I fragment in pRS415 backbone. A *BamH*I site and an *Spe*I site were previously engineered between the *GAL1* promoter and the *CYC1* terminator for cloning purposes. To create pRSG414 vector, The *Hind*III-*Sac*I fragment from pRSG415 was cloned into pRS414, a *CEN* vector with a *TRP1* marker [15].

To clone *RAD52* into the pRSG415 vector, the single *Bam*HI site within the *RAD52* ORF was removed by a silent mutation via site-directed mutagenesis (5'-CGACAGAGAAGGACCCCGTTGTAG-3'). The *RAD52* coding sequence starting from the first (GAL1-RAD52F1), the third (GAL1-RAD52F3) or the fifth ATG (GAL1-RAD52F5) to the stop codon was amplified by PCR to introduce a *Bam*H1 site at the 5' and an *Spe*I site at the 3', and subcloned into pRSG415, placing the coding sequence downstream of the *GAL1* promoter but upstream of the *CYC1* terminator. To create GAL1-RAD52F1ATG1, the second, third, fourth and fifth ATG in GAL1-RAD52F1 were mutated to ATC by site-directed mutagenesis. To create GAL1-RAD52F3ATG3, the fourth and fifth ATG in GAL1-RAD52F3 were mutated to ATC by site-directed mutagenesis. For selection with the *TRP1* marker, the *Hind*III-*Sac*I fragments containing *RAD52*, the *GAL1* promoter, and the *CYC1* terminator were inserted into the pRSG414 vector to generate GAL1b-RAD52F1, GAL1b-RAD52F3 and GAL1b-RAD52F5.

For overexpression of Rad51 and Rad59, the *RAD51* and *RAD59* genes were amplified from genomic DNA and cloned into pRSG415 between the *Bam*H1 and the *Spe*I sites, placed downstream of the *GAL1* promoter but upstream of the *CYC1* terminator.

Western blotting

Yeast proteins were prepared following a procedure from the laboratory of Steven Hahn (www.fhcrc.org/lab/hahn). Equal amounts of proteins, determined by Bradford method (Pirece), were separated on 10% SDS-PAGE and blotted onto polyvinylidene difluoride membrane (Amersham Pharmacia Biotech). Rad52 was detected with a goat anti-Rad52 antibody RAD52 yC-17 (Santa Cruz Biotech) followed by a rabbit anti-goat IgG HRP (Sigma). The membrane was stripped and probed with a rabbit anti-G-6-PDH antibody (Sigma) followed by a goat anti-rabbit IgG HRP (Sigma) as a loading control.

MMS sensitivity assay

The strains harboring galactose-inducible gene constructs were cultivated in appropriate dropout liquid medium containing 2% raffinose as the sole carbon source to mid-log phase. 10-fold serial dilutions were prepared and 10 to 10^6 cells were spotted on appropriate solid medium containing 2% raffinose and 0.05% galactose with or without MMS at concentrations specified in figure legends. The plates were then incubated at 30°C for 3 or 4 days and photographed. The strains harboring gene constructs controlled by the genomic promoter were evaluated in the same way except that the liquid and solid culture medium contained 2% glucose as the carbon source.

RNA dot blotting

Total RNA was prepared by extraction with hot acidic phenol following the protocol described in **Short Protocols In Molecular Biology**, Fourth Edition. Total RNA (4 μg or 0.4 μg) was dot-blotted onto nylon membranes (Amersham Pharmacia Biotech) and UV-crosslinked. Blotted membranes were hybridized with a ^{32}P-radiolabeled *RAD52* DNA probe or a *TDH4* DNA probe. Hybridization probes were labeled with [α-^{32}P] dCTP using random primer DNA labeling kit (Invitrogen). Hybridization was performed in 0.5M NaH_2PO_4/Na_2HPO_4 pH7.2, 7% SDS, 10 mM EDTA, at 60°C, according to Church and Gilbert [16]. The membrane was exposed to phosphorescent screens and the images were scanned with Phosphorimager (Molecular Dynamics). The signals were quantified using ImageQuant software (Molecular Dynamics).

RT-PCR

cDNA was synthesized using Superscript II reverse transcriptase (Invitrogen). Total RNA (5 μg) was mixed with 12.5 pmole of a *RAD52* specific primer (5'-TTTTCACCAGGTTCTTCGTCG-3') and 20 nmole of dNTPs. The mixture was incubated at 65°C for 5 min and quickly chilled on ice. Following addition of First Strand buffer (Invitrogen) and DTT (Invitrogen), the mixture was incubated at 42°C for 2 min. Reverse transcriptase was added to half of the mixture, 1μl of DEPC-treated H_2O was added to the remaining half as the control. cDNA was synthesized at 42°C for 50 min. The cDNA was then amplified using a pair of *RAD52* specific primers (5'-GAGAAGAAGCCCGTTTTC-3' and 5'-CGGGTATTGTTGTTGTTC-3") and Taq polymerase (Promega).

Primer extension

An oligonucleotide probe (5'-TTACTCTCCAACCTTCG-3') was labeled with [γ-^{32}P] dATP using T4 polynucleotide kinase (New England Biolabs). Total RNA (12 μg) was hybridized to the radiolabeled probe in 150 mM KCl, 10 mM Tris-HCl pH 8.3, 1 mM EDTA at 65°C for 90 min. Extension reaction was carried out in reaction buffer containing 20 mM Tris-HCl pH 8.3, 10 mM $MgCl_2$, 5 mM DTT, 0.15 mg/ml actinomycin D, 0.15 mM dNTPs, 5 U of AMV reverse transcriptase (Invitrogen). The reaction was performed at 42°C for 60 min. Reaction mix was then digested with RNase and extracted with phenol/chloroform and precipitated with ethanol. The reaction products were resolved in a 6% PAGE/7 M Urea gel. The gel was dried on a vacuum gel drier at 80°C for 1 hour and exposed to phosphorescent screens and scanned with Phosphorimager (Molecular Dynamics).

RESULTS

Determining the translation initiation site(s) of the Rad52 protein

There are five in-frame ATG triplets at the 5' end of the *RAD52* genomic sequence. Recent studies suggest that the third ATG (99 bp downstream from the first ATG) is likely to be the translation initiation codon [5, 14]. I examined the possible translation initiation sites using a more systematic approach. I mutated four of the five ATG triplets to ATC in different combinations, keeping a single ATG for translation initiation. These *RAD52* variants were named *RAD52ATG1, 2, 3, 5*, indicating the presence of the corresponding ATG (Figure 2-1A). Low copy plasmids carrying these variants of *RAD52* controlled by the endogenous promoter were tested for their ability to

complement a *rad52Δ* strain using sensitivity to the DNA damaging agent MMS as an assay (Figure 2-1B). Compared to the wild type strain (JP166) expressing the endogenous *RAD52*, the *rad52Δ* strain, JP166L1, is at least 10,000 times more sensitive. Neither *RAD52ATG1* nor *RAD52ATG2* could complement *rad52Δ*. In contrast, the plasmid carrying wild type *RAD52*, *RAD52ATG3*, or *RAD52ATG5* fully complemented the sensitive phenotype of *rad52Δ*. To confirm that the Rad52 protein initiated from the fifth ATG is functional, we tested *rad52d103-120*, a *rad52* mutant lacking the six amino acids downstream of the third ATG to the fifth ATG (Figure 2-1A). This deletion mutant indeed complemented the MMS sensitive phenotype of *rad52Δ* cells (Figure 2-1C). I also examined the level of Rad52 protein expressed by these variants. Consistent with the results of the complementation test, Rad52 protein in *RAD52ATG3* and *RAD52ATG5* containing cells was expressed at a level similar to that of endogenous Rad52 in the wild type strain JP166, while no Rad52 protein was detected in *RAD52ATG1* and *RAD52ATG2* expressing cells (Figure 2-1D). To examine whether the ATG to ATC mutations in *RAD52ATG1* or *RAD52ATG2* impaired transcription of *RAD52*, RT-PCR was performed. *RAD52* transcripts existed in both *RAD52ATG1* and *RAD52ATG2* expressing cells (Figure 2-1E). Next I measured the *RAD52* mRNA level. *RAD52* mRNA was transcribed at similar levels from all the variants tested as shown by RNA dot blotting analysis (Figure 2-1F), indicating that the absence of Rad52 in *RAD52ATG1* and *RAD52ATG2* expressing cells is likely caused by a posttranscriptional defect. Taken together, these results indicate that efficient complementation of *rad52Δ* can be achieved by exogenous expression of the *RAD52* gene expressed under the control of the endogenous promoter. However, it appears that only the third or fifth, and possibly the

fourth ATG, can be used as translation initiation sites *in vivo*. The first and the second ATG do not serve as translation initiation sites. The failure of *RAD52ATG1* and *RAD52ATG2* to complement the MMS sensitivity of *rad52Δ* is due to a lack of Rad52 protein expression as a result of posttranscriptional defects.

Overexpression of *RAD52* has a strong negative effect on DNA damage repair induced by MMS

Both *in vivo* and *in vitro* data suggest that cells are sensitive to changes in the level of Rad52, especially under DNA damaging conditions [6-8]. To directly examine the effect of *RAD52* overexpression on DNA damage repair, I cloned the coding sequence downstream of the galactose-inducible *GAL1* promoter, which results in high level of expression. Since Rad52 proteins initiated from the third and fifth ATG were both found to be functional, I engineered constructs starting from the third or the fifth ATG into the pRSG415 vector, designated as GAL1-RAD52F3 and GAL1-RAD52F5, respectively (Figure 2-2A). Previous studies on the effect of Rad52 overexpression utilized constructs containing *RAD52* starting from the first ATG [9, 10]. Thus, I also tested a similar construct, GAL1-RAD52F1 (Figure 2-2A), as a control and to compare my results with the previous studies. These three constructs were tested for their ability to complement the MMS sensitive phenotype of *rad52Δ* by spot assays. Surprisingly, *RAD52* expressed from the *GAL1* promoter induced phenotypes different from those of genes expressed from the endogenous promoter. Expression of GAL1-RAD52F3 or GAL1-RAD52F5 did not complement the MMS sensitivity of *rad52Δ*, while that of GAL1-RAD52F1 restored the MMS resistance of *rad52Δ* cells to a level similar to that of the wild type strain JP166 expressing the chromosomal copy of *RAD52* (Figure 2-2B).

Since the GAL1-RAD52F3 construct contains three candidates for translation initiation codon, ATG 3, 4 and 5, I mutated the forth and fifth ATG to ATC, and tested this new construct named GAL1-RAD52F3ATG3 (Figure 2-2A). Similar to the result with GAL1-RAD52F3, this construct did not complement the MMS sensitive phenotype of *rad52Δ* (Figure 2-2C). In the absence of MMS, cells expressing these constructs showed no apparent defect in growth compared to wild type cells (Figure 2-2B).

The observed phenotypic differences between different *RAD52* constructs prompted me to investigate the expression level of *RAD52*. The *RAD52* RNA level was increased to similar high levels (37-89 fold) in GAL1-RAD52F1, GAL1-RAD52F3 or GAL1-RAD52F5 expressing cells compared to that of wild type cells expressing the genomic *RAD52* (Figure 2-3A). The level of Rad52 protein expressed by GAL1-RAD52F3 or GAL1-RAD52F5 was also increased significantly compared to that of the wild type strain (Figure 2-3B). In contrast, Rad52 protein in GAL1-RAD52F1 expressing cells was increased less than 5 fold (Figure 2-3B). A quantitative comparison revealed a 40-fold increase in Rad52 level expressed from GAL1-RAD52F3 compared to that expressed from GAL1-RAD52F1 (Figure 2-3C). To investigate the possible cause for the relatively low level of Rad52 protein expressed from GAL1-RAD52F1, a primer extension experiment was performed to examine the *RAD52* transcripts. Most of the overexpressed transcripts were initiated upstream of the first ATG (Figure 2-3D). Only a minor species was transcribed from the natural initiation site, i.e. downstream of the second but upstream of the third ATG, for the endogenous *RAD52* transcripts in the wild type cells (Figure 2-3D). This result suggests that the relatively low level of Rad52 protein expression by GAL1-RAD52F1 is not due to defects in transcription initiation or

decreased transcript stability. It appears that the additional sequences at the 5' of *RAD52* mRNA transcribed from GAL1-RAD52F1 are deleterious for protein accumulation. The existence of the longer *RAD52* transcripts in GAL1-RAD52F1 suggests possible utilization of the first ATG for translation initiation. I constructed GAL1-RAD52F1ATG1 by mutating all but the first ATG to ATC in GAL1-RAD52F1 (Figure 2-2A). Unexpectedly, GAL1-RAD52F1ATG1 failed to complement *rad52Δ* (Figure 2-3E), and no Rad52 protein could be detected (Figure 2-3F). These results suggest that the first ATG can not initiate translation, and Rad52 protein expressed by GAL1-RAD52F1 is translated from a downstream ATG.

In summary, removal of the sequence between the first and the third ATG greatly increases Rad52 protein expression level controlled by the *GAL1* promoter. A high level of Rad52 expression has a strong negative effect on DNA damage repair induced by MMS.

Overexpression of *RAD51* suppresses the negative effect of *RAD52* overexpression

Since Rad52 physically interacts with other components of the homologous recombination repair pathway, including Rad51, Rad59 and RPA, the negative effect of Rad52 overexpression may be due to the sequestration of these interaction partners. To test this hypothesis, I co-overexpressed Rad52 with Rad51 or Rad59 to examine whether the negative effect of Rad52 overexpression could be at least partially rescued (Figure 2-4A). The fragments containing the *GAL1* promoter, *RAD52* and the *CYC1* terminator from GAL1-RAD52F1, GAL1-RAD52F3 and GAL1-RAD52F5 were subcloned into pRS414 to create GAL1b-RAD52F1, GAL1b-RAD52F3 and GAL1b-RAD52F5, respectively. Overexpression of Rad51 or Rad59 by themselves could not rescue the

MMS sensitive phenotype of *rad52Δ* cells, indicating the essential role of Rad52 in DNA damage repair. Overexpression of Rad51 or Rad59 showed no effect in GAL1b-RAD52F1 expressing cells, suggesting that Rad51 or Rad59 overexpression has no negative effect on DNA damage repair. Overexpression of Rad51 almost completely rescued the MMS sensitive phenotype of cells expressing GAL1b-RAD52F3 or GAL1b-RAD52F5. In contrast, overexpression of Rad59 had no effect. This is not due to a lack of Rad59 expression or malfunction, since the same Rad59 construct can complement the MMS sensitive phenotype of a *rad59Δ* strain (Figure 2-4B). I also confirmed high level of Rad52 expression by GAL1b-RAD52F3 and GAL1b-RAD52F5 in Rad51 overexpressing cells (Figure 2-4C). Thus, the above results suggest that the negative effect of Rad52 overexpression is likely due to the sequestration of Rad51.

Overexpression of a *rad52* mutant with a specific defect in interaction with Rad51 has a greatly reduced defect in DNA damage repair.

The ability of overexpressed Rad51 to rescue the defect in DNA damage repair as a result of Rad52 overexpression suggests that the Rad51-dependent pathway of homologous recombination is affected in GAL1-RAD52F3 or GAL1-RAD52F5 expressing cells. I tested this possibility in a more direct approach by examining the effect of overexpressing *rad52d409-412*, a *rad52* mutant that has a specific defect in interaction with Rad51 [17]. In contrast to the highly sensitive phenotype of GAL1-RAD52F3, *rad52Δ* cells expressing GAL1-RAD52F3d409-412 showed only a slightly increased MMS sensitivity (figure 2-5A). Cells containing GAL1-RAD52F3 or GAL1-RAD52F3d409-412 express similar level of Rad52 (figure2-5B). Therefore,

overexpression of a Rad52 mutant protein with a specific defect in Rad52-Rad51 interaction has a greatly reduced negative effect on DNA damage repair.

RAD52 overexpression affects a _RAD51_-independent DNA damage repair pathway(s)

I also examined whether other DNA repair pathways are affected by Rad52 overexpression. If a Rad51-dependent pathway is the major repair pathway for the damages induced by MMS, the effects on other pathways might not be readily detected in the presence of Rad51. Therefore, I examined GAL1-RAD52F3 and GAL1-RAD52F5 in a *rad51Δ* strain, JP166W1. As shown in Figure 2-6A, *rad51Δ* cells were highly sensitive to 0.005% MMS treatment (the same concentration used in earlier experiments). GAL1-RAD52F3 and GAL1-RAD52F5 did not significantly alter the MMS sensitivity of *rad51Δ* cells. Therefore, we reduced the MMS concentration to 0.001%, under which condition the sensitivity of the *rad51Δ* cells was significantly reduced (figure 2-6B), whereas *rad52Δ* cells were still highly sensitive (data not shown). Under this condition, *rad51Δ* cells expressing GAL1-RAD52F3 or GAL1-RAD52F5 did show a significantly higher MMS sensitivity than cells containing the control vector. Thus, these results suggest that Rad52 overexpression has a negative effect on a RAD51-independent repair pathway(s).

Since recombination repair pathways in yeast consist of the Rad51- and the Rad59-dependent pathways, we examined whether the negative effect observed in *rad51Δ* cells was due to an impaired Rad59-dependent pathway. Rad52 and Rad59 were co-overexpressed in a *rad52Δ rad51Δ* strain BY20031 (Figure 2-6D). Overexpression of Rad59 alone did not alter cells' ability to repair DNA damages induced by MMS. Overexpression of Rad52 alone from GAL1b-RAD52F3 or GAL1b-RAD52F5 resulted in

a MMS sensitive phenotype similar to that shown in Figure 2-6B. Co-overexpression of Rad52 with Rad59 did not restore the MMS resistance (Figure 2-6D). Thus, the additional negative effect of Rad52 overexpression observed in *rad51Δ* cells is not likely caused by a defective Rad59-dependent pathway. It is possible that other DNA damage repair pathways are affected when Rad52 is overexpressed.

DISCUSSION

In this study, I demonstrated that overexpression of Rad52 has a specific negative effect on DNA damage repair induced in response to MMS. First, cell growth under DNA damaging conditions is negatively affected by Rad52 overexpression. Second, this negative effect can be suppressed by Rad51 overexpression, but not Rad59 overexpression. This study provides *in vivo* evidence that the ratio between Rad52 and Rad51 is critical in homologous recombination mediated DNA damage repair. In addition, our results also suggest that Rad52 overexpression affects a *RAD51*-independent DNA damage repair pathway(s). I also tested possible translation initiation sites of Rad52. Among the five in-frame ATGs at the 5' end of the *RAD52* sequence, the third, fourth and fifth ATG can be used as a translation start codon. I also demonstrated that Rad52 translated from the fifth ATG is as competent as that translated from the third ATG in DNA damage repair induced by MMS.

Translation initiation site(s) of Rad52

The existence of five in-frame ATG triplets at the 5' of the *RAD52* sequence has caused confusion as to which of these serves as *in vivo* translation initiation site(s). Previous studies have suggested that the first and the second ATG are not used to initiate

translation *in vivo* [5, 14]. However, which of the remaining three ATGs is in fact used for translation initiation is unclear. By mutating four of the five ATGs in different combinations and keeping only one intact, I examined Rad52 translated from a certain ATG under the control of its own promoter. When only the third or the fifth ATG is available to initiate translation, Rad52 protein can be expressed at a level similar to the endogenous protein in wild type cells (Figure 2-1D). More importantly, Rad52 translated from the third and the fifth ATG have same ability to fully complement the MMS sensitivity of *rad52Δ* (Figure 2-1B). However, when only the first or the second ATG is intact, no Rad52 protein can be detected (Figure 2-1D). This is consistent with the result of an S1 nuclease protection analysis, which reveals that the 5' end of a major *RAD52* transcript is located between the second and the third ATG [14].

A number of reports studied Rad52 by placing the coding sequence from the first ATG under the control of a heterologous promoter. It is unclear whether the *RAD52* mRNA start site was altered under those conditions, hence producing Rad52 with additional 5' sequences. When the entire *RAD52* coding sequence is placed under the control of the *GAL1* promoter, the majority of *RAD52* mRNA is transcribed from upstream of the first ATG (Figure 2-3D). However, the first ATG is not likely to initiate translation as demonstrated by the lack of Rad52 expression from GAL1-RAD52F1ATG1 (Figure 2-3F), which only has the first ATG available for translation initiation. Therefore, although *RAD52* mRNA can be transcribed from upstream of the first ATG, Rad52 protein translation is still initiated from a downstream ATG. Furthermore, it appears that the additional sequences at the 5' end of *RAD52* mRNA are deleterious for protein accumulation. Although expression from GAL1-RAD52F1 results

in a ~90-fold increase in *RAD52* mRNA compared to the endogenous level (Figure2-3A), there is a less than 5-fold increase in Rad52 protein level (Figure 2-3B). In contrast, removal of the sequence between the first and the third ATG leads to at least a 40-fold increase in Rad52 protein level (Figure 2-3C). It is likely that the addition sequences transcribed from GAL1-RAD52F1 block the protein translation machinery.

Effects of *RAD52* overexpression on DNA damage repair

Rad52 is the central player in homologous recombination. It is involved in multiple direct protein-protein interactions, including self-association and interactions with RPA, Rad51, and Rad59 [18-21]. Changes in cellular concentration of components involved in hetero-multimeric complexes will result in imbalance among the components. Such imbalance often leads to distinct phenotypes [22]. Consistent with this idea, Rad52 should be kept at a level ~1/10 of the amount of Rad51 to achieve its maximal mediator function in strand exchange reactions [7]. In vivo, Rad52 protein level is tightly controlled by both transcriptional and posttranslational regulation [6]. When overproduced, Rad52 exerts a negative effect on DNA damage repair (Figure 2-2B). In fact, a similar negative effect has been observed for Rad54 overexpression [23]. The negative effect of Rad52 overexpression results mainly from sequestration of Rad51, since overexpression of Rad51 can completely suppress such effect (Figure 2-4A). Indeed, overexpression of *rad52d409-412*, which is defective in interaction with Rad51, displays a greatly reduced effect on DNA damage repair (Figure 2-5A). It is possible that when overexpressed, *rad52d409-412* may have residual Rad51-binding activity which enables it to mediate Rad51 function. This could account for its relative resistance to MMS treatment.

The negative effect of overexpression of Rad52 observed in our study is not caused by malfunction of the Rad52 protein. Overexpression of Rad51 can not rescue the MMS sensitive phenotype of *rad52Δ* cells (Figure 2-4A). Only when Rad52 and Rad51 are overexrepssed simultaneously, is MMS sensitivity of *rad52Δ* rescued (Figure 2-4A), indicating that Rad52 expressed from GAL1-RAD52F3 or GAL1-RAD52F5 is functional.

The strong negative effect of *RAD52* overexpression demonstrated by our results does not agree with the previous observation that overexpression of *RAD52* has no appreciable effect on DNA damage repair [10]. In the previous study, the *RAD52* overexpression construct was made by placing *RAD52* gene from the first ATG under the control of the *ENO1* promoter. Although the authors showed that the RNA level of *RAD52* was 10-fold higher than that of wild type cells, they did not examine the steady state protein level. In fact, the sequence between the first ATG and the third ATG seems to block protein translation (discussed above). In addition, this sequence appears to contain a competent promoter. GAL1-RAD52F1 can complement the MMS sensitivity of *rad52Δ* in non-inducing medium (Figure 2-7). pRS415RAD52B, a *RAD52* construct with neither a heterologous promoter nor the genomic sequence upstream of the first ATG, can also complement the MMS sensitivity of *rad52Δ* cells (Figure 2-8). Therefore, it is possible that the expression of Rad52 by GAL1-RAD52F1 is driven by a potential control element within the sequence between the first and the third ATG. Indeed, the primer extension study revealed a *RAD52* mRNA species with a 5' end identical to that of the endogenous *RAD52* transcript (Figure 2-3D). It is highly likely that Rad52

translated from this species accounts for the MMS resistance of the *rad52Δ* cells expressing GAL1-RAD52F1.

Significance of the ratio between Rad52 and Rad51 in DNA damage repair *in vivo*

Recent studies on Rad51 and its partner protein Brca2 suggest that the site in Rad51 involved in Rad52 binding is the same site for Rad51-Rad51 interaction. Human Rad51 contains a conserved motif (85-GFTTATE-91, a comparable region of ScRad51 has a sequence of 143-GFVTAAD-149) which serves as the interface for Rad51 oligomerization [24, 25]. Mutation of this sequence prevents DNA damage-induced Rad51 foci formation [24]. This motif was initially recognized in the BRC repeats of Brca2, a Rad51 interacting protein. X-ray structure study and mutational analysis have shown that such a motif in Brca2 is indeed responsible for Rad51 binding [24, 25]. Interestingly, the C-terminus of ScRad52 which interacts with Rad51 contains a similar sequence 315-TFVTAKA-321 [25]. Indeed, a *rad52* mutant (*rad52K353E*), which is defective in Rad51 interaction, has a single amino acid substitution in this motif [26].

The sharing of a single binding site of Rad51 for two different protein interactions would explain the inhibition of Rad51-mediated DNA damage repair by excessive Rad52 and provide a plausible mechanism for Rad51 action. The rate limiting step of Rad51 nucleoprotein filament assembly is the nucleation step, after which the filament elongates rapidly [27]. The Rad52-Rad51 interaction, as well as Brca2-Rad51 interaction, recruits Rad51 to DNA damage sites [25, 28]. Rad52 then facilitates initial RPA displacement by Rad51 [27]. After nucleation, the free form of Rad51 can interact with Rad51 and with DNA to form Rad51-DNA nucleoprotein filament. However, excess amount of Rad51 interacting protein would exclude Rad51 from oligomerization during filament formation.

Consistent with this model, Rad51 is of higher cellular abundance than Rad52. Since they form stable stoichiometric complexes as demonstrated in co-immunoprecipitation experiments, most of the cellular Rad51 is free from interaction with Rad52 [7, 8].

Effects of *RAD52* overexpression on *RAD51*-independent DNA damage repair pathways

Rad51-dependent and Rad59-dependent pathways are the major pathways in homologous recombination repair in *S. cerevisiae* (reviewed in [2]. *rad51Δ rad59Δ* double mutants display similar phenotypes as *rad52Δ* mutants [2, 29]. However, the additional DNA damage repair defect observed in *rad51Δ* strain from Rad52 overexpression is not likely due to an impaired Rad59-dependent pathway, since overexpression of *RAD59* can not rescue the defect (Figure 2-6D). Nucleotide excision repair and base pair excision repair can repair DNA damages induced by MMS [30]. It is possible that the additional negative effect is mediated by nonspecific association of overexpressed Rad52 with protein components involved in other DNA damage repair pathways. Alternatively, DNA lesions caused by MMS are channeled to repair pathways which normally do not function in repairing these damages when Rad51-dependent pathway is functional. Therefore, this effect may only be observed in the absence of Rad51.

SUMMARY

In summary, the present study has demonstrated that overexpression of Rad52 has a strong negative effect on DNA damage repair induced by MMS. This effect is caused mainly by sequestration of Rad51 by excess amount of Rad52. Overexpression of Rad52

also has a negative effect on a Rad51-independent DNA damage repair pathway(s). This effect appears to be nonspecific. In addition, the experiments reveal that the third, fifth, and possibly the fourth ATG at the 5' end of *RAD52* can be used as a translation initiation codon *in vivo*. The sequences between the first and the third ATG appears to contain a promoter, and these sequences have a strong negative effect on Rad52 protein expression controlled by a heterologous *GAL1* promoter.

APPENDIX 2: FIGURES AND TABLES FOR CHAPTER 2

Table 2-1. *S. cerevisiae* strains used in this study

strain	Genotype
JP166 [a]	*MATa his3Δ leu2Δ ura3Δ tlc1Δ pRS316TLC1*
JP166L1 [b]	*MATa his3Δ leu2Δ ura3Δ rad52Δ::HIS3 tlc1Δ pRS316TLC1*
JP166W1 [b]	*MATa his3Δ leu2Δ ura3Δ rad51Δ::HIS3 tlc1Δ pRS316TLC1*
JP166W2 [b]	*MATa his3Δ leu2Δ ura3Δ rad59Δ::HIS3 tlc1Δ pRS316TLC1*
BY4735 [c]	*MATα ade2Δ::hisG his3Δ200 leu2Δ0 met15Δ0 trp1Δ63 Ura3Δ0*
BY4735L1 [d]	*MATα ade2Δ::hisG his3Δ200 leu2Δ0 met15Δ0 trp1Δ63 Ura3Δ0 rad52Δ::HIS3*
BY20031 [d]	*MATα ade2Δ::hisG his3Δ200 leu2Δ0 met15Δ0 trp1Δ63 Ura3Δ0 rad52Δ::HIS3 rad51Δ::KANMX6 tlc1Δ::Met15 pRS316TLC1*

[a] From Dr. John Prescott (University of California, San Francisco)

[b] Derivative of JP166; this study

[c] Obtained from ATCC

[d] Derivative of BY4735; this study

Table 2-2. Constructs used in this study

Plasmid	Description
pRS415	A *CEN* shuttle vector with a *LEU2* marker
pRS414	A *CEN* shuttle vector with a *TRP1* marker
pRSG415	*GAL1* promoter and *CYC1* terminator are inserted into pRS415
pRSG414	*GAL1* promoter and *CYC1* terminator are inserted into pRS414
pRSG415RAD52F1 (GAL1-RAD52F1)	*RAD52* gene from the first ATG to stop codon is cloned into pRSG415, placed under the control of the *GAL1* promoter
pRSG415RAD52 F1ATG1 (GAL1-RAD52F1ATG1)	The second, third, fourth and fifth ATG were mutated to ATC in GAL1-RAD52F1
pRSG415RAD52F3 (GAL1-RAD52F3)	*RAD52* gene from the third ATG to stop codon is cloned into pRSG415, placed under the control of the *GAL1* promoter
pRSG415RAD52F3M 38-40I (GAL1-RAD52F3ATG3)	The fourth and the fifth ATG in GAL1-RAD52F3 are mutated to ATC
pRSG415RAD52F5 (GAL1-RAD52F5)	*RAD52* gene from the fifth ATG to stop codon is cloned into pRSG415, placed under the control of the *GAL1* promoter
pRSG414RAD52 F1 (GAL1b-RAD52F1)	*RAD52* gene from the first ATG to stop codon is cloned into pRSG414, placed under the control of the *GAL1* promoter
pRSG414RAD52F3 (GAL1b-RAD52F3)	*RAD52* gene from the third ATG to stop codon is cloned into pRSG414, placed under the control of the *GAL1* promoter
pRSG414RAD52F5 (GAL1b-RAD52F5)	*RAD52* gene from the fifth ATG to stop codon is cloned into pRSG414, placed under the control of the *GAL1* promoter

Table 2-2. Constructs used in this study (Continued)

pRSG415RAD51 (GAL1-RAD51)	*RAD51* gene is placed under the control of *GAL1* promoter
pRSG415RAD59 (GAL1-RAD59)	*RAD59* gene is placed under the control of *GAL1* promoter
pRS415RAD52B	*RAD52* gene from the first ATG to stop codon followed by *CYC1* terminator is cloned into pRS415
pRS415RAD52 (RAD52)	The *Sal*I fragment containing genomic copy of *RAD52* gene (from ~1kb upstream to ~0.8 kb downstream) {Adzuma, 1984 #2} is cloned into pRS415
pRS415RAD52d103-120 (RAD52d103-120)	The 6 amino acids from downstream of the third ATG to the fifth ATG are deleted from pRS415RAD52
pRS415RAD52ATG1 (RAD52ATG1)	pRS415RAD52 with only the first ATG kept intact, all others are mutated to ATC
pRS415RAD52ATG3 (RAD52ATG3)	pRS415RAD52 with only the third ATG kept intact, all others are mutated to ATC
pRS415RAD52ATG5 (RAD52ATG5)	pRS415RAD52 with only the fifth ATG kept intact, all others are mutated to ATC

Figure 2-1 Analysis of the MMS sensitivity of *rad52Δ* cells expressing *RAD52* variants containing a single translation initiation site and controlled by *RAD52* genomic promoter

A. Schematic representation of *RAD52* variants

Open circles represent ATG triplets. Closed circles represent ATC triplets. The *Sal*I genomic fragment containing *RAD52* coding sequence and its own promoter was cloned into the pRS415 vector. Four out of the five 5'-terminal in-frame ATG triplets were mutated to ATC to leave a single ATG for translation initiation. The variants were named *RAD52ATG1, 2, 3* or *5*, corresponding to the individual ATG triplets. *rad52d103-120* was constructed by deleting the six amino acids downstream of the third ATG to the fifth ATG. The deletion is indicated as a dashed line. The arrows indicate the transcription start sites based on previous reports [5, 14].

B. MMS sensitivity of *rad52Δ* cells expressing *RAD52, RAD52ATG1, RAD52ATG2, RAD52ATG3, or RAD52ATG5*

The wild type strain JP166 expressing genomic *RAD52* and the *rad52Δ* strain JP166L1 expressing *RAD52* variants or the control vector were cultivated in SC-Ura-Leu medium containing 2% glucose to mid-log phase. 10-fold serial dilutions containing 10^6 to 10 cells were spotted on SC-Ura-Leu solid medium containing 2% glucose with or without 0.005% MMS.

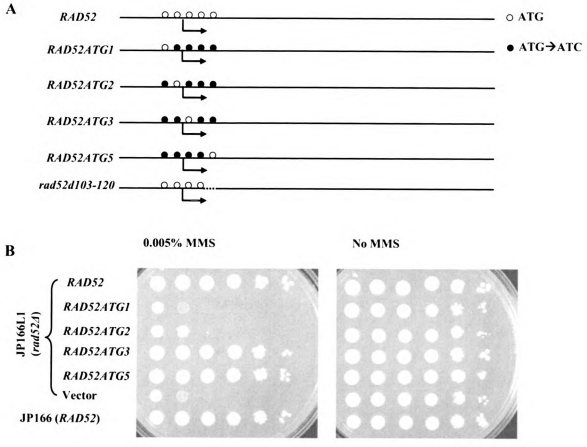
A
RAD52
RAD52ATG1
RAD52ATG2
RAD52ATG3
RAD52ATG5
rad52d103-120
○ ATG
● ATG→ATC
B
0.005% MMS
No MMS
JP166L1 (rad52-1)
RAD52
RAD52ATG1
RAD52ATG2
RAD52ATG3
RAD52ATG5
Vector
JP166 (RAD52)

Figure 2-1

C. Complementation of the MMS sensitive phenotype of *rad52Δ* cells with *rad52d103-120*

rad52103-120 expresses a *rad52* gene with a deletion of nucleotide 103-120 (encoding the 6 amino acids from downstream of the third ATG to the fifth ATG) and under the control of *RAD52* genomic promoter. The wild type strain JP166 expressing genomic *RAD52* and the *rad52Δ* strain JP166L1 expressing *RAD52ATG5* or *rad52d103-120* were cultivated in SC-Ura-Leu medium containing 2% glucose to mid-log phase. 10-fold serial dilutions containing 10^6 to 10 cells were spotted on SC-Ura-Leu solid medium containing 2% glucose with or without 0.005% MMS.

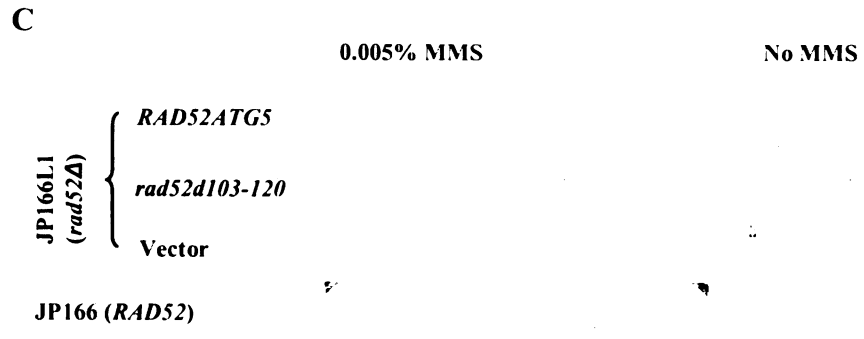
C
0.005% MMS
No MMS
JP166L1
(rad52Δ)
RAD52ATG5
rad52d103-120
Vector
JP166 (RAD52)

Figure 2-1

D. Analysis of Rad52 protein expression in *rad52Δ* cells expressing *RAD52ATG1*, *RAD52ATG2*, *RAD52ATG3*, *or RAD52ATG5*

Proteins were extracted from cells cultivated in medium containing 2% glucose. The Western blot was probed with an anti-Rad52 antibody, after which the membrane was stripped and probed with an anti-glucose-6-phosphate dehydrogenase (G-6-PDH) antibody.

D

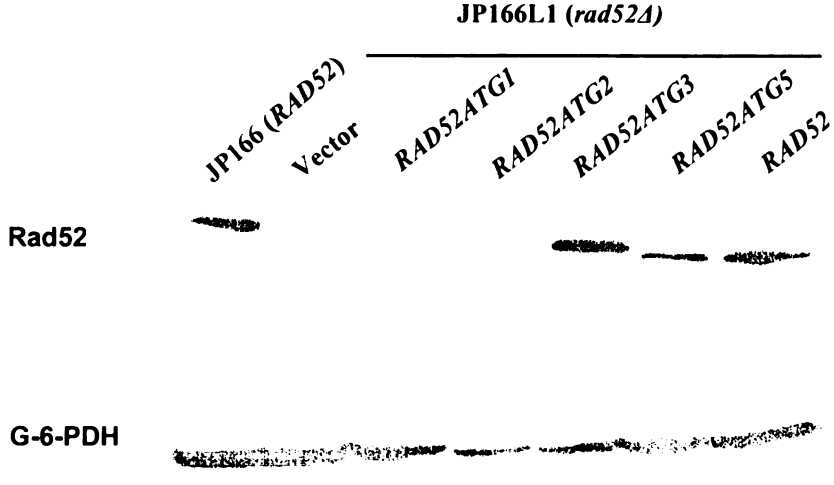
JP166L1 (rad52Δ)
JP166 (RAD52)
Vector
RAD52ATG1
RAD52ATG2
RAD52ATG3
RAD52ATG5
RAD52
Rad52
G-6-PDH

Figure 2-1

E. Analysis of *RAD52* mRNA in *rad52A* cells expressing *RAD52ATG1* or *RAD52ATG2*

Total RNA from the wild type strain JP166 or the *rad52A* strain JP166L1 expressing *RAD52ATG1*, *RAD52ATG2* or the control vector was subjected to RT-PCR. cDNA was synthesized using a *RAD52* specific primer, and then amplified by a pair of *RAD52* specific primers. The expected RT-PCR product is 570 bp in length.

E

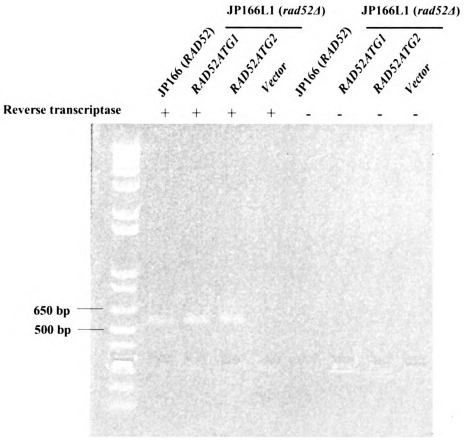
JP166L1 (rad52Δ)
JP166L1 (rad52Δ)
JP166 (RAD52)
RAD52ATG1
RAD52ATG2
Vector
JP166 (RAD52)
RAD52ATG1
RAD52ATG2
Vector
Reverse transcriptase
+ + + + - - - -
650 bp
500 bp

Figure 2-1

F. *RAD52* mRNA level in *rad52A* cells expressing *RAD52ATG1*, *RAD52ATG2*, *RAD52ATG3 or RAD52ATG5*

4 μg of total RNA was dot-blotted and probed with *RAD52* DNA. At the same time, 0.4 μg of total RNA was dot-blotted and probed with *TDH4* DNA as the loading control. The ratio of *RAD52* to *TDH4* counts was calculated and compared to that of JP166, which was standardized as 1.

F

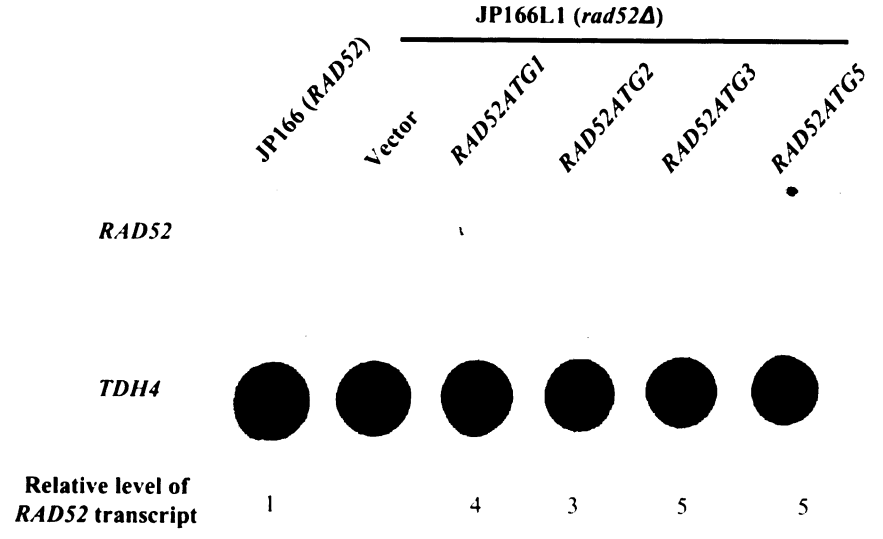
JP166L1 (rad52Δ)
JP166 (RAD52)
Vector
RAD52ATG1
RAD52ATG2
RAD52ATG3
RAD52ATG5
RAD52
TDH4
Relative level of RAD52 transcript
1
4
3
5
5

Figure 2-1

Figure 2-2 Analysis of the MMS sensitivity of *rad52Δ* cells expressing different *RAD52* constructs controlled by the galactose-inducible *GAL1* promoter

A. Schematic representation of *RAD52* constructs for galactose-inducible overexpression

Open circles represent ATG triplets. Closed circles represent ATG→ATC mutations. The *RAD52* coding sequence starting from the first ATG (RAD52F1), the third ATG (RAD52F3) or the fifth ATG (RAD52F5) was cloned into a pRSG415 vector, and placed downstream of the *GAL1* promoter. GAL1-RAD52F1ATG1was constructed by mutating the second, third, forth and fifth ATG in GAL1-RAD53F1. GAL1-RAD53F3ATG3 was constructed by mutating the forth and fifth ATG in GAL1-RAD53F3. Rad52 protein expression was induced by addition of galactose into medium at 0.05%.

B. MMS sensitivity of a *rad52Δ* strain expressing GAL1-RAD52F1, GAL1-RAD52F3, or GAL1-RAD52F5

The wild type strain JP166 and the rad52Δ strain JP166L1 expressing GAL1-RAD52F1, GAL1-RAD52F3, GAL1-RAD52F5, or the control vector, were cultivated in SC-Ura-Leu medium containing 2% raffinose to mid-log phase. 10-fold serial dilutions containing 106 to 10 cells of each strain were spotted on SC-Ura-Leu plates containing 2% raffinose and 0.05% galactose with or without 0.005% MMS.

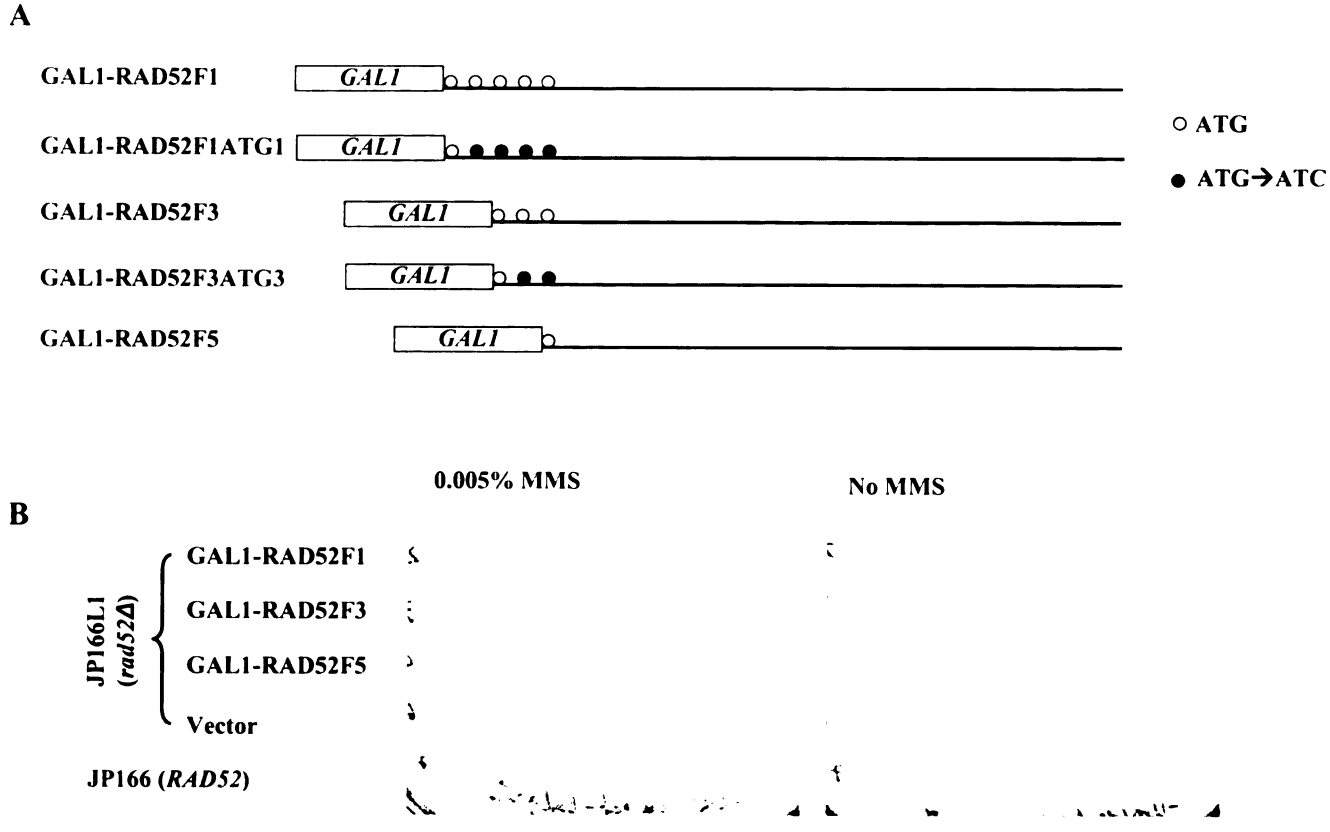
A
GAL1-RAD52F1
GAL1
GAL1-RAD52F1ATG1
GAL1
GAL1-RAD52F3
GAL1
GAL1-RAD52F3ATG3
GAL1
GAL1-RAD52F5
GAL1
○ ATG
● ATG→ATC
B
0.005% MMS
No MMS
JP166L1
(rad52Δ)
GAL1-RAD52F1
GAL1-RAD52F3
GAL1-RAD52F5
Vector
JP166 (RAD52)

Figure 2-2

C. MMS sensitivity of a *rad52Δ* strain expressing GAL1-RAD52F3ATG3

GAL1-RAD52F3ATG3 expresses the *RAD52* gene starting from the third ATG, and the forth and the fifth ATG are mutated to ATC. JP166L1 expressing GAL1-RAD52F3, GAL1-RAD52F3ATG3, or the control vector, were cultivated in SC-Ura-Leu medium containing 2% raffinose to mid-log phase. Spot assays were performed as described in ***B***.

C

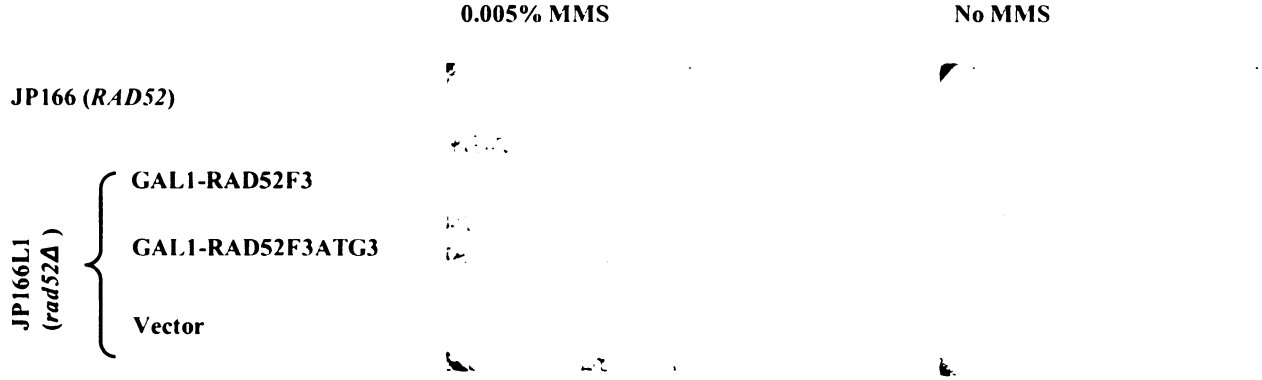
0.005% MMS
No MMS
JP166 (RAD52)
JP166L1 (rad52Δ)
GAL1-RAD52F3
GAL1-RAD52F3ATG3
Vector

Figure 2-2

Figure 2-3 Analysis of *RAD52* expression level in *rad52*Δ cells expressing different *RAD52* constructs controlled by the *GAL1* promoter

A. *RAD52* mRNA level in *rad52A* cells expressing GAL1-RAD52F1, GAL1-RAD52F3 or GAL1-RAD52F5

Total RNA was extracted from cells cultivated in medium containing 2% raffinose and 0.05% galactose for induction of *RAD52* expression. 4 μg of total RNA was dot-blotted and probed with *RAD52* DNA. At the same time, 0.4 μg of total RNA was dot-blotted and probed with *TDH4* DNA. . The ratio of *RAD52* to *TDH4* counts was calculated and compared to that of JP166, which was standardized as 1.

A

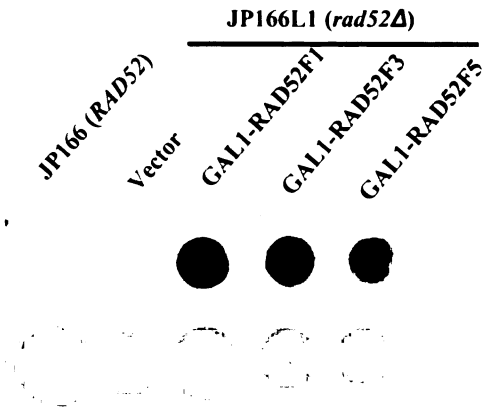

Relative level of *RAD52* transcript	**1**	**89**	**59**	**37**

Figure 2-3

B. Comparison of the steady state protein level of Rad52 in *rad52Δ* cells expressing GAL1-RAD52F1, GAL1-RAD52F3 and GAL1-RAD52F5

Proteins were extracted from cells cultivated in medium containing 2% raffinose and 0.05% galactose. JP166 was cultivated in media containing 2% glucose. The Western blot was probed with an anti-Rad52 antibody, after which the membrane was stripped and probed with an anti-G-6-PDH antibody.

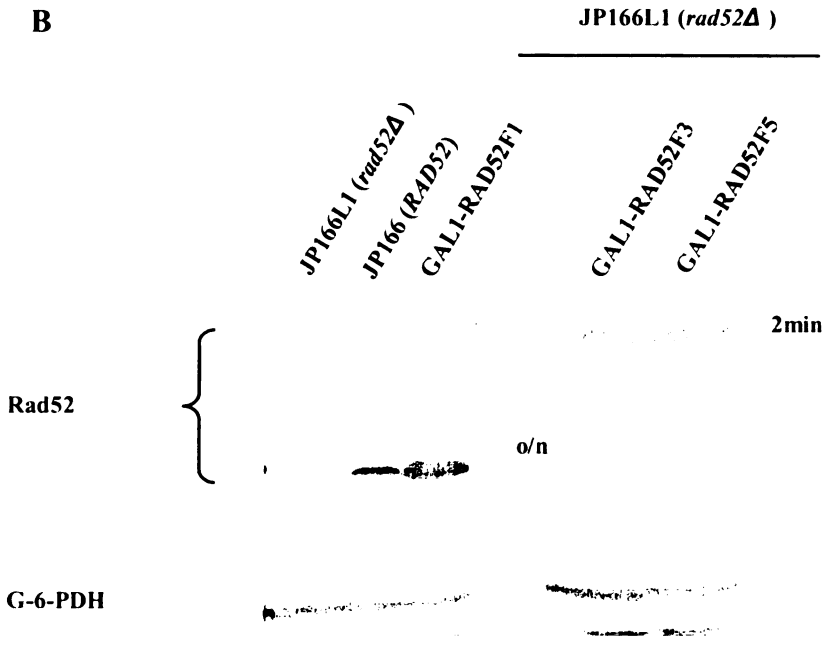
B
JP166L1 (rad52Δ)
JP166L1 (rad52Δ)
JP166 (RAD52)
GAL1-RAD52F1
GAL1-RAD52F3
GAL1-RAD52F5
2min
Rad52
o/n
G-6-PDH

Figure 2-3

C. Quantitative comparison of the Rad52 protein level in *rad52Δ* cells expressing GAL1-RAD52F1 or GAL1-RAD52F3

Proteins were extracted from cells cultivated in medium containing 2% raffinose and 0.05% galactose. The amount of total protein loaded is indicated above each lane. The Western blot was probed with an anti-Rad52 antibody, after which the membrane was stripped and probed with an anti-G-6-PDH antibody.

C

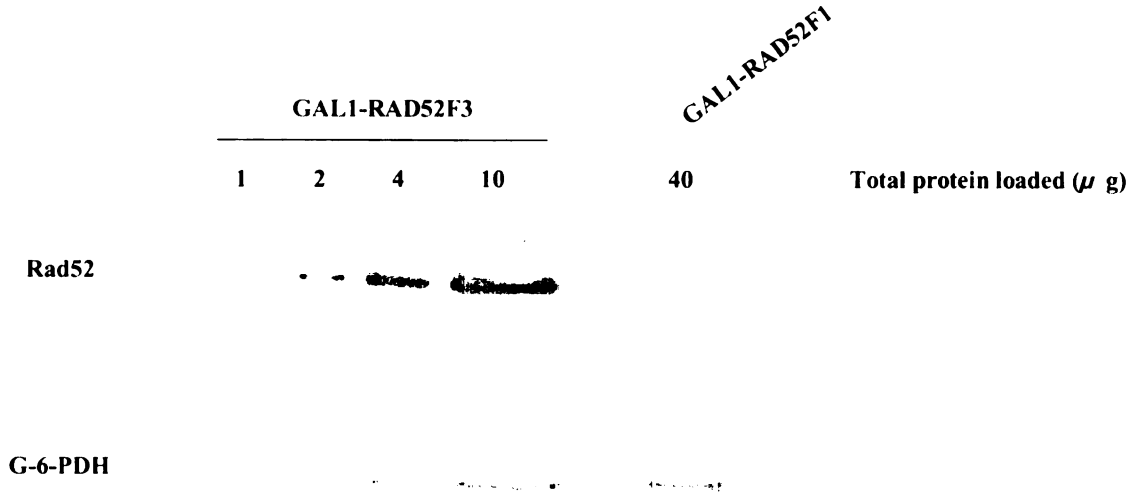
GAL1-RAD52F3
GAL1-RAD52F1
1
2
4
10
40
Total protein loaded (μ g)
Rad52
G-6-PDH

Figure 2-3

D. Examination of *RAD52* mRNA transcribed in *rad52Δ* cells expressing GAL1-RAD52F1

Total RNA was prepared from JP166 (*RAD52*), JP166L1 (*rad52Δ*), and JP166L1 expressing GAL1-RAD52F1 cultivated in medium containing 2% raffinose and 0.05% galactose. The radioactive labeled probe hybridizes to nucleotide 243-259 of the *RAD52* sequence. The nucleotide positions of the first, second and third ATG are indicated. The expected sizes for mRNA transcribed from upstream of the first, second or third ATG are also indicated. *RAD52* transcripts detected only in JP166L1 GAL1-RAD52F1 are indicated by a bracket. The transcript with a 5' end identical to the endogenous *RAD52* transcript is indicated by an arrowhead.

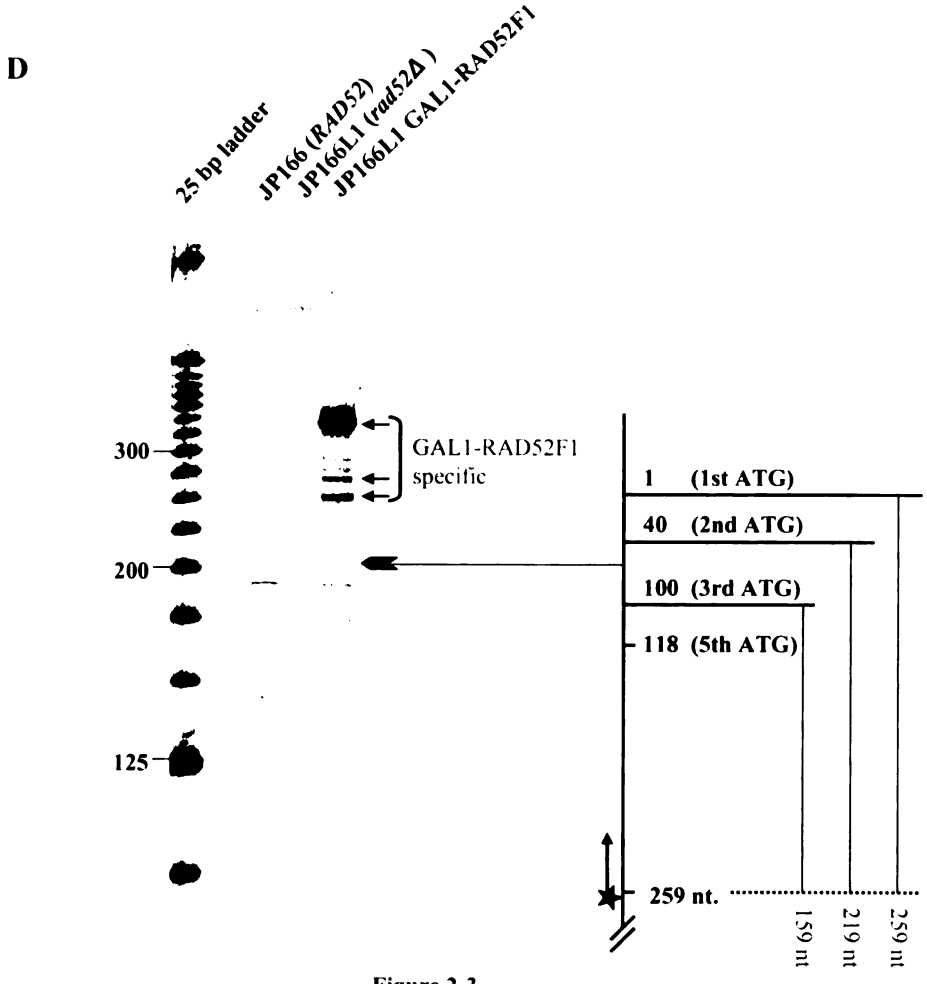
D
25 bp ladder
JP166 (RAD52)
JP166L1 (rad52Δ)
JP166L1 GAL1-RAD52F1
300
200
125
GAL1-RAD52F1
specific
1 (1st ATG)
40 (2nd ATG)
100 (3rd ATG)
118 (5th ATG)
259 nt.
159 nt
219 nt
259 nt

Figure 2-3

E. Analysis of the MMS sensitivity of *rad52Δ* cells expressing GAL1-RAD52F1ATG1

The wild type strain JP166 and the *rad52Δ* strain JP166L1 expressing GAL1-RAD52F1, GAL1-RAD52F1ATG1, or the control vector, were cultivated in SC-Ura-Leu medium containing 2% raffinose to mid-log phase. 10-fold serial dilutions containing 10^6 to 10 cells of each strain were spotted on SC-Ura-Leu plates containing 2% raffinose and 0.05% galactose with or without 0.005% MMS.

F. Examination of Rad52 protein expression in *rad52Δ* cells expressing GAL1-RAD52F1ATG1

Proteins were extracted from cells cultivated in medium containing 2% raffinose and 0.05% galactose for induction of Rad52 expression. The Western blot was probed with an anti-Rad52 antibody, after which the membrane was stripped and probed with an anti-G-6-PDH antibody.

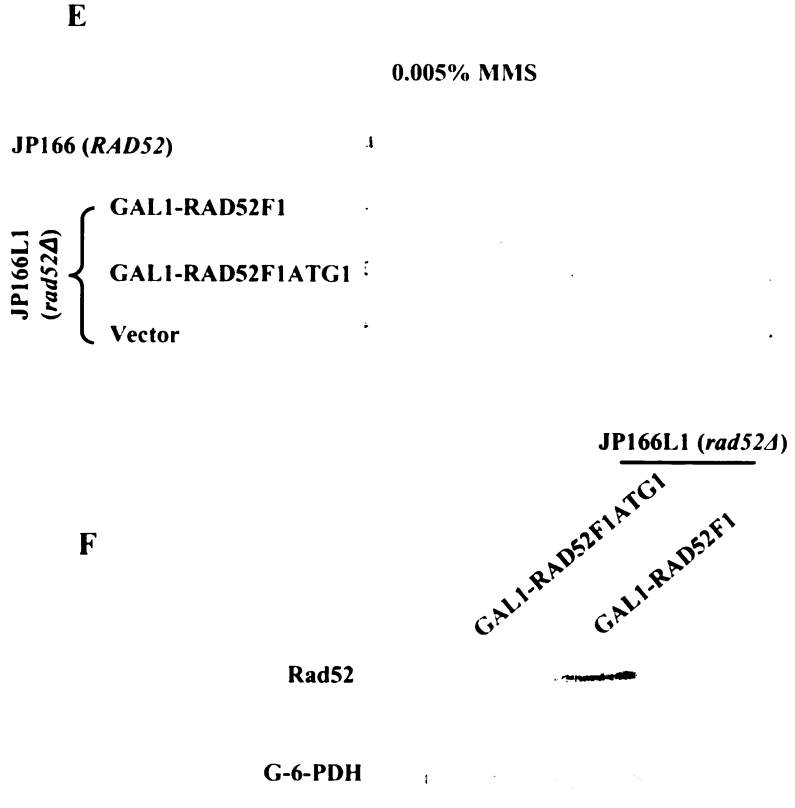
E
0.005% MMS
No MMS
JP166 (RAD52)
JP166L1 (rad52Δ)
GAL1-RAD52F1
GAL1-RAD52F1ATG1
Vector
F
JP166L1 (rad52Δ)
GAL1-RAD52F1ATG1
GAL1-RAD52F1
Rad52
G-6-PDH

Figure 2-3

Figure 2-4 Analysis of the MMS sensitivity of *rad52Δ* cells co-overexpressing *RAD52* with *RAD51* or *RAD59*

A. MMS sensitivity of *rad52Δ* cells co-expressing different *RAD52* overexpression constructs with a *RAD51* or a *RAD59* overexpression construct

The fragments containing the *GAL1* promoter, *RAD52* and the *CYC1* terminator from GAL1-RAD52F1, GAL1-RAD52F3 and GAL1-RAD52F5 were subcloned into pRSG414 to create GAL1b-RAD52F1, GAL1b-RAD52F3 and GAL1b-RAD52F5. Those three *RAD52* constructs or the control vector pRSG414 were introduced into a *rad52A* strain BY4735L1 carrying either the *RAD51* or the *RAD59* overexpression construct (GAL1-RAD51, GAL1-RAD59, respectively) or the empty vector (pRSG415). Cells were cultivated in SC-Leu-Trp medium containing 2% raffinose to mid-log phase. 10-fold serial dilutions containing 10^6 to 10 cells of each strain were spotted on SC-Leu-Trp solid medium containing 2% raffinose and 0.05% galactose with or without 0.005% MMS.

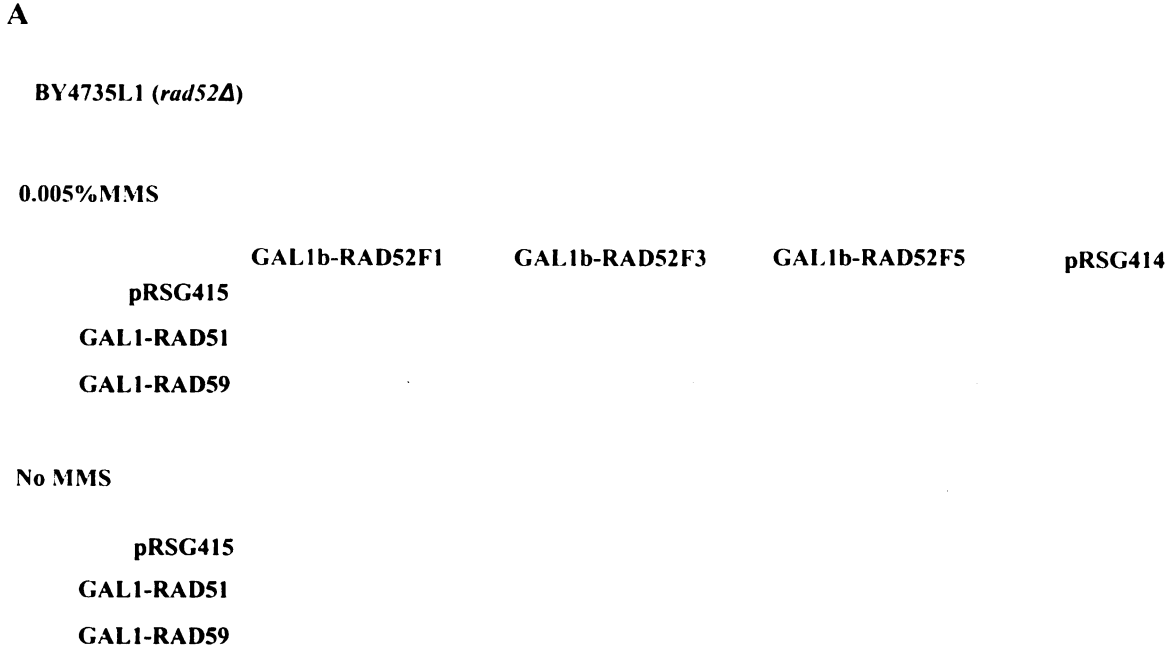
A
BY4735L1 (rad52Δ)
0.005%MMS
GAL1b-RAD52F1
GAL1b-RAD52F3
GAL1b-RAD52F5
pRSG414
pRSG415
GAL1-RAD51
GAL1-RAD59
No MMS
pRSG415
GAL1-RAD51
GAL1-RAD59

Figure 2-4

B. Complementation of the MMS sensitive phenotype of *rad59Δ* cells with GAL1-RAD59

JP166W2 (*rad59Δ*) strain expressing GAL1-RAD59 or the control vector was cultivated in SC-Ura-Leu medium containing 2% raffinose to mid-log phase. 10-fold serial dilutions containing 10^6 to 10 cells of each strain were spotted on SC-Ura-Leu solid medium containing 2% raffinose and 0.05% galactose with or without 0.01% MMS.

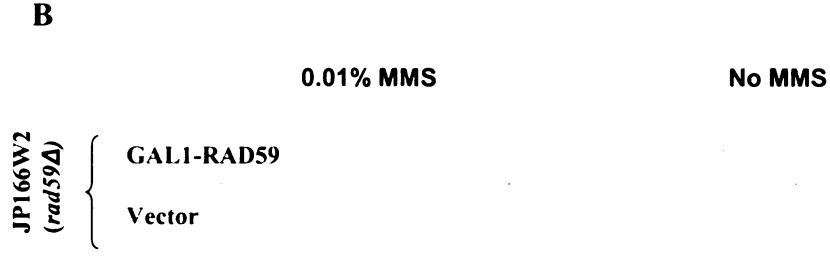

Figure 2-4

C. Analysis of Rad52 protein level in *rad52Δ* cells co-expressing GAL1-RAD51 with GAL1b-RAD52F1, GAL1b-RAD52F3 or GAL1b-RAD52F5

Proteins were extracted from cells cultivated in medium containing 2% raffinose and 0.05% galactose. The Western blot was probed with an anti-Rad52 antibody, after which the membrane was stripped and probed with an anti-G-6-PDH antibody.

C

BY4735L1 (*rad52Δ*)

GAL1-RAD51

GAL1b-RAD52F1 | GAL1b-RAD52F3 | GAL1b-RAD52F5

Rad52

G-6-PDH

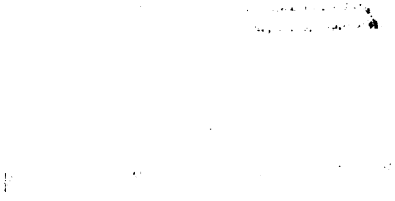

Figure 2-4

Figure 2-5 Analysis of the MMS sensitivity of *rad52Δ* cells overexpressing a mutant Rad52 with a defect in interaction with Rad51

A. MMS sensitivity of *rad52Δ* cells expressing GAL1-RAD52F3 or GAL1-RAD52F3d409-412

RAD52F3d409-412 encodes a mutant Rad52 that has a specific defect in interaction with Rad51. JP166L1 (*rad52Δ*) strain expressing GAL1-RAD52F3 or GAL1-RAD52F3d409-412 was cultivated in SC-Ura-Leu medium containing 2% raffinose to mid-log phase. 10-fold serial dilutions containing 10^6 to 10 cells of each strain were spotted on SC-Ura-Leu solid medium containing 2% raffinose and 0.05% galactose with or without 0.005% MMS.

B. Comparison of Rad52 protein level in *rad52Δ* cells expressing GAL1-RAD52F3 or GAL1-RAD52F3d409-412

Proteins were extracted from cells cultivated in medium containing 2% raffinose and 0.05% galactose. The Western blot was probed with an anti-Rad52 antibody, after which the membrane was stripped and probed with an anti-G-6-PDH antibody.

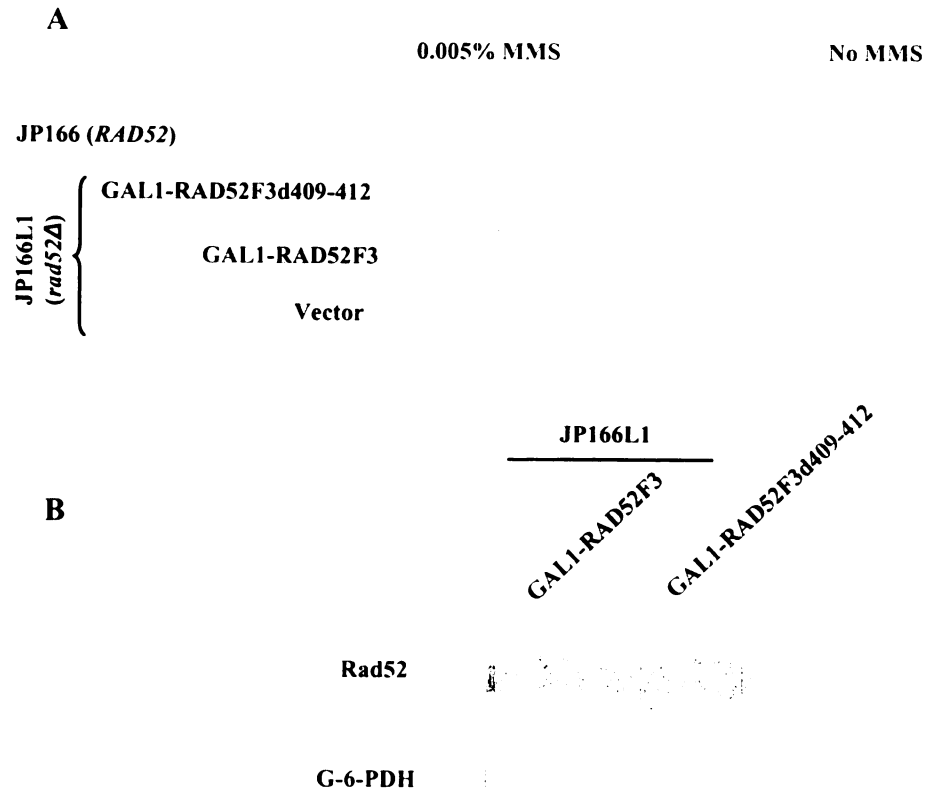
A
0.005% MMS
No MMS
JP166 (RAD52)
JP166L1 (rad52Δ)
GAL1-RAD52F3d409-412
GAL1-RAD52F3
Vector
B
JP166L1
GAL1-RAD52F3
GAL1-RAD52F3d409-412
Rad52
G-6-PDH

Figure 2-5

Figure 2-6 Analysis of the MMS sensitivity of rad51Δ strains overexpressing Rad52, or co-overexpressing Rad52 with Rad59

A-C. MMS sensitivity of a *rad51Δ* strain JP166W1 expressing GAL1-RAD52F3 or GAL1-RAD52F5

JP166W1 (*rad51Δ*) cells expressing GAL1-RAD52F3, GAL1-RAD52F5 or the control vector were cultivated in SC-Ura-Leu medium containing 2% raffinose to mid-log phase. 10-fold serial dilutions containing 10^6 to 10 cells of each strain were spotted on SC-Ura-Leu solid medium containing 2% raffinose and 0.05% galactose with 0.005% MMS (***A***), 0.001% MMS (***B***) or no MMS (***C***).


A 0.005%MMS
B 0.001%MMS
C No MMS
JP166W1 (rad51Δ)
Vector
GAL1-RAD52F3
GAL1-RAD52F5

Figure 2-6

D. MMS sensitivity of BY20031 strain (*rad52Δ rad51Δ*) co-overexpressing Rad52 with Rad59

Rad52 was overexpressed by introducing the GAL1b-RAD52F3 or GAL1b-RAD52F5 constructs into BY20031 harboring the Rad59 overexpression construct GAL1-RAD59. Cells were cultivated in SC-Ura-Leu-Trp medium containing 2% raffinose to mid-log phase. 10-fold serial dilutions containing 10^6 to 10 cells of each strain were spotted on SC-Ura-Leu-Trp solid medium containing 2% raffinose and 0.05% galactose with or without 0.001% MMS.

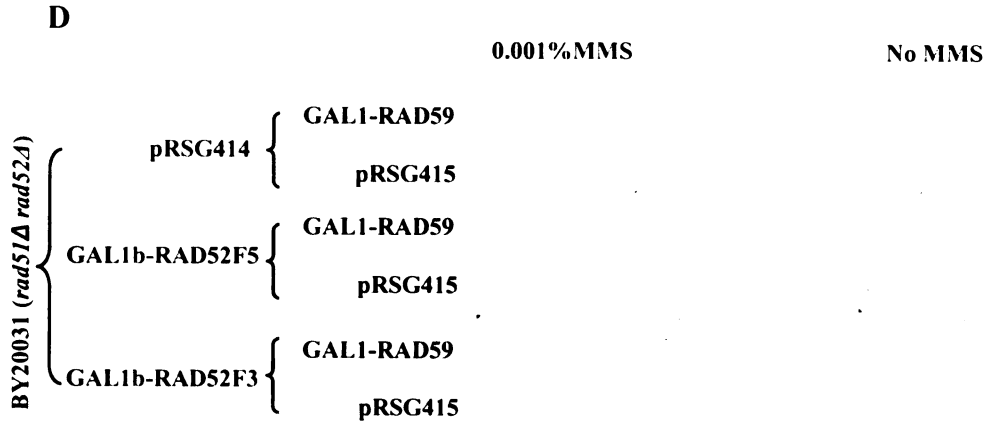
D
0.001%MMS
No MMS
BY20031 (rad51Δ rad52Δ)
pRSG414
GAL1-RAD59
pRSG415
GAL1b-RAD52F5
GAL1-RAD59
pRSG415
GAL1b-RAD52F3
GAL1-RAD59
pRSG415

Figure 2-6

Figure 2-7 Complementation of the MMS sensitive phenotype of *rad52Δ* cells with GAL1-RAD52F1 on non-inducing medium

JP166 (*RAD52*) and JP166L1 (*rad52-1*) expressing GAL1-RAD52F1 or the control vector were cultivated in SC-Ura-Leu medium containing 2% glucose (non-inducing condition for genes controlled by the *GAL1* promoter) to mid-log phase. 10-fold serial dilutions containing 10^6 to 10 cells of each strain were spotted on SC-Ura-Leu solid medium containing 2% glucose with or without 0.005% MMS.

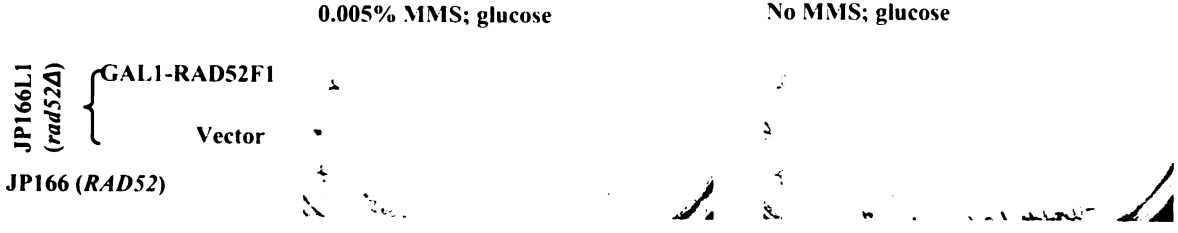
0.005% MMS; glucose
No MMS; glucose
JP166L1 (rad52Δ)
GAL1-RAD52F1
Vector
JP166 (RAD52)

Figure 2-7

Figure 2-8 Complementation of the MMS sensitive phenotype of a *rad52Δ* strain with pRS415RAD52B

pRS415RAD52 harbors the *RAD52* coding sequence and its genomic promoter. pRS415RAD52B harbors only the *RAD52* coding sequence without the sequence upstream of the first ATG or a heterologous promoter. Both constructs were introduced into JP166L1 (*rad52Δ*). Cells were cultivated in SC-Ura-Leu medium containing 2% glucose to mid-log phase. 10-fold serial dilutions containing 10^6 to 10 cells of each strain were spotted on SC-Ura-Leu solid medium containing 2% glucose with or without 0.005% MMS.

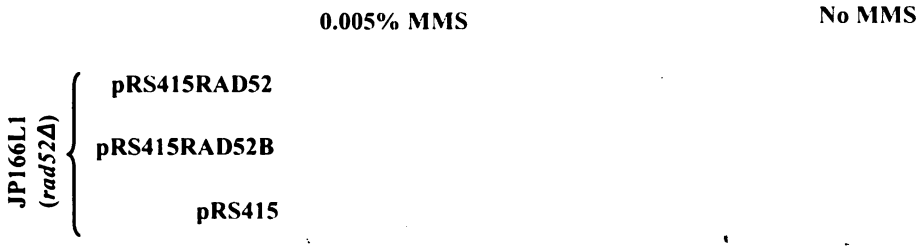
0.005% MMS
No MMS
JP166L1
(rad52Δ)
pRS415RAD52
pRS415RAD52B
pRS415

Figure 2-8

REFERENCES

1. Kraus, E., W.Y. Leung, and J.E. Haber, *Break-induced replication: a review and an example in budding yeast.* Proc Natl Acad Sci U S A, 2001. **98**(15): p. 8255-62.

2. Paques, F. and J.E. Haber, *Multiple pathways of recombination induced by double-strand breaks in Saccharomyces cerevisiae.* Microbiol Mol Biol Rev, 1999. **63**(2): p. 349-404.

3. Symington, L.S., *Role of RAD52 epistasis group genes in homologous recombination and double-strand break repair.* Microbiol Mol Biol Rev, 2002. **66**(4): p. 630-70, table of contents.

4. Bai, Y., A.P. Davis, and L.S. Symington, *A novel allele of RAD52 that causes severe DNA repair and recombination deficiencies only in the absence of RAD51 or RAD59.* Genetics, 1999. **153**(3): p. 1117-30.

5. Mortensen, U.H., et al., *A molecular genetic dissection of the evolutionarily conserved N terminus of yeast Rad52.* Genetics, 2002. **161**(2): p. 549-62.

6. Asleson, E.N. and D.M. Livingston, *Investigation of the stability of yeast rad52 mutant proteins uncovers post-translational and transcriptional regulation of Rad52p.* Genetics, 2003. **163**(1): p. 91-101.

7. Song, B. and P. Sung, *Functional interactions among yeast Rad51 recombinase, Rad52 mediator, and replication protein A in DNA strand exchange.* J Biol Chem, 2000. **275**(21): p. 15895-904.

8. Sung, P., *Function of yeast Rad52 protein as a mediator between replication protein A and the Rad51 recombinase.* J Biol Chem, 1997. **272**(45): p. 28194-7.

9. Milne, G.T. and D.T. Weaver, *Dominant negative alleles of RAD52 reveal a DNA repair/recombination complex including Rad51 and Rad52.* Genes Dev, 1993. **7**(9): p. 1755-65.

10. Dornfeld, K.J. and D.M. Livingston, *Effects of controlled RAD52 expression on repair and recombination in Saccharomyces cerevisiae.* Mol Cell Biol, 1991. **11**(4): p. 2013-7.

11. Longtine, M.S., et al., *Additional modules for versatile and economical PCR-based gene deletion and modification in Saccharomyces cerevisiae.* Yeast, 1998. **14**(10): p. 953-61.

12. Lorenz, M.C., et al., *Gene disruption with PCR products in Saccharomyces cerevisiae.* Gene, 1995. **158**(1): p. 113-7.

13. Agatep, R., R.D. Kirkpatrick, D.L. Parchaliuk, R.A. Woods, and R.D. Gietz, *Transformation of Sacchromyces cerevisiae by the lithium acetate/single-stranded carrier DNA/polyethylene glycol (LiAc/ss-DNA/PEG ptotocol.* Technical Tips Online (http://tto.trends.com), 1998.

14. Adzuma, K., T. Ogawa, and H. Ogawa, *Primary structure of the RAD52 gene in Saccharomyces cerevisiae.* Mol Cell Biol, 1984. **4**(12): p. 2735-44.

15. Sikorski, R.S. and P. Hieter, *A system of shuttle vectors and yeast host strains designed for efficient manipulation of DNA in Saccharomyces cerevisiae.* Genetics, 1989. **122**(1): p. 19-27.

16. Church, G.M. and W. Gilbert, *Genomic sequencing.* Proc Natl Acad Sci U S A, 1984. **81**(7): p. 1991-5.

17. Krejci, L., et al., *Interaction with Rad51 is indispensable for recombination mediator function of Rad52.* J Biol Chem, 2002. **277**(42): p. 40132-41.

18. Hays, S.L., et al., *Studies of the interaction between Rad52 protein and the yeast single-stranded DNA binding protein RPA.* Mol Cell Biol, 1998. **18**(7): p. 4400-6.

19. Davis, A.P. and L.S. Symington, *The yeast recombinational repair protein Rad59 interacts with Rad52 and stimulates single-strand annealing.* Genetics, 2001. **159**(2): p. 515-25.

20. Hays, S.L., A.A. Firmenich, and P. Berg, *Complex formation in yeast double-strand break repair: participation of Rad51, Rad52, Rad55, and Rad57 proteins.* Proc Natl Acad Sci U S A, 1995. **92**(15): p. 6925-9.

21. Shinohara, A., et al., *Rad52 forms ring structures and co-operates with RPA in single-strand DNA annealing.* Genes Cells, 1998. **3**(3): p. 145-56.

22. Phizicky, E.M. and S. Fields, *Protein-protein interactions: methods for detection and analysis.* Microbiol Rev, 1995. **59**(1): p. 94-123.

23. Clever, B., et al., *Specific negative effects resulting from elevated levels of the recombinational repair protein Rad54p in Saccharomyces cerevisiae.* Yeast, 1999. **15**(9): p. 721-40.

24. Pellegrini, L., et al., *Insights into DNA recombination from the structure of a RAD51-BRCA2 complex.* Nature, 2002. **420**(6913): p. 287-93.

25. Shin, D.S., et al., *Full-length archaeal Rad51 structure and mutants: mechanisms for RAD51 assembly and control by BRCA2.* Embo J, 2003. **22**(17): p. 4566-76.

26. Krejci, L., et al., *Molecular dissection of interactions between Rad51 and members of the recombination-repair group.* Mol Cell Biol, 2001. **21**(3): p. 966-76.

27. Sugiyama, T. and S.C. Kowalczykowski, *Rad52 protein associates with replication protein A (RPA)-single-stranded DNA to accelerate Rad51-mediated displacement of RPA and presynaptic complex formation.* J Biol Chem, 2002. **277**(35): p. 31663-72.

28. Sugawara, N., X. Wang, and J.E. Haber, *In vivo roles of Rad52, Rad54, and Rad55 proteins in Rad51-mediated recombination.* Mol Cell, 2003. **12**(1): p. 209-19.

29. Bai, Y. and L.S. Symington, *A Rad52 homolog is required for RAD51-independent mitotic recombination in Saccharomyces cerevisiae.* Genes Dev, 1996. **10**(16): p. 2025-37.

30. Xiao, W. and B.L. Chow, *Synergism between yeast nucleotide and base excision repair pathways in the protection against DNA methylation damage.* Curr Genet, 1998. **33**(2): p. 92-9.

CHAPTER 3

NOVAL ALLELES OF *RAD52* THAT DEFERENTIALLY AFFECT THE TWO SURVIVOR PATHWAYS IN *S. CEREVISIAE*

ABSTRACT

Immortalized human cells without the telomerase activity avoid senescence and maintain their viability by the Alternative Lengthening of Telomere (ALT) mechanism(s). *Saccharomyces cerevisiae* activates two telomerase-independent pathways for telomere lengthening and maintenance. The type I pathway is manifested by homologous recombination and amplification of the subtelomeric Y' elements, and the type II pathway is characterized by a sudden increase in the number of the telomeric $C_{1\text{-}3}A/TG_{1\text{-}3}$ repeats. While Rad52 is essential for both pathways, other Rad52 epistasis group genes contribute to telomere maintenance more specifically: type I survivors depend on Rad51, 54, 55, and 57; type II survivors require Rad59, Rad50, Mre11, and Xrs2. In the current work, the highly conserved amino-terminal half of Rad52 that catalyzes homologous pairing was subjected to mutagenesis to identify amino acid residues critical for survival through senescence. R70G, K159E, and R171S mutants all are defective in type II survival without apparent effects on the type I pathway. A fourth mutation, D164G, has defects in both type I and type II pathways. To further test the molecular mechanisms underlying these phenotypes, all four mutants were tested for their ability to mediate homologous recombination involving heteroalleles on non-homologous chromosomes, and two direct repeats on the same chromosome. Consistent with the type

II specific survival defects, R70G, K159E and R171S showed deficiency in recombination between direct repeats, but were normal in the interchromosomal recombination tests. In contrast, the D164G mutation suffered from severe defects in interchromosomal recombination, consistent with its defects in type I survival. Surprisingly, even though there was no obvious defect in overall recombination efficiency between two direct repeats on the same chromosome, nearly all of the D164G recombinants in this test were generated via the pop-out mechanism. We speculate that the prevalence of excising the intervening sequence between two homologous elements may account for the defect in the type II pathway.

INTRODUCTION

Telomeres are specialized DNA-protein complexes at the ends of eukaryotic chromosomes. They contribute to the stable maintenance of chromosomes by providing protection against degradation and end-to-end fusion. They also shield chromosome ends from the DNA damage checkpoint (reviewed in Zakian, Cold Spring Harbor Monograph Series 29, 1995, 107-137). In wild type *Saccharomyces cerevisiae*, telomeres contain 300 ± 75 bps of $T(G)_{2-3}(TG)_{1-6}$ repeats [1]. Immediately internal to the simple repeats are two classes of telomere associated sequences, X and Y'. Compared to the more diverse X elements, which range from 0.3 to 3.75 kb, Y' elements are highly conserved with about 1% divergence within a strain [2]. Y' elements exist as either 6.7 kb Y'- long or 5.2 kb Y'-short [2, 3].

Telomeres provide substrates for telomere-specific DNA replication. In wild type yeast cells, telomeres are elongated by telomerase, a ribonucleoprotein that contains an RNA subunit (*TLC1*), which serves as template and a catalytic protein subunit (*EST2*)

with reverse transcriptase activity. In the absence of telomerase, telomeres shorten progressively with each cell division (reviewed in [4]). Most telomerase-negative cells will cease division after 50-100 generations. However, survivors that resume normal cell division arise spontaneously from such cultures [5]. In survivor cells, telomeres are maintained by Rad52-dependent homologous recombination[5-10]. Genetic studies defined two telomerase-independent pathways in yeast which require different components of the *RAD52* epistasis group [9, 10]. While *RAD52* is essential for both pathways, *RAD51, RAD54, Rad55* and *RAD57* are required for the type I pathway, and *RAD50*, *RAD59*, *MRE11* and *XRS2* are required for the type II pathway. These two pathways generate two types of survivors with characteristic telomeres [5, 9, 11]: type I survivors maintain relatively short telomere repeats and increased tandem repeats of Y' elements, whereas type II survivors have long and heterogeneous telomere repeats with little Y' amplification.

Alternative mechanisms of telomere lengthening also exist in human cells ([12] and reviewed in [13]). About 31% of human tumor samples do not have detectable telomerase activity. Although not all of the telomerase-negative tumors display abnormally long telomeres, a subset of tumor samples (4%) acquire >20 kb terminal restriction fragments. Those telomeres are maintained by a Alternative Lengthening of Telomere (ALT) pathway. ALT exists in about 30% of human cell lines. Rapid elongation of telomeres following gradual shortening has been observed in human ALT cells [14]. The long and heterogeneous telomeres observed in ALT cells are similar to those in type II yeast survivors, suggesting that human ALT is mediated by a recombination process similar to that which occurs in the type II survivor pathway in *S.*

cerevisiae [11, 15]. Indeed, DNA sequences can be copied from telomere to telomere in human ALT cells [16]. Human ALT cells contain ALT-associated PML bodies (APB), novel promyelocytic leukemia (PML) bodies [17]. Telomeric DNA, Rad51 and Rad52 have been detected in APB. Noticeably, the appearance of APB coincides with the activation of ALT. The existence of Rad52 in APB suggests a possible role for Rad52 in human ALT.

Rad52 is involved in virtually all homologous recombination in yeast. It is conserved throughout eukaryotes, especially at its N-terminus which contains the core activities, including DNA-binding and self-association [18-20]. This region alone is able to catalyze homologous pairing [18, 21]. Rad52 interacts with Rad59 through the N-terminus [22, 23]. This interaction stimulates Rad52's function in single strand annealing *in vivo* [24].The C-terminus of Rad52 interacts with replication protein A (RPA) and Rad51. Rad52 can efficiently anneal short complementary oligonucleotides [19]. However, it needs RPA to eliminate secondary structures in long DNA molecules for efficient annealing [25]. Rad52 acts as a mediator between RPA and Rad51 to facilitate Rad51 nucleation onto ssDNA substrates [26-29]. Rad52 also stimulates strand exchange by stabilizing Rad51 presynaptic filaments [30].

Although the functions of Rad52 in homologous recombination have been studied in detail, it remains unclear as to how Rad52 differentially participates in the two telomere maintenance pathways in survivor cells. Similarly, while an increasing number of *rad52* mutants have been identified and characterized, the effects of Rad52 mutants on survivor pathways have not yet been studied. In this work, the well-conserved N-terminus of Rad52 was subjected to random mutagenesis to identify residues that are critical for its

functions in survivor pathways. I identified mutations differentially affecting the two survivor pathways. R70G, K159E and R171S mutations cause defects in the type II pathway, and this phenotype correlates well with a reduced efficiency in carrying out direct repeat recombination. D164G results in defects in both type I and type II pathways. It also leads to a severe defect in interchromosomal recombination. Interestingly, while the overall recombination efficiency between two direct repeats remains normal, nearly all the recombinants are generated via intrachromatid pop-out events. These mutants may provide tools for detailed studies of telomere maintenance in the absence of telomerase.

MATERIALS AND METHODS

Yeast Strains, media, and genetic methods

Yeast strains used in this study are listed in Table 3-1. JP166 was generously provided by Dr. John Prescott (University of California, San Francisco). A type I survivor strain, JP166S10, was created by selecting for 5-fluoroorotic acid (5-FOA) resistant clones of JP166 followed by five re-streakings on YPD. JP166L1, a *rad52Δ* strain derived from JP166, was constructed by replacing the *RAD52* with the *HIS3* gene. JP166L041 was constructed by replacing the *RAD51* gene with *KanMX6* [31] first, then replacing the *RAD52* with the *HIS3* gene. JP166L042 was constructed by replacing the *RAD59* gene with *KanMX6* first, then replacing *RAD52* with *HIS3*. All gene disruptions were complete deletions of the open reading frames and were constructed by transforming the cells with a PCR-generated gene disruption cassette [32]. W2078 and W2014-5C were kindly provided by Dr. Rodney Rothstein (Columbia University).

S. cerevisiae strains were propagated at 30°C in dropout media lacking the amino acids required for plasmid selection. Yeast transformation was performed according to Agatep. R. *et al.* [33].

Plasmids and mutations

Plasmids used in this study are listed in table 3-2. Vector pRSG415 (generously provided by Dr. John Prescott, UCSF) used for galactose-inducible expression, contains the *GAL1* promoter and the *CYC1* terminator [34] in pRS415 backbone, a *CEN* vector with a *LEU2* selectable marker (Stratagene). An *Sma*I site was previously engineered between the *GAL1* promoter and the *CYC1* terminator. The *RAD52* coding sequence starting from 117 bp downstream of the first ATG to the stop codon was subcloned into the *Sma*I site of pRSG415. The single *Bam*HI site in the coding sequence was deleted by a silent mutation. A *BamH*I site was introduced into the 5' end of the coding sequence. An *Spe*I site was introduced at nucleotide 711 for cloning purposes, resulting in a lysine to serine mutation. This mutation does not affect Rad52 functions (data not shown). The resulting construct was designated as pLL1.

pLL2 was constructed by ligating the *Sal*I fragment containing *RAD52* and its genomic promoter [35], amplified by PCR from genomic DNA of JP166, into the *Sal*I site of pRS415. R70G, K159E, D164G and R171S mutations were introduced into pLL2 individually by site-directed mutagenesis (Stratagene) to create pLL2a, pLL2b, pLL2c and pLL2d, respectively. Mutations were confirmed by DNA sequencing. The *Xho*I/*Spe*I fragment from these plasmids was inserted into pRS414 (Stratagene) to generate pLL3 (for *RAD52*), pLL3a (for R70G), pLL3b (for K159E), pLL3c (for D164G) and pLL3d (for R171S).

Random mutagenesis and yeast co-transformation

Random mutagenesis of the *RAD52* gene was carried out using Taq polymerase (Promega) as previously described [36]. Reaction mixtures contained 1x mutagenic PCR buffer (7 mM $MgCl_2$, 50 mM KCl, 10 mM Tris-HCl pH 8.3, 0.01% (w/v) gelatin), 1x dNTP mix (200 μM dGTP, 200 μM dATP, 1 mM dCTP and 1 mM dTTP), 20 fmoles of pLL1 as input DNA, 30 pmoles of each primer (5'-CATTTTCGGTTTGTATTACTTC -3' (anneals to a sequence within the *GAL1* promoter); 5'-TTTTCACCAGGTTCTTCGT CG -3'), with addition of $MnCl_2$ at 0.5 mM. The reaction was carried out for 30 cycles for 1 min at 94°C, 1 min at 45°C, and 3 min at 72°C.

To create a *rad52* library, the purified mutagenized PCR fragments and linear pLL1 lacking the *Bam*HI/*Spe*I fragment were co-introduced into JP166S10.Yeast co-transformation was performed using the LiAc/ss-DNA/PEG method [33].

Genetic screen for *rad52* alleles

Transformants of JP166S10 carrying randomly mutagenized *rad52* on pRSG415 were replica plated first onto SC-Leu plates containing 2% raffinose and 0.8% galactose with 0.001% methylmethanesulfonate (MMS), then onto SC-Leu plates containing 2% glucose with 0.001% MMS as a growth control. Clones displaying increased MMS sensitivity were recovered from glucose-containing plates and patched on test plates (SC-Leu plates containing 2% raffinose and 0.8% galactose) and control plates (SC-Leu plates containing 2% glucose). Plates were incubated for 3 days. Cells from the test plates were then patched onto test plates and control plates one additional time. Clones showing a deficient growth phenotype on test plates, judged by small colonies or the lack of overall growth, were then streaked on test plates once. The candidates were recovered from the

control plates. Plasmids were recovered and re-introduced into JP166S10 to confirm the phenotype. Plasmids were subjected to DNA sequencing to identify mutations.

Protein preparation and Western blotting analysis

Yeast proteins were prepared following a procedure from the laboratory of Steven Hahn (www.fhcrc.org/lab/hahn). Briefly, yeast cultures were harvested at OD_{600} ~1.0, and washed in cold extraction buffer (200 mM Tris pH 8.0, 150 mM $(NH_4)_2SO_4$, 10% glycerol, 1 mM EDTA) containing 2 mM DTT and protease inhibitor (Roche). Cells were then resuspended in cold extraction buffer with 2 mM DTT and protease inhibitor. 60% volume of acid-washed glass beads (425 - 600 microns, Sigma) were added to each sample. Samples were then vertexed at top speed for 1 min at 4°C for 5 times. Between each vortex, samples were kept on ice for at least 1min. Cell debris and glass beads were removed by centrifugation. Equal amounts of protein, determined by the Bradford method (Pirece), were separated on 10% SDS-PAGE and blotted onto polyvinylidene difluoride membrane (Amersham Pharmacia Biotech). Rad52 was detected with a goat anti-Rad52 antibody RAD52 yC-17 (Santa Cruz Biotech) followed by a rabbit anti-goat IgG HRP (Sigma). Membranes were stripped and probed with a rabbit anti-G-6-PDH antibody (Sigma) followed by a goat anti-rabbit IgG HRP (Sigma) for a loading control.

Determination of MMS sensitivity

Yeast cells were grown in appropriate dropout media to mid-log phase. Cells were collected and washed twice with ddH_2O. 10-fold serial dilutions containing 10 to 10^6 cells were spotted on plates with or without methlmethane sulfonate at concentration

specified in figure legends. Plates were incubated at 30°C for three to four days and photographed.

Liquid growth potential assay

JP166L1, JP166041, or JP166042 carrying either wild type *RAD52* or mutant *rad52* were selected using 5-FOA for loss of pRS316TLC1. Individual *tlc1Δ* colonies for each strain were inoculated into appropriate dropout media. Growth potential was monitored as described previously [8, 10]. Briefly, every 21 hours, cells were counted using a hemocytometer and inoculated into fresh media at $3x10^5$ cells/ml. The growth potential of each culture was presented as an average cell density at the end of each day.

Formation of survivors

Survivors were obtained as previously described with slight modifications [9, 11]. For liquid assays, 3 independent transformants of JP166L1 carrying either wild type *RAD52* or mutant *rad52* were selected by 5-FOA to lose the pR316TLC1 plasmid. 10 individual *tlc1Δ* colonies from each transformant were inoculated into appropriate dropout media and cultivated for 3 days. Cells were then inoculated into fresh media with a 1:10,000 dilution. This process was repeated five times to allow cellular senescence to occur and survivors to appear. Alternatively, survivors were obtained by single colony assay. 10 to 20 individual *tlc1Δ* colonies from each transformant were streaked on solid plates until colony sizes reached ~0.5 mm. For strains displaying high mortality during senescence, more colonies were picked from the first streaks for subsequent re-streaking in order to obtain a certain number of survivors. All plates were incubated for three to four days before colonies were picked.

DNA preparation and Southern blotting analysis

Cell pellets collected from each overnight culture were suspended in SEB (1 M D-Sorbital, 100 mM EDTA (pH 8.0), 14.4 mM 2-mercaptoethanol) containing 1 mg/ml of zymolyase (ICN Biomedicals. Inc) and incubated at 37° with shaking for 30 min. After brief centrifugation, the pellets were suspended in EDS (50 mM EDTA pH8.0, 2% SDS, 0.025 N NaOH) and incubated at 65°C for 15 min. Following addition of NH_4OAC, samples were precipitated at 4°C for 30 min. The supernatant was precipitated with isopropanol. The resulting pellets were resuspended in TE (10 mM Tris-HCl pH 8.0, 1mM EDTA pH 8.0) containing 20 μg/ml RNase. Equal amounts of genomic DNA judged by ethidium bromide staining were digested with *Xho*I to completion and resolved in 1% agarose gel and then blotted onto positively charged nylon membrane (Amersham Pharmacia Biotech) in 1.5M NaCl, 0.5M NaOH following manufacture's manual. After UV-crosslinking, the membrane was hybridized to a yeast telomere probe (5'-TGTGGTGTGTGGGTGTGGTGT-3') labeled with [γ-^{32}P] dATP using T4 polynucleotide kinase (New England Biolabs). Hybridization was carried out in 0.5M NaH_2PO_4/Na_2HPO_4 pH 7.2, 7% SDS, 1 mM EDTA pH 8.0 at 55°C for overnight (modified from Church and Gilbert [37]). The membranes were exposed to phosphorescent screens and the images were scanned with Phosphorimager (Molecular Dynamic).

Determination of mitotic recombination rates

Mitotic recombination between *leu2-ΔEco*RI and *leu2-ΔBst*EII heteroalleles was examined in diploid strains (W2078; for interchromosomal recombination) or in haploid strains (W2014-5C; direct-repeat recombination) as described previously [38]. Briefly,

wild type *RAD52* or mutant *rad52* on pRS414 backbone (pLL3, pLL3a, pLL3b, pLL3c and pLL3d) were introduced into W2078 or W2014-5C. Fresh transformants were inoculated into SC-Trp medium at $2x10^4$ cells/ml and grown to $2x10^7$ cells/ml. Plating efficiency and the number of recombinants were determined by plating an appropriate number of cells on SC-Trp and SC-Trp-Leu plates, respectively. For each mutant *rad52*, five to seven independent transformants were analyzed. Recombination rate and standard deviation were determined as previously described [39]. A two-tailed *t*-test was used to determine the significance of differences between *rad52* and *RAD52*.

To detect the deletion of the *URA3* marker in direct-repeat recombination events, Leu^- recombinants from SC-Trp-Leu plates were patched onto SC-Ura plates to determine the percentage of Ura^- recombinants.

RESULTS

Experimental strategy

There are five in-frame ATG triplets at the 5' end of *RAD52*. In Chapter II, I have shown that the third, forth and the fifth ATG can serve as the translation initiation site *in vivo*, and that Rad52 translated from the fifth ATG has the same function as that translated from the third ATG. Therefore I cloned *RAD52* starting from the fifth ATG into the pRSG415 vector to create pLL1, in which *RAD52* expression is under the control of the galatose-inducible *GAL1* promoter. The well-conserved N-terminal region, about 230 amino acids, of Rad52 was targeted for random mutagenesis using pLL1 as the template by error-prone PCR-based mutagenesis [36]. The mutagenized PCR products were introduced into a survivor strain JP166S10, along with the linearized pLL1 lacking

the targeted region of *RAD52*. Gap repair of the linear vector with the PCR fragment gives rise to a circular plasmid (Figure 3-1). Approximately 24,000 transformants were screened by a two-step screening scheme illustrated in Figure 3-2. The first step was to screen for mutants conferring higher sensitivity to the DNA damaging agent MMS. About 1,700 clones displayed increased MMS sensitivity. These clones were further screened for defects in survivor growth (Figure 3-3). Seventy-three candidate clones were isolated.

DNA sequencing revealed 57 different *rad52* mutants (Table 3-3), among which 7 mutants had single amino acid changes, 19 had two, 17 had three, and 14 had four to six mutations. 37 of the 94 mutated residues are conserved between HsRad52 and ScRad52 (Figure 3-4). Some residues were mutated in 6-8 different mutants (Figure 3-4). This high frequency of mutation at certain positions suggests that these residues are probably critical for Rad52 function. It is also possible that these mutations were generated at certain hot spots during PCR mutagenesis. However, at least some residues, for example, Asp164 and Arg171, are indeed critical for Rad52 functions (see below).

The growth defects displayed by these *rad52* alleles are specific for survivor cells, since a wild type strain, JP166, harboring these alleles showed normal growth phenotype (data not shown). To study whether the growth defects of survivor cells were caused by defects in telomere maintenance, four single mutations, R70G, K159E, D164G and R171S, were examined in detail. These four residues are evolutionarily conserved and some were studied by others [21, 38, 40]. These mutations were introduced into *RAD52* carried on pRS415 or pRS414, low copy vectors in which *RAD52* is controlled by its own

promoter. The constructs were introduced into *rad52Δ* strains to study the effects of these mutations on telomerase-independent telomere maintenance.

Mutant *rad52* displays increased MMS sensitivity

The four *rad52* mutants were first examined for their ability to complement the MMS sensitivity of a *rad52Δ* strain JP166L1 by spot assays. Cells expressing R70G, K159E, or R171S showed similar sensitivity to MMS as cells carrying the control vector (Figure 3-5). Cells expressing D164G were more resistant to MMS treatment than the other three mutants. However, they were significantly more sensitive than cells expressing *RAD52* (Figure 3-5). Therefore, R70G, K159E, and R171S cannot complement the MMS sensitivity of *rad52Δ*, and D164G partially complemented *rad52Δ*. Next I examined whether these mutations caused defects in Rad52 protein expression. While R70G and R171S did not affect Rad52 level, K159E and D164G reduced Rad52 expression (Figure 3-6). However, a low level of protein expression is not likely the cause for the phenotypes of K159E and D164G. D164G, while expressed at a lower level, is the only allele that could partially complement *rad52Δ*. In addition, though present at similar levels, K159E and D614G alleles display distinctive phenotypes in survivor pathways and perform homologous recombination with different efficiencies (See below).

Rad52 mutations lead to early senescence

To study the effects of Rad52 mutations on survivor pathways, we examined the growth potential of *tlc1Δ* cells expressing *rad52*. Growth potential was measured by diluting liquid cultures to $3x10^5$cells/ml and examining cell densities every 21 hours. Cell

densities for each day were plotted to generate "grow-out-of senescence" curves. A yeast culture gradually loses the capacity to repopulate as cells enter senescence due to telomere shortening. This process is reflected by decreased cell densities on grow-out curves. When cells recover from senescence, cell density will return to a normal level, indicating survivors have been generated [9, 10]. The abilities of *rad52* mutants to generate survivors were compared to that of *RAD52*. R70G, K159E, D164G and R171S entered senescence on the third or forth day after telomerase activity was eliminated by shuffling out the *URA3* plasmid bearing the sole copy of *TLC1*, whereas *RAD52* cells entered senescence on the fifth and sixth day, suggesting that these mutations cause early senescence (Figure 3-7). All four mutants recovered from senescence, indicating that these mutations do not have an apparent effect on survivor generation.

Rad52 mutations differentially affect the two survivor pathways

Yeast cells employ either a type I or type II pathway to generate survivors [9]. These two survivor pathways have different genetic requirements. Loss of certain genes causes cells to preferentially utilize one survivor pathway over the other, or even completely blocks the second pathway. To examine whether Rad52 mutations deferentially affect the two survivor pathways, I analyzed survivor types by Southern blot analysis. The two types of survivors arise at different frequencies depending on growth conditions [11]. In general, most of the survivors are type I when there is no growth competition, such as growing cells on solid medium where individual colonies form independently (single colony assay) [11]. However, when growth competition exists, such as growing cells in liquid culture (liquid assay), most of the survivors are type II due to their higher growth rate [11]. The exact ratio between the two survivor types under

these conditions is strain-dependent [9, 11]. When cultivated in liquid medium, *RAD52* generated roughly an equal number of type I and type II survivors. Like *RAD52*, D164G generated both type I and type II survivors at a similar frequency. In contrast, R70G, K159E and R171S generated only type I survivors. (Figure 3-8 and Table 3-4), suggesting that these three mutations have negative effects on the type II pathway. When streaked on solid medium, R70G, K159E and R171S showed similar phenotypes as *RAD52* in that type I survivors occurred predominantly. In contrast, 40% of the survivors generated by D164G were type II. The increase of type II survivors in single colony assays suggests that D164G mutation has a negative effect on the type I pathway, or results in a more active type II pathway, or both (Figure 3-9 and Table 3-4). Taken together, the above results indicate that R70G, K159E and R171S survive senescence preferentially through type I pathway. D164G has a preference for type II pathway as shown by single colony assays. However, the frequency of type II survivors was not increased in liquid assay, which favors type II pathway. It is possible that D164G is also defective in generating type II survivors, though to a lesser degree than generating type I survivors. Alternatively, the D164G mutation may have negative effects on the proliferation of type II survivors. Therefore, the growth advantage of type II survivors over type I survivors in liquid cultures is diminished, and results in changes in the ratio of the two survivor types.

To further provide genetic evidence for the differential utilization of type I or II survivor pathways by these *rad52* mutants, we introduced each allele into *rad52Δ rad51Δ* (JP166041) and *rad52Δ rad59Δ* (JP166042) strains. Deleting *RAD51* or *RAD59* forces cells to use, if available, only the type II or type I pathway, respectively. Liquid growth

potential assays were performed to examine cell growth and survivor generation. When introduced into the *rad51Δ* strain, R70G, 159E and R171S showed declined growth potential similar to that of *RAD52* after telomerase activity was eliminated. However, they did not generate survivors, whereas *RAD52* recovered from senescence (Figure 3-10), indicating that these three mutants rely mainly on type I pathway to generate survivors. In the absence of Rad51, none of these *rad52* mutants displayed discernible type II survival, indicating that the mutations cause severe defects in the type II pathway. In contrast, two out of five D164G were able to generate survivors, at much later time points compared to *RAD52* (Figure 3-10). Thus, D164G is also defective in the type II pathway, though to a lesser degree than the other three mutants. The same *rad51Δ rad52* mutant strains were also tested on solid plates for survivor generation. 24 samples were tested for each strain. Consistent with the liquid assay, cells expressing R70G, K159E or R171S did not generate any survivors, whereas D164G generated survivors at a reduced frequency (data not shown). Together, these results suggest that all four mutants are defective in eliciting type II survival. When introduced into the *rad59Δ* strain, all four mutants were able to generate survivors in liquid media (Figure 3-11). However, cells expressing K159E or D164G displayed a more profound senescence phenotype (Figure 3-11). The accelerated decline in growth potential is similar to that of *rad52Δ* described previously [9]. Deletion of Rad59 does not change the ability of the mutants to generate survivors as all the mutants were still able to survive senescence. Since *rad59Δ* mutation selectively eliminates type II pathway, these results indicate that all four mutants maintain an appreciable portion of the type I survival function.

***rad52* mutants perform homologous recombination with different efficiencies**

Based on the telomere DNA sequences in survivor strains and the genetic requirement of the two survivor pathways, it has been proposed that the type I pathway arises from recombination between the Y' elements on different chromosomes and the type II pathway may be caused by recombination between the telomere repeats on the same (looping back) or different chromosomes [9, 11, 41]. Since the four Rad52 mutations appear to display differential effects on survivor pathways, it is possible that corresponding effects can be seen in selective homologous recombination events. To test this, I examined the efficiency of recombination between two homologous alleles present on different chromosomes or as tandem repeats on the same chromosome.

The interchromosomal heteroallelic recombination efficiency of each *rad52* mutant was determined by introducing the mutant into a homozygous *rad52Δ* strain carrying two nonfunctional *leu2* alleles, *leu2ΔBst*EII and *leu2ΔEco*RI (Figure 3-12A) [38, 42]. In the absence of *RAD52*, the rate of *LEU2* recombinant formation was 8-fold lower than in wild type. R70G and R171S displayed a 2 to 3-fold increase in recombination rate compared to wild type (Figure 3-12B). K159E had a recombination rate similar to *RAD52*. In contrast, D164G reduced the recombination rate by 14-fold. These results indicate that while R70G, K159E and R171S mutations do not have significant effects on interchromosomal recombination, the D164G mutation causes a severe defect similar to *rad52Δ*.

The direct-repeat recombination rate was examined by using a haploid *rad52Δ* strain carrying the *leu2ΔBst*EII and the *leu2ΔEco*RI alleles as tandem repeats on chromosome V (Figure 3-12C) [38, 43]. A *URA3* marker is flanked by the two *leu2*

alleles. *LEU2* recombinants can be generated via different mechanisms, including pop-out events that result in the loss of the intervening *URA3* marker, gene conversion events that replace one of the two repeats, unequal sister chromatid exchange that produces a triplication product and events that create disomes (Figure 3-12C) [38]. The preference for certain mechanisms reflects changes in the functions of homologous recombination proteins, and will inevitably affect the outcome of biological processes that are mediated by such events. The percentage of pop-out is of particular interest since such events could have devastating effects on telomere maintenance if it occurred between telomere repeats. The recombination rate was 30-fold lower in *rad52Δ* cells than the *RAD52* cells. R70G and R171S caused a moderate decrease of 1.5 to 2-fold in recombination rates. K159E displayed a 15-fold reduction in the recombination rate. The tendency of popping out the intervening *URA3* gene of these three mutants as evidenced by assaying the percentage of Leu^+/Ura^- recombinants was similar to that of *RAD52*, which was ~60%. D164G displayed overall recombination efficiency similar to that of *RAD52*. Interestingly, nearly all of the Leu^+ recombinants generated in D164G strain were produced by pop-out events ((Figure 3-12D). Thus, R70G, K159E and R171S negatively affect the recombination between two direct repeats. These mutations do not change the tendency of deletion events. As much as 40% of the recombinants retain the intervening sequence. In contrast, D164G does not affect overall efficiency of direct-repeat recombination. However, it results in elevated pop-out activity. Most of the recombinants produced by D164G lose the intervening sequence.

DISCUSSION

Rad52 plays a central role in yeast survivor pathways [5, 9, 10]. *tlc1Δ rad52Δ* mutants cannot survive senescence. The highly conserved N-terminal region of Rad52 can catalyze homologous pairing [21]. Thus, the core activity of Rad52 appears to reside in this region [18, 21]. In this study, we identified amino acid residues critical for Rad52 functions in survivor pathways by screening for *rad52* mutants that were randomly mutated at the N-terminal region. The functions of 4 residues, Arg70, Lys159, Asp164 and Arg171, were examined in detail. We demonstrated that mutations of these residues differentially affect the two survivor pathways, as well as different homologous recombination events (summarized in Figure 3-13). R70G, R171S and K159E cause defects in the type II pathway specifically. These three mutants perform interchromosomal recombination at near wild type efficiencies, but are moderately defective in direct-repeat recombination. D164G is defective in both type I and type II pathways. It also has a severe defect in interchromosomal recombination. While D164G does not result in an apparent reduction in direct-repeat recombination, most of the recombinants are produced through the intrachromatid pop-out mechanism. The correlation between the two survivor pathways and different recombination events provides further support that the type I pathway is mediated by recombination between telomeres on different chromosomes and the type II pathway is mediated most likely by telomere "looping back" [9].

Effects of Rad52 mutations on survivor pathways

The ratio between the two types of survivor is strain-dependent [5, 9, 11]. The changes in the activity of the two pathways can be assessed by comparing this ratio

between *tlc1Δ* cells expressing wild type *RAD52* and those expressing mutant *rad52*. While the *tlc1Δ RAD52* strain generates a similar number of type I and II survivors when grown in liquid medium, it generates only type I survivors when streaked for individual colonies. *R70G, K159E,* and *R171S* are defective in the type II pathway since *tlc1Δ* cells expressing these mutants do not generate any type II survivors in either liquid or single colony assays (Figure 3-8 & Table 3-4). Consistent with this defect, these cells can not recover from senescence in the absence of Rad51 where cells rely solely on the type II pathway for survival (Figure 3-10). These alleles appear to have normal type I activity since they can recover from senescence and proliferate normally even in the absence of Rad59 (Figure 3-11). Several pieces of evidence suggest that *D164G* is defective in both type I and type II pathways. There is a significant increase in type II survivors in single colony assays that favors the type I pathway, suggesting that D164G mutation results in a defective type I pathway, and/or an elevated type II activity. However, in the absence of Rad51 where cells rely on the type II pathway to survive through senescence, *D164G* generates survivor at a later time point and with a reduced frequency, suggesting that the D614G mutation has a negative effect on the type II pathway as well. Thus, the change in the ratio of the survivor types is possibly due to different degrees of defects in the two pathways.

Contribution of inter- and intra- chromosomal recombination to the two survivor pathways

Based on the genetic requirement of the survivor pathways and the nature of the survivor telomeres, it has been widely accepted that the type I pathway is mediated by recombination between Y' elements on different chromosomes, and the type II pathway

is mediated by recombination between the telomere repeats [9, 11, 41]. However, for the type II pathway, it remains unclear as to whether the recombination between telomere repeats is via interchromosomal or intrachromosomal mechanisms. The defects of *R70G, K159E,* and *R171S* in the type II pathway correlate well with their defects in direct-repeat recombination, and their ability to carry out the type I pathway is consistent with their near wild type efficiency in performing interchromosomal recombination. The defect of *D164G* in the type I pathway is in accord with its marked deficiency in interchromosomal recombination. These results support the role of interchromosomal recombination in the type I pathway. Our results also suggest that type II survivor telomeres are maintained mainly by telomere looping back to copy the $T(G)_{2\text{-}3}(TG)_{1\text{-}6}$ repeats intrachromosomally. Consistent with this idea, the high incidence of excising the intervening sequence between two direct repeats may account for the defects of *D164G* in the type II pathway. There is evidence that telomeres form t-loops, in which telomeres loop back and the 3' single-stranded tails of G-strands pair with the duplex telomeric DNA [44, 45]. t-loops have been observed in evolutionarily unrelated organisms [44, 45], suggesting they are a conserved feature of eukaryotic telomeres. Similar structures have been proposed to mediate telomere length regulation and the transcriptional regulation of genes placed in subtelomeric region in yeast [46-49]. This structure is likely disintegrated by illegitimate excision of the intervening sequence between the paired regions. Indeed, a mutation in TRF2, a human telomere binding protein, induces t-loop deletion and results in rapid telomere shortening [50].

Possible structural basis of the observed phenotypes of *rad52* mutants

The *R70G, R171S and K159E* alleles display similar phenotypes in homologous recombination. They are able to perform interchromosomal recombination normally, but are moderately defective in recombination between two direct repeats located on the same chromosome. Genetic studies show that intrachromosomal recombination requires *RAD59* [41, 51]. Consistent with their defects in direct repeats recombination, all three mutant alleles are defective in the Rad59-depedent type II pathway. Rad59 physically interacts with Rad52 at the N-terminal region of Rad52 that coincides with its self-association region [24] [52]. Thus, the defects of these mutants in the type II pathway and direct-repeat recombination could result from the disruption of Rad52-Rad59 interaction. It would be important to examine the interaction between Rad59 and Rad52 mutants by co-immunoprecipitation experiments. However, no suitable antibodies are available at present.

Arg55 and Arg156 of the human Rad52, corresponding to Arg70 and Arg171 of the yeast Rad52, are important for DNA binding [21]. Substituting these residues with alanine results in severe defects in ssDNA and/or dsDNA binding by HsRad52. Arg70 and Arg171 of ScRad52 do not appear to be essential for DNA binding, since *R70G* and *R171S* are normal in interchromosomal recombination. This is further supported by the previously identified *R70A* and *R171A* alleles that show no defects in interchromosomal or direct-repeat recombination [38].

D164G allele is defective in interchromosomal recombination. It has no obvious defect in direct-repeat recombination. However, it preferentially generates pop-out recombinants. *D164G* is also defective in both type I and type II pathways. These phenotypes suggest that D164G mutation might compromise the DNA binding and/or

self-association functions, which will lead to defects in multiple genetic processes. It is possible that this allele is also defective in interaction with Rad59 for the same reason discussed for the other three mutant alleles.

Secondary structure prediction places Lys159, Asp164 and Arg171 on the same α-helix. Their spacing is such that Asp164 and Arg171 are located on the same side of the α-helix, and Lys159 is located on the opposite side. The crystal structure of the N-terminal domain of human Rad52 reveals that the corresponding residues, Lys144, Asp149 and Arg156, are also located on a α-helix. Arg156 is part of a DNA binding site. In the ring structure formed by Rad52 monomers, Lys144 forms a hydrogen bond with Asp149 of the neighboring monomer. This structure predicts similar phenotypes for mutations at Lys144 and Asp149 which disrupt the hydrogen bond. However, K159E and D164G mutations of the yeast Rad52 display different phenotypes. The difference could be due to, at least in part, different degrees of disruption of the interactions between Rad52 monomers. It is possible that there are subtle structural differences between ScRad52 and HsRad52. The fact that Arg171 of ScRad52 appears not to be important for DNA binding supports such notion.

SUMMARY

In summary, I identified 57 *rad52* alleles with defects in responding to MMS toxicity. Of these, I characterized in greater details 4 alleles for their phenotypes in telomerase-independent telomere maintenance and homologous recombination. *rad52R70G*, *rad52K159E* and *rad52R171S* have defects specifically in the type II survivor pathway. *rad52D164G* is defective in both type I and type II pathways. The defects in telomere maintenance correlate well with mutant phenotypes in homologous

recombination. A mutant with a defect in the type II pathway is also defective in intrachromosomal direct-repeat recombination. A mutant with a defect in the type I pathway is also defective in interchromosomal heteroallelic recombination. These results provide further support for the proposed mechanisms of the two telomere maintenance pathways in the absence of telomerase [9, 11, 41]. Since the amino acid residues mutated in these alleles are highly conserved, analogous mutations in Rad52 homologues may have similar effects on their functions.

APPENDIX 3: FIGURES AND TABLES FOR CHAPTER 3

Table 3-1 *S. cerevisiae* strains used in this study

strain	genotype
JP166 [a]	*MATa his3Δ leu2Δ ura3Δ tlc1Δ pRS316TLC1*
JP166L1 [b]	*MATa his3Δ leu2Δ ura3Δ tlc1Δ rad52Δ::HIS3 pRS316TLC1*
JP166L041 [b]	*MATa his3Δ leu2Δ ura3Δ tlc1Δ rad51Δ::KanMX6 rad52Δ::HIS3 pRS316TLC1*
JP166L042 [b]	*MATa his3Δ leu2Δ ura3Δ tlc1Δ rad59Δ::KanMX6 rad52Δ::HIS3 pRS316TLC1*
W2014-5C [c]	*MATa rad52::HIS5 SUP4-o::CAN1-HIS3::sup4*$^{+}$ *leu2-ΔEco*RI*::URA3::leu2-ΔBst*EII
W2078 [c]	*MATa/α rad52::HIS5/ rad52::HIS5 leu2-ΔEco*RI*/ leu2-ΔBst*EII

[a] From Dr. John Prescott (University of California, San Francisco)

[b] Derivative of JP166, This study.

[c] From R. Rothstein's laboratory {Mortensen, 2002 #4}.

Table 3-2 Plasmids used in this study

Plasmid	description
pRS415 [a]	a *CEN* vector with a *LEU2* marker
pRS414 [a]	a *CEN* vector with a *TRP1* marker
pLL2	*RAD52* and its own promoter is cloned into pRS415
pLL2a	R70G mutation is introduced into pLL2
pLL2b	K159E mutation is introduced into pLL2
pLL2c	D164G mutation is introduced into pLL2
pLL2d	R171S mutation is introduced into pLL2
pLL3	The *Xho*I/*Spe*I fragment from LL2 containing *RAD52* and its promoter is cloned into pRS414
pLL3a	The *Xho*I/*Spe*I fragment from LL2a containing *rad52R70G* and its promoter is cloned into pRS414
pLL3b	The *Xho*I/*Spe*I fragment from LL2 containing *rad52K159E* and its promoter is cloned into pRS414
pLL3c	The *Xho*I/*Spe*I fragment from LL2 containing *rad52D164G* and its promoter is cloned into pRS414
pLL3d	The *Xho*I/*Spe*I fragment from LL2 containing *rad52R171S* and its promoter is cloned into pRS414
pRSG415 [b]	a *GAL*1 promoter and a *CYC*1 terminator is cloned into pRS415
pLL1	*RAD52* coding sequence lacking the first 117 nucleotide is cloned into pRSG415 between the *GAL*1 promoter and the *CYC*1 terminator. The single *Bam*H1 in the RAD52 sequence is removed by a silent mutation. An *Spe*I is inserter at position 711.

[a] From Stratagene

[b] From Dr. John Prescott (University of California, San Francisco)

Figure 3-1 Construction of *rad52* library

pLL1 harbors *RAD52* starting from the fifth ATG under the control of the *GAL1* promoter. *RAD52* expression is induced by galactose, but repressed by glucose. The 5'~700 bp of *RAD52* was replaced with randomly mutagenized PCR fragments of the same region by gap repair. pLL1mut represents the resulting plasmids.

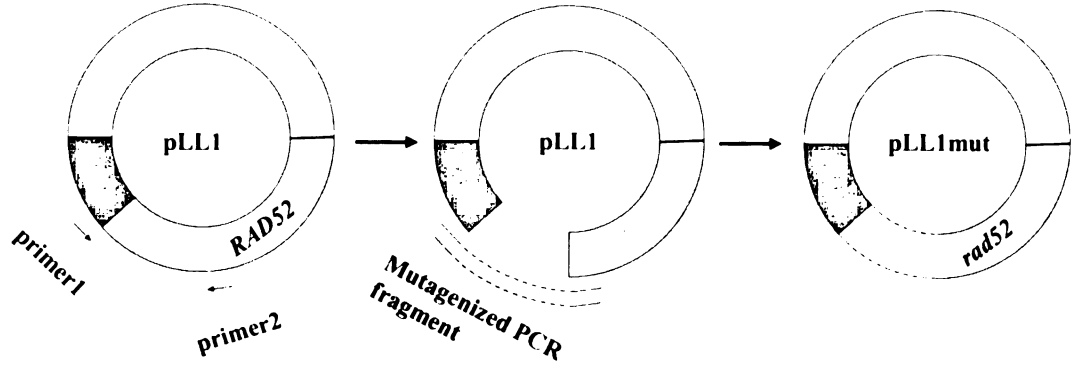
pLL1
RAD52
primer1
primer2
pLL1
Mutagenized PCR fragment
pLL1mut
rad52

Figure 3-1

Figure 3-2 Screening scheme for rad52 mutants

JP166S10 (a survivor strain) carrying wild type *RAD52*, mutant *rad52* or control vector were plated on SC-Leu/glucose (noninducing) plates, after which colonies were replica plated onto SC-Leu/galactose (inducing) plates containing 0.001% MMS, then onto SC-Leu/glucose plates containing 0.001% MMS. Clones showed higher sensitivity to MMS on galactose-containing plates were recovered from glucose-containing plates, and patched onto SC-Leu/galactose plates twice to identify the ones that grew poorly. At the same time cells were also patched onto SC-Leu/glucose plates serving as control for cell growth, as well as for recovering candidates. Candidate clones were further streaked on SC-Leu plates to examine the growth phenotype. Plasmid DNA recovered from the candidates was used to transform JP166S10 and other strains mentioned in the text, and for DNA sequencing.

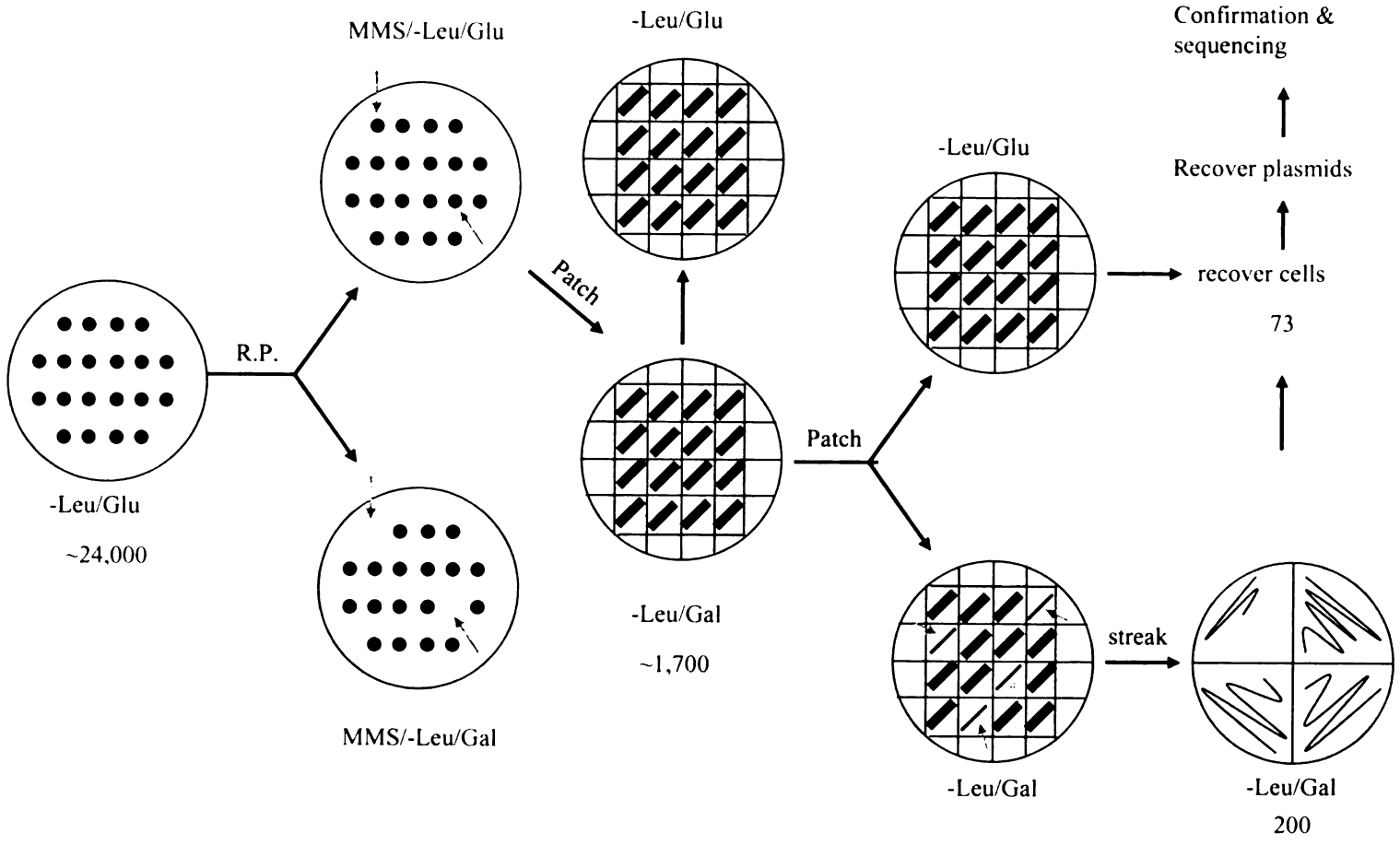
MMS/-Leu/Glu
-Leu/Glu
Confirmation &
sequencing
-Leu/Glu
Recover plasmids
Patch
recover cells
73
R.P.
Patch
-Leu/Glu
~24,000
-Leu/Gal
~1,700
streak
MMS/-Leu/Gal
-Leu/Gal
-Leu/Gal
200

Figure 3-2

Figure 3-3 Growth phenotype of JP166S10 expressing rad52 alleles

This figure shows a plate from the last step of the screening procedure illustrated in Figure 3-2. JP166S10 harboring the control vector expresses the genomic copy of *RAD52*. It served as the control for comparing growth phenotype. JP166S10 expressing *RAD52* showed normal growth. JP166S10 expressing *rad52-215* or *rad52-507* displayed deficient growth phenotype. These two clones were identified as candidates. The other four clones shown in the figure displayed less severe or no apparent growth phenotype. These clones were not investigated further.

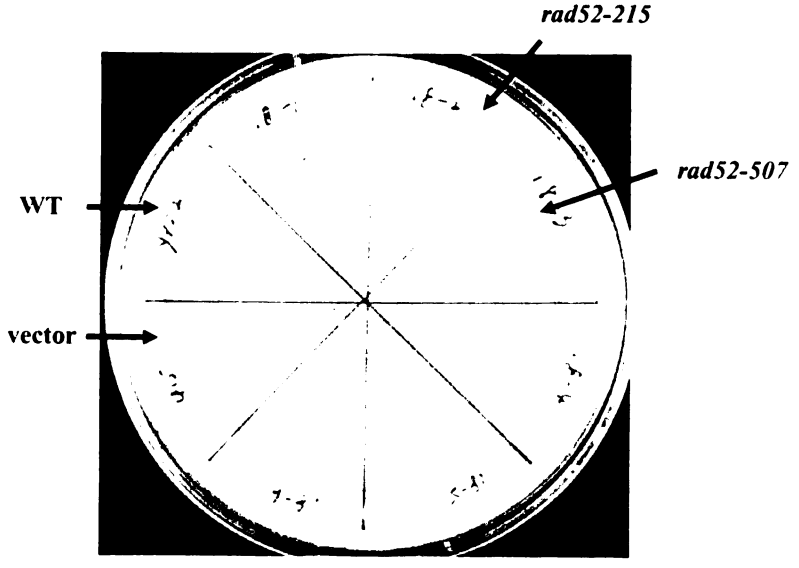

Figure 3-3

Table 3-3 *rad52* alleles identified in this study

	Mutant I.D.	Mutations
Single mutants	rad52-101	K60E
	rad52-102	K61N
	rad52-103	P64H
	rad52-104	R70G
	rad52-105	K159E
	rad52-106	D164G
	rad52-107	R171S
Double mutants	rad52-201	E113G; V193E
	rad52-202	R70G; N203I
	rad52-203	K60E; F206S
	rad52-204	D164V; N204D
	rad52-205	K61E; R217G
	rad52-206	K167R; R171G
	rad52-207	F73S; D164G
	rad52-208	E65D; N232D
	rad52-209	K69E; N179D
	rad52-210	R171G; I190S
	rad52-211	K61N; N204Y
	rad52-212	R207G; Q229P
	rad52-213	K61E; T75P
	rad52-214	K69E; N242Y
	rad52-215	R171S; E202K
	rad52-216	K57N; Y80D
	rad52-217	D41V; K61E
	rad52-218	I120L; F195I
	rad52-219	R171S; N219S

Table 3-3 *rad52* alleles identified in this study (continued)

Triple mutants	Mutant I.D.	Mutations
	rad52-301	V126I; K167R; T218A
	rad52-302	T163M; N204S; E223A
	rad52-303	R207G; N242S; P245L
	rad52-304	R171G; I212N; N242D
	rad52-305	T163K; T220S; N232S
	rad52-306	R207G; E211V; Q229L
	rad52-307	I120M; V193M; H222L
	rad52-308	D41H; D164G; Q229R
	rad52-309	T75A; D164G; N204D
	rad52-310	N146D; L237M; S247P
	rad52-311	Y80D; R85S; F195S
	rad52-312	N97D; K117M; Y141F
	rad52-313	K61E; I78T; K192R
	rad52-314	K184N; D210E; P231S
	rad52-315	E52N; T134S; D164G
	rad52-316	Y66H; L205S; E223V
	rad52-317	K184E; R207G; N244Y
Quadruple mutants	rad52-401	F73S; T75A; D164G; D199G
	rad52-402	R77G; I81T; L187P; S215N
	rad52-403	F110I; I120V; N175D; N203D
Quintuple mutants	rad52-501	D53G; D201E;R217K;N232D;D246Y
	rad52-502	F47Y; D112G;K167R; E214V; Q227R
	rad52-503	K159N; E211G; S213R; L221S; K233E
	rad52-504	L62I; G63R; I120V; E155G; D199G
	rad52-505	E42K; V86A; D164N; D201V; D210E
	rad52-506	K167E; N179S; D199G; E223K; Q239H
	rad52-507	E147V; P231T; R234G; S239N; N244Y
	rad52-508	P64L; G74E; W84R; Q115R; L237S
	rad52-509	V46A; T101A; I190N; E223G; V240I
Sextuple mutants	rad52-601	Y80N; S105R; F195I; P197S; S215G; Y230H
	rad52-602	N97Y; L111M; T163M; D201E; T218A; L221F

Figure 3-4 Distribution of mutations

Ninety-four residues were mutated in fifty-seven mutants. Only residues shared by at least two mutants are shown. Seven mutants have single amino acid substitution. Those mutated residues are indicated by open boxes. Residues indicated by open ovals are conserved between hsRad52 and Scrad52 (Only residues up to amino acid 171 are shown.). The numbers next to certain residues indicate the number of mutants that have mutations at that position.

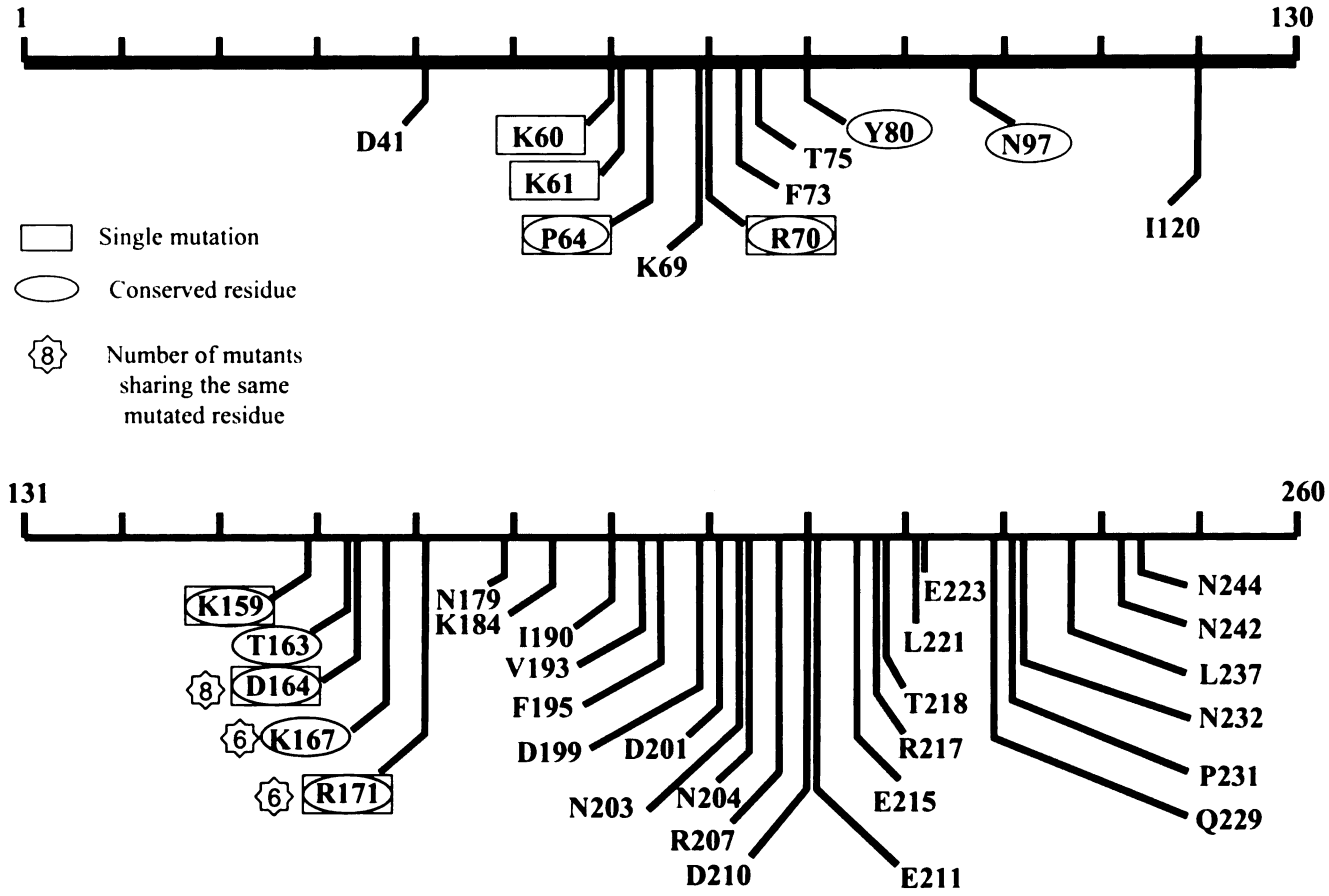
1
130
D41
K60
K61
P64
K69
R70
T75
F73
Y80
N97
I120
Single mutation
Conserved residue
8
Number of mutants sharing the same mutated residue
131
260
K159
T163
8
D164
6
K167
6
R171
N179
K184
I190
V193
F195
D199
D201
N203
N204
R207
D210
E211
E215
R217
T218
L221
E223
N244
N242
L237
N232
P231
Q229

Figure 3-4

Figure 3-5 MMS sensitivity assay of *rad52* mutants

JP166L1 (a *rad52Δ* strain) expressing wild type *RAD52*, *rad52R70G*, *rad52K159E*, *rad52D164G*, *rad52R171S*, or the control vector were cultivated overnight to mid-log phase. 10-fold serial dilutions containing 10 to 10^6 cells of each strain were spotted on plates with or without 0.005% MMS. MMS sensitivity was evaluated after 3 or 4 days of incubation.

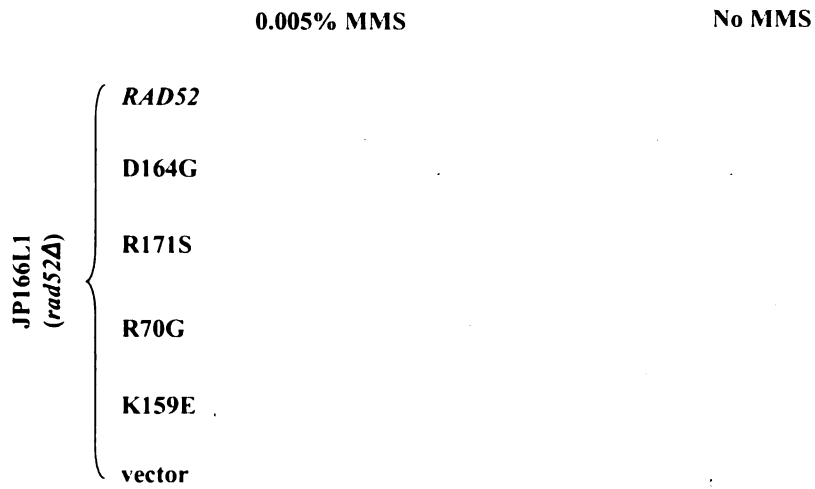
0.005% MMS
No MMS
JP166L1
(rad52Δ)
RAD52
D164G
R171S
R70G
K159E
vector

Figure 3-5

Figure 3-6 Steady state protein levels of *rad52* alleles

Yeast proteins (60 μg) were prepared from strains with the indicated genotypes. The proteins were separated in 10% SDS-PAGE. The membrane was probed with an antibody against Rad52, after which the membrane was stripped and probed with an antibody against G-6-PDH.

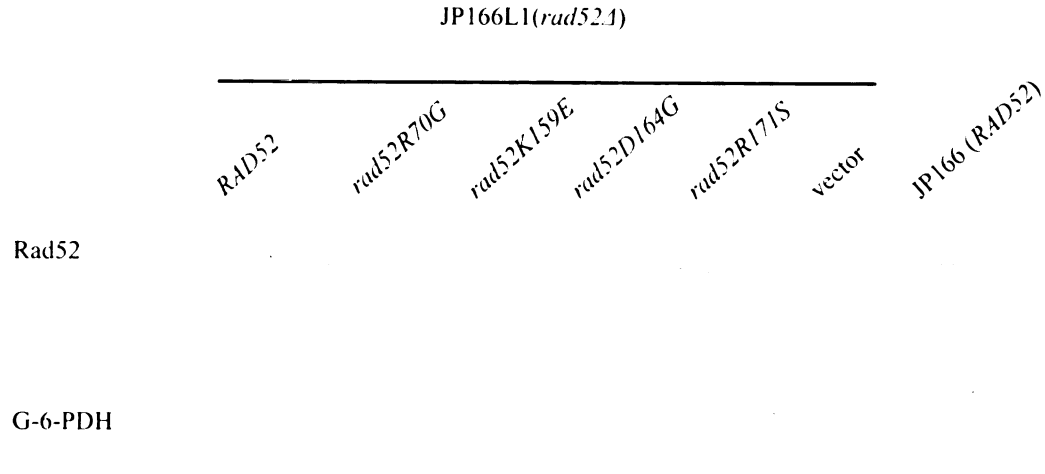
JP166L1(rad52-1)
RAD52
rad52R70G
rad52K159E
rad52D164G
rad52R171S
vector
JP166 (RAD52)
Rad52
G-6-PDH

Figure 3-6

Figure 3-7 Growth potential of *rad52* mutants through senescence and recovery process

JP166L1 (*rad52Δ*) expressing wild type *RAD52*, *rad52R70G*, *rad52K159E*, *rad52D164G* or *rad52R171S* was plated on solid SC-Leu medium containing 5-FOA to lose the sole copy of *TLC1* bearing on a *URA3* plasmid. Individual *tlc1Δ* colonies were cultivated in liquid SC-Leu medium to examine growth potential through senescence and recovery process. Cells were counted every 21 hours and inoculated into fresh media at $3x10^5$ cells/ml. This process was repeated for 11 days to generate "grow-out-of-senescence" curves. The curves shown are the average of 5 samples for each genetic background. Error bars represent standard deviation.

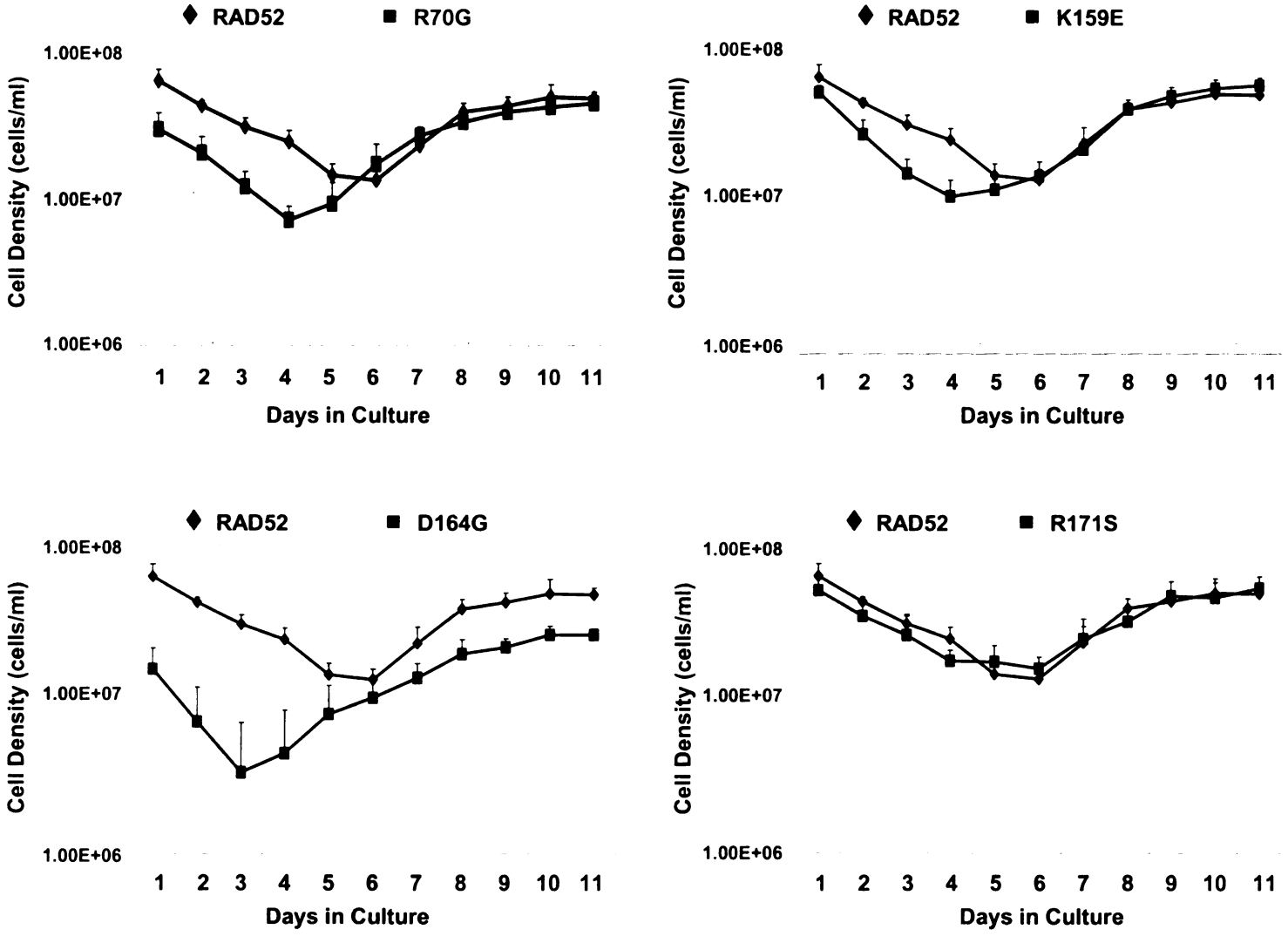
RAD52
R70G
1.00E+08
1.00E+07
1.00E+06
Cell Density (cells/ml)
1 2 3 4 5 6 7 8 9 10 11
Days in Culture
RAD52
K159E
1.00E+08
1.00E+07
1.00E+06
Cell Density (cells/ml)
1 2 3 4 5 6 7 8 9 10 11
Days in Culture
RAD52
D164G
1.00E+08
1.00E+07
1.00E+06
Cell Density (cells/ml)
1 2 3 4 5 6 7 8 9 10 11
Days in Culture
RAD52
R171S
1.00E+08
1.00E+07
1.00E+06
Cell Density (cells/ml)
1 2 3 4 5 6 7 8 9 10 11
Days in Culture

Figure 3-7

Figure 3-8 Southern blot analysis of telomeric DNA in survivors obtained by liquid assay

JP166L1 expressing wild type *RAD52*, *rad52R70G*, *rad52K159E*, *rad52D164G* or *rad52R171S* was selected on solid medium containing 5-FOA to lose the pRS316TLC1 plasmid. Individual *tlc1Δ* colonies were inoculated into liquid SC-Leu medium and cultivated for 3 days. Cultures were then diluted 1:10,000 with fresh medium. This process was repeated five times until survivors appeared. Genomic DNA was digested with *Xho*I, which cuts within the Y' elements once. The filters were hybridized to a poly(dG-dT) probe. Type II telomeres, indicated by triangles above lanes, are characterized by multiple bands with various sizes. All others samples are type I telomeres. **A**: *RAD52*. **B**: *rad52R70G*. **C**: *rad52K159E*. D: *rad52D164G*. **E**: *rad52R171S*.

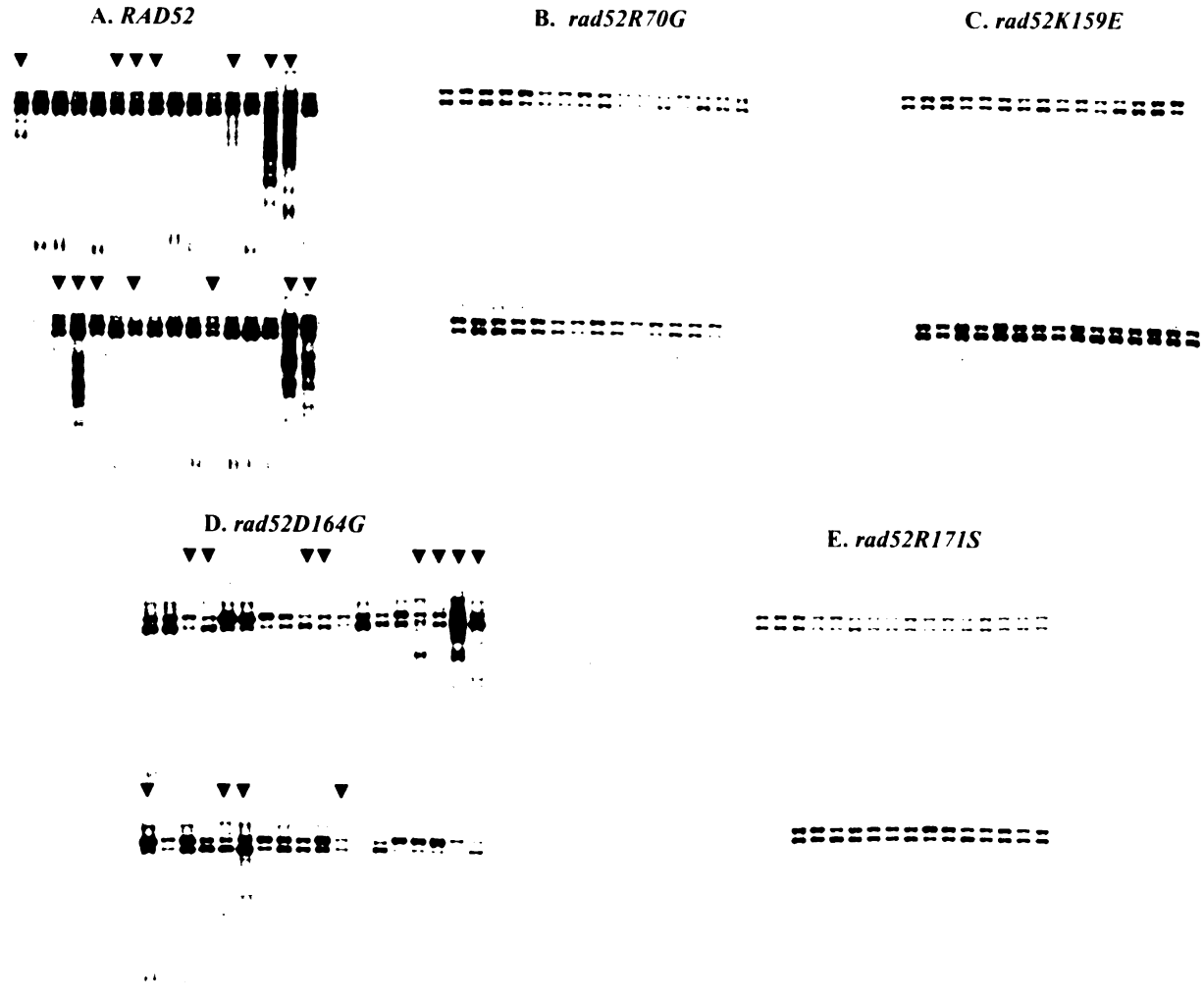

Figure 3-8

Figure 3-9 Southern blot analysis of telomeric DNA in survivors obtained by single colony assay

JP166L1 expressing wild type *RAD52*, *rad52R70G*, *rad52K159E*, *rad52D164G* or *rad52R171S* was selected on solid medium containing 5-FOA to lose the pRS316TLC1 plasmid. Individual *tlc1Δ* colonies were streaked on solid SC-Leu medium. Single colonies were then picked for the next streaking. This process was repeated five to seven times until survivors appeared. Survivors were cultivated in liquid medium for overnight and collected for analyzing telomeres. Genomic DNA was digested with *Xho*I, which cuts within the Y' elements once. The filters were hybridized to a poly(dG-dT) probe. Type II telomeres are indicated by triangles above lanes. All other samples are type I telomeres. **A**: *RAD52*. **B**: *rad52R70G*. **C**: *rad52K159E*. D: *rad52D164G*. **E**: *rad52R171S*.

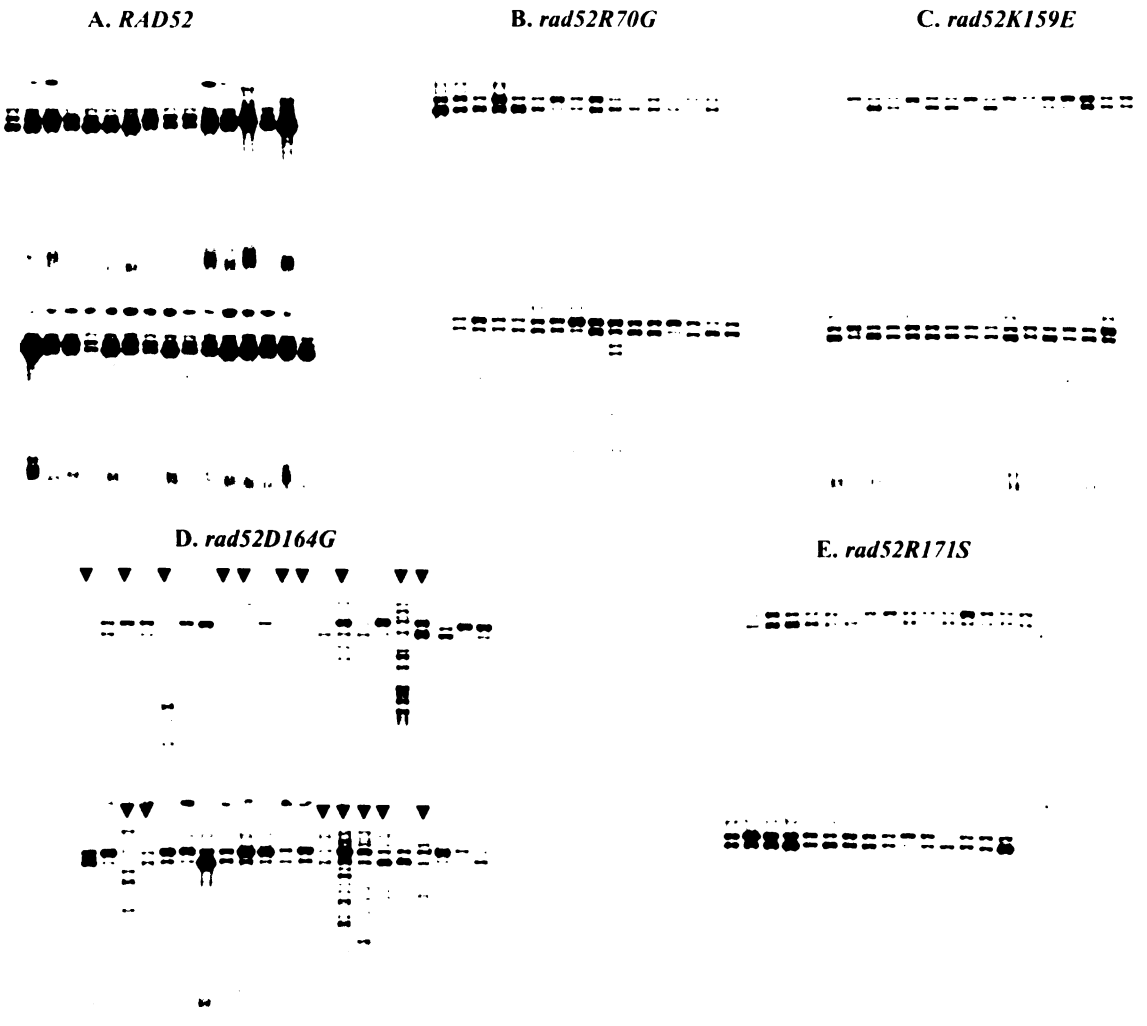

Figure 3-9

Table 3-4 Differential utilization of the two survivor pathways by rad52 mutants

	Single colony assay			Liquid assay		
	Type I	Type II	TypeI/typeII	Type I	Type II	TypeI/typeII
tlc1Δ RAD52	30	0	N/A	16	14	1.1
tlc1Δ rad52R70G	30	0	N/A	30	0	N/A
tlc1Δ rad52K159E	30	0	N/A	30	0	N/A
tlc1Δ rad52D164G	25	17	1.5	17	12	1.4
tlc1Δ rad52R171S	30	0	N/A	30	0	N/A

N/A: not applicable

Figure 3-10 Growth potential of *rad52* mutants in a *rad51*Δ strain through senescence and recovery process

RAD52 or *rad52* mutants were introduced into JP166041 (*rad51Δ rad52Δ*) strain which relies solely on the type II pathway to survive through senescence. After telomerase activity was eliminated by shuffling out the *URA3* plasmid bearing the sole copy of *TLC1*, individual *tlc1Δ* colonies were inoculated into SC-Leu medium. Cell density was examined every 21 hours and cells were inoculated into fresh media at $3x10^5$ cells/ml. This process was repeated for 10-12 days to generate grow-out-of senescence curves. The curves shown are the average of 5 samples for each genetic background except for D614G. D164Ga represents three samples that did not recover from senescence. D164Gb and D164Gc represent the two samples that recovered from senescence at day 7 and day 12 of the experiment, respectively. The error bars represent standard deviation.

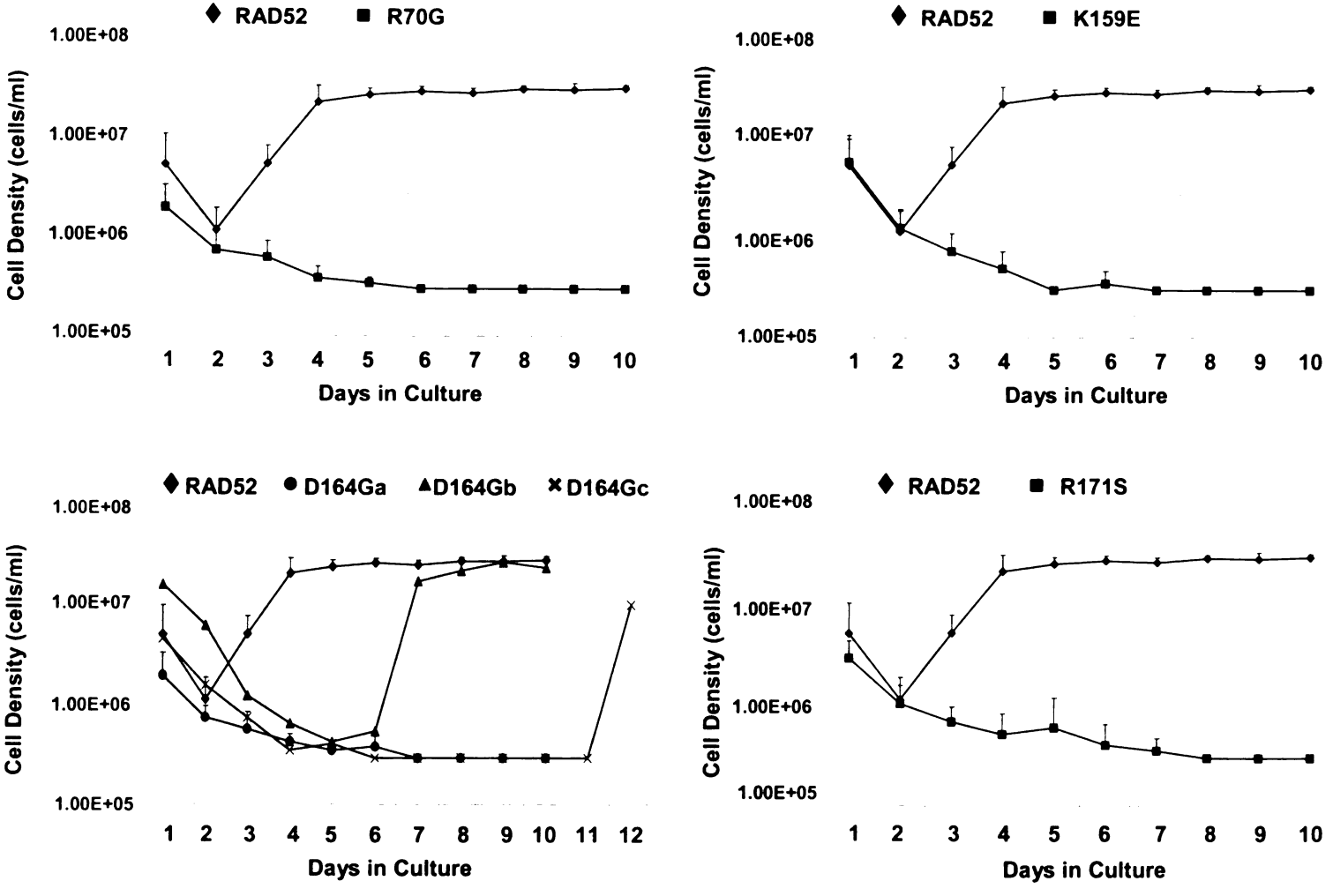

Figure 3-10 ***RAD52*** **or** ***rad52*** **mutants in JP166** ***rad51Δ rad52Δ***

Figure 3-11 Growth potential of *rad52* mutants in a *rad59Δ* strain through senescence and recovery process

RAD52 or *rad52* mutants were introduced into JP166042 (*rad59Δ rad52Δ*) strain which relies solely on the type I pathway to survive through senescence. After telomerase activity was eliminated by shuffling out the *URA3* plasmid bearing the sole copy of *TLC1*, individual *tlc1Δ* colonies were inoculated into SC-Leu medium. Cell density was examined every 21 hours and cells were inoculated into fresh media at $3x10^5$ cells/ml. This process was repeated for 12 days to generate grow-out-of-senescence curves. The curves shown are the average of 5 samples for each genetic background. The error bars represent standard deviation.

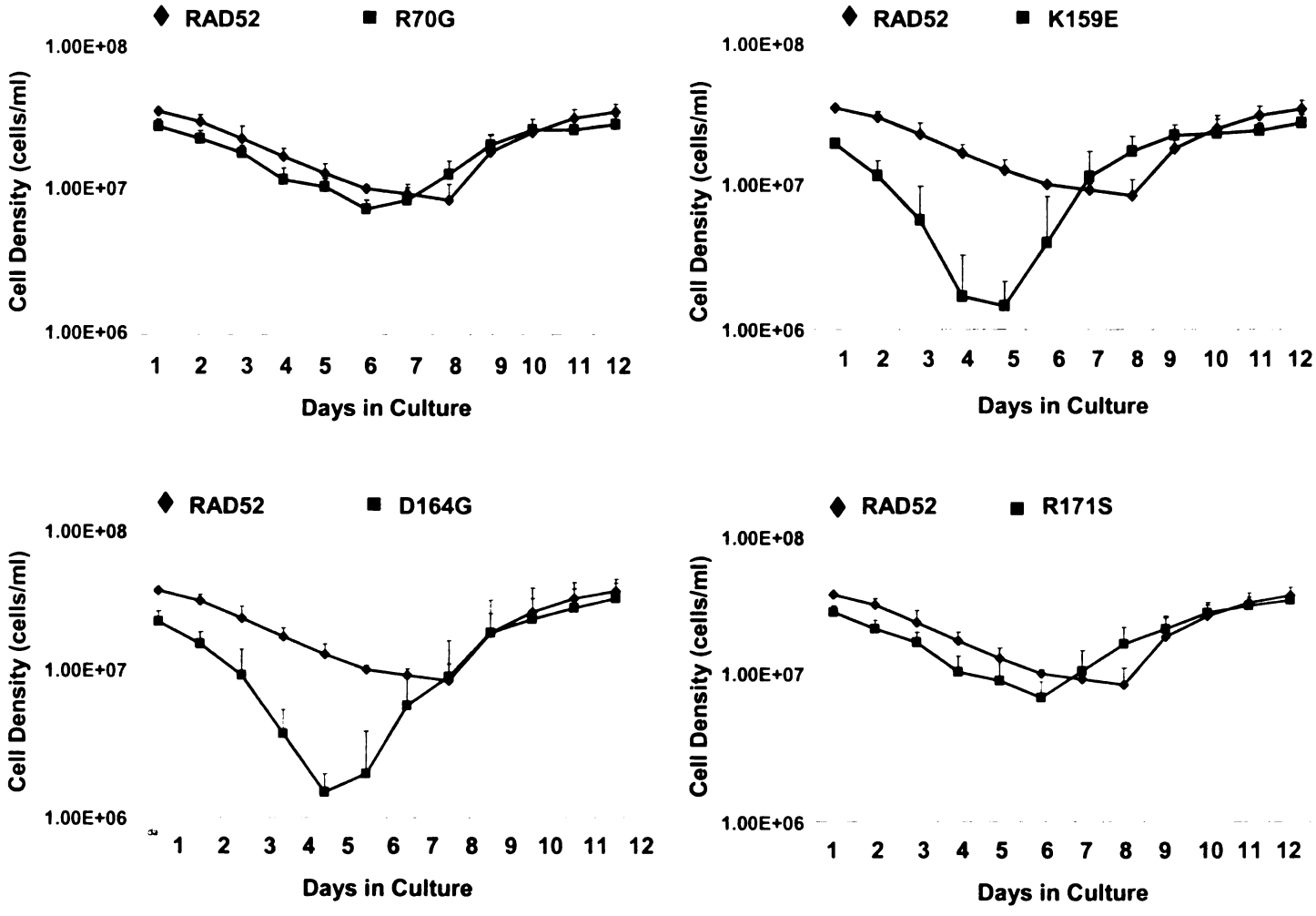

Figure 3-11 ***RAD52*** **or** ***rad52*** **mutants in JP166** ***rad59Δ rad52Δ***

Figure 3-12 Effect of Rad52 mutations on interchromosomal recombination and direct-repeat recombination

A. Possible recombination events in interchromosomal recombination.

In interchromosomal recombination, *LEU2* recombinants can arise through (a) reciprocal exchange, (b) gene conversion of *ΔBst*EII allele, and (c) gene conversion of *ΔEco*RI allele.

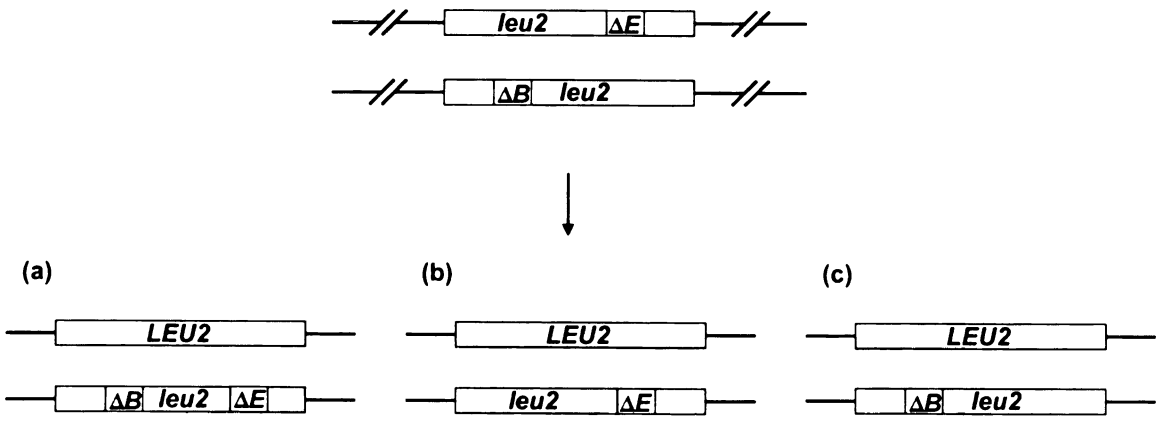

Figure 3-12A

Adopted from Mortensen, UH et al.
Genetics 161: 549-562 (2002)

B. Effect of Rad52 mutations on interchromosomal recombination.

Recombination rates are calculated as events per cell per generation. Relative recombination efficiency is also indicated. A two-tailed *t*-test is used to determine the significance of differences between *rad52* and *RAD52*. *P* value: D164G 0.032; K159E: 0.599; R70G 0.064; R171S 0.064.

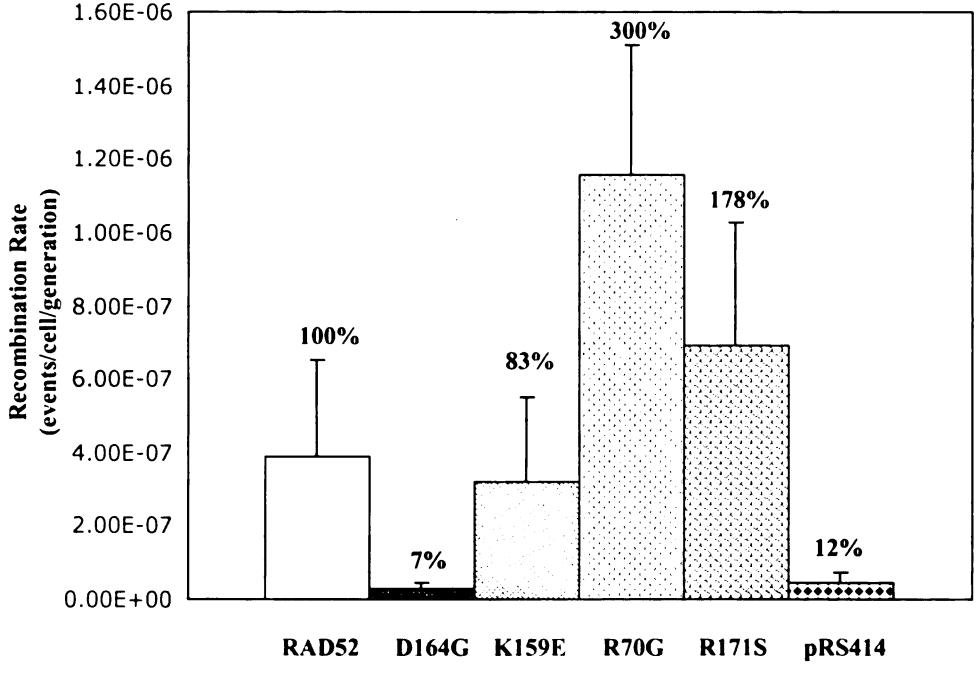
1.60E-06
1.40E-06
1.20E-06
1.00E-06
8.00E-07
6.00E-07
4.00E-07
2.00E-07
0.00E+00
Recombination Rate
(events/cell/generation)
100%
7%
83%
300%
178%
12%
RAD52
D164G
K159E
R70G
R171S
pRS414

Figure 3-12B

C. Possible recombination events in direct-repeat recombination.

In direct repeats recombination, *LEU2* recombinants can arise through (a) "pop-our" recombination, (b) *ΔBst*EII replacement, (c) *ΔEco*RI replacement, (d) triplication, and (e) disome with pop-out on one chromosome and the parental construct on the other.

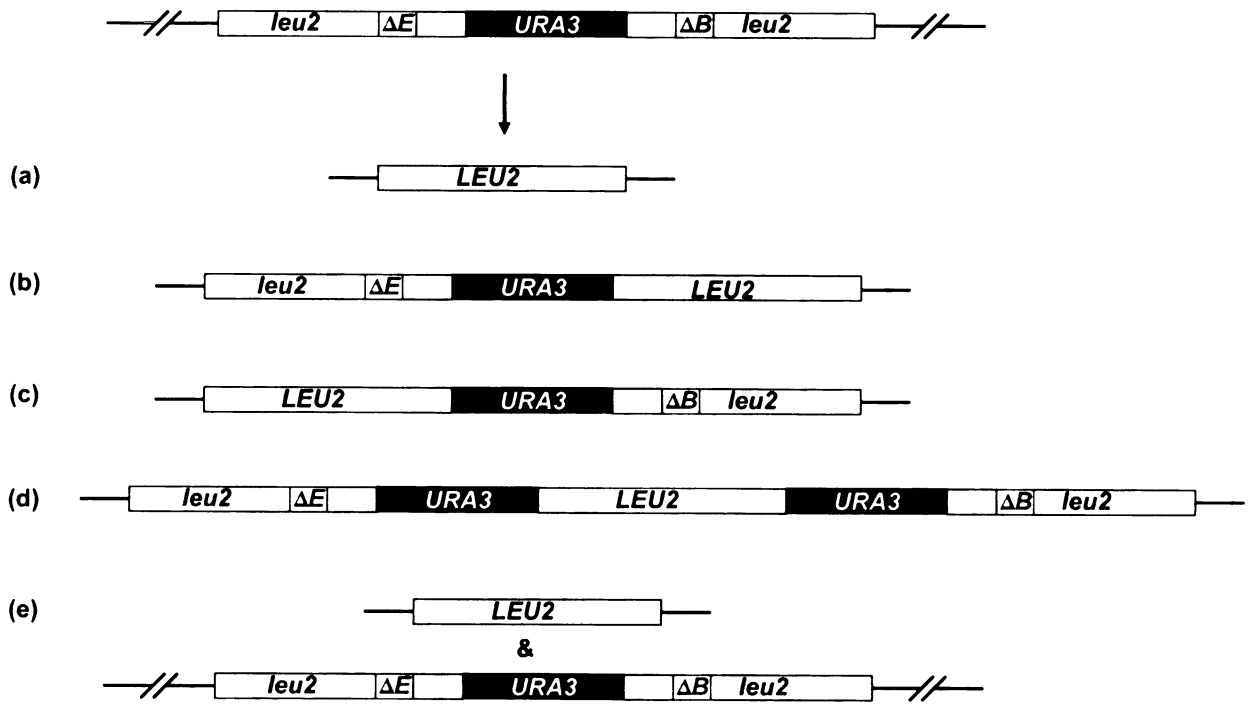

Figure 3-12C

Adopted from Mortensen, UH et al.
Genetics 161: 549-562 (2002)

D. Effect of Rad52 mutations on direct-repeat recombination.

Recombination rates are calculated as events per cell per generation. Relative recombination efficiency is also indicated. A two-tailed *t*-test is used to determine the significance of differences between *rad52* and *RAD52*. *P* value: D164G 0.083; K159E: 0.002; R70G 0.001; R171S 0.001.

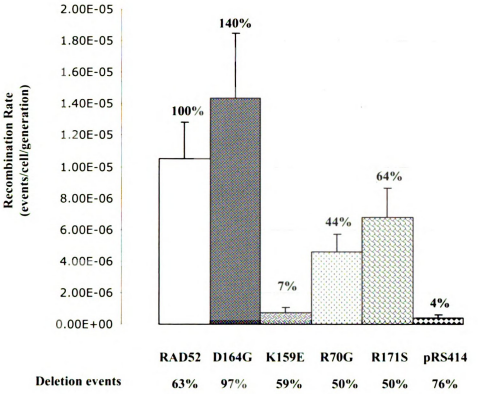
Recombination Rate
(events/cell/generation)
2.00E-05
1.80E-05
1.60E-05
1.40E-05
1.20E-05
1.00E-05
8.00E-06
6.00E-06
4.00E-06
2.00E-06
0.00E+00
100%
140%
7%
44%
64%
4%
RAD52
D164G
K159E
R70G
R171S
pRS414
Deletion events
63%
97%
59%
50%
50%
76%

Figure 3-12D

Figure 3-13 Effects of Rad52 mutations on survivor pathways and homologous recombination

R70G, K159E and R171S mutations cause defects in the type II pathway and direct-repeat recombination. They do not affect type I pathway or interchromosomal recombination. D164G results in defects in both type I and type II pathways, as well as reduced interchromosomal recombination. It does not change the overall efficiency of direct-repeat recombination, but strongly favors the pop-out mechanism. The correlation between the type I pathway and interchromosomal recombination provides further proof that type I telomeres are maintained by recombination between Y' on different chromosomes. The correlation between the type II pathway and direct-repeat recombination argues that type II telomeres are maintained most likely by t-loop elongation, in which telomeres loop back to copy telomere repeats intrachromosomally. This is further supported by the phenotypes of D164G. The t-loop structure could become abortive due to the elevated activity of excising the intervening sequences, and results in a defect in the type II pathway.

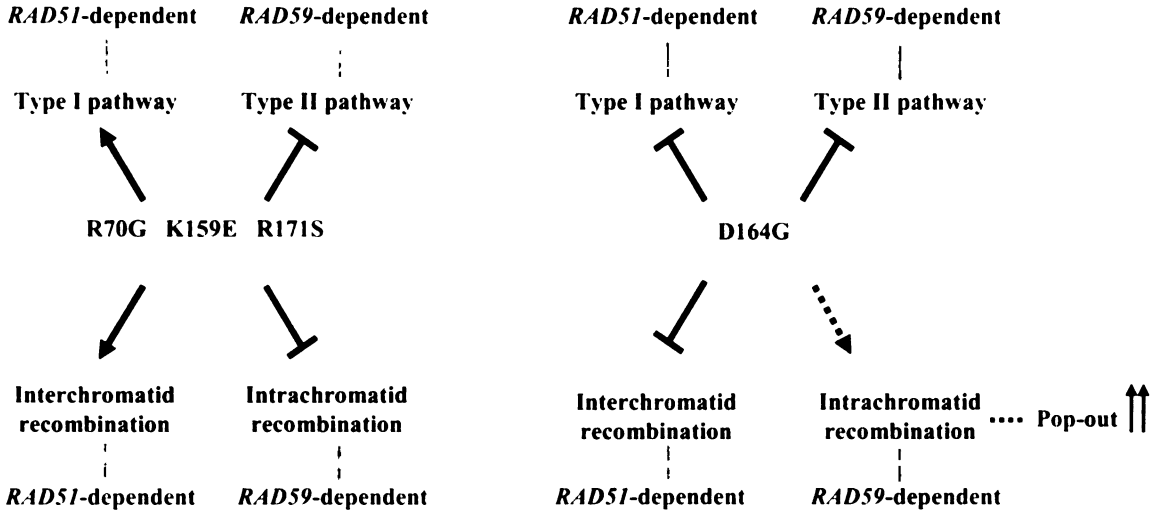
RAD51-dependent
RAD59-dependent
Type I pathway
Type II pathway
R70G
K159E
R171S
Interchromatid recombination
Intrachromatid recombination
RAD51-dependent
RAD59-dependent
RAD51-dependent
RAD59-dependent
Type I pathway
Type II pathway
D164G
Interchromatid recombination
Intrachromatid recombination
Pop-out
RAD51-dependent
RAD59-dependent

Figure 3-13

REFERENCES

1. Shampay, J., J.W. Szostak, and E.H. Blackburn, *DNA sequences of telomeres maintained in yeast.* Nature, 1984. **310**(5973): p. 154-7.

2. Louis, E.J. and J.E. Haber, *The structure and evolution of subtelomeric Y' repeats in Saccharomyces cerevisiae.* Genetics, 1992. **131**(3): p. 559-74.

3. Louis, E.J. and J.E. Haber, *The subtelomeric Y' repeat family in Saccharomyces cerevisiae: an experimental system for repeated sequence evolution.* Genetics, 1990. **124**(3): p. 533-45.

4. Zakian, V.A., *Structure, function, and replication of Saccharomyces cerevisiae telomeres.* Annu Rev Genet, 1996. **30**: p. 141-72.

5. Lundblad, V. and E.H. Blackburn, *An alternative pathway for yeast telomere maintenance rescues est1- senescence.* Cell, 1993. **73**(2): p. 347-60.

6. Lundblad, V. and J.W. Szostak, *A mutant with a defect in telomere elongation leads to senescence in yeast.* Cell, 1989. **57**(4): p. 633-43.

7. Lendvay, T.S., et al., *Senescence mutants of Saccharomyces cerevisiae with a defect in telomere replication identify three additional EST genes.* Genetics, 1996. **144**(4): p. 1399-412.

8. Singer, M.S. and D.E. Gottschling, *TLC1: template RNA component of Saccharomyces cerevisiae telomerase.* Science, 1994. **266**(5184): p. 404-9.

9. Chen, Q., A. Ijpma, and C.W. Greider, *Two survivor pathways that allow growth in the absence of telomerase are generated by distinct telomere recombination events.* Mol Cell Biol, 2001. **21**(5): p. 1819-27.

10. Le, S., et al., *RAD50 and RAD51 define two pathways that collaborate to maintain telomeres in the absence of telomerase.* Genetics, 1999. **152**(1): p. 143-52.

11. Teng, S.C. and V.A. Zakian, *Telomere-telomere recombination is an efficient bypass pathway for telomere maintenance in Saccharomyces cerevisiae.* Mol Cell Biol, 1999. **19**(12): p. 8083-93.

12. Bryan, T.M., et al., *Evidence for an alternative mechanism for maintaining telomere length in human tumors and tumor-derived cell lines.* Nat Med, 1997. **3**(11): p. 1271-4.

13. Henson, J.D., et al., *Alternative lengthening of telomeres in mammalian cells.* Oncogene, 2002. **21**(4): p. 598-610.

14. Reddel, R.R., T.M. Bryan, and J.P. Murnane, *Immortalized cells with no detectable telomerase activity. A review.* Biochemistry (Mosc), 1997. **62**(11): p. 1254-62.

15. Lundblad, V., *Telomere maintenance without telomerase.* Oncogene, 2002. **21**(4): p. 522-31.

16. Dunham, M.A., et al., *Telomere maintenance by recombination in human cells.* Nat Genet, 2000. **26**(4): p. 447-50.

17. Yeager, T.R., et al., *Telomerase-negative immortalized human cells contain a novel type of promyelocytic leukemia (PML) body.* Cancer Res, 1999. **59**(17): p. 4175-9.

18. Asleson, E.N., R.J. Okagaki, and D.M. Livingston, *A core activity associated with the N terminus of the yeast RAD52 protein is revealed by RAD51 overexpression suppression of C-terminal rad52 truncation alleles.* Genetics, 1999. **153**(2): p. 681-92.

19. Mortensen, U.H., et al., *DNA strand annealing is promoted by the yeast Rad52 protein.* Proc Natl Acad Sci U S A, 1996. **93**(20): p. 10729-34.

20. Shinohara, A., et al., *Rad52 forms ring structures and co-operates with RPA in single-strand DNA annealing.* Genes Cells, 1998. **3**(3): p. 145-56.

21. Kagawa, W., et al., *Crystal structure of the homologous-pairing domain from the human Rad52 recombinase in the undecameric form.* Mol Cell, 2002. **10**(2): p. 359-71.

22. Cortes-Ledesma, F., F. Malagon, and A. Aguilera, *A Novel Yeast Mutation, rad52-L89F, Causes a Specific Defect in Rad51-Independent Recombination That Correlates With a Reduced Ability of Rad52-L89F to Interact With Rad59.* Genetics, 2004. **168**(1): p. 553-7.

23. Symington, L.S., *Role of RAD52 epistasis group genes in homologous recombination and double-strand break repair.* Microbiol Mol Biol Rev, 2002. **66**(4): p. 630-70, table of contents.

24. Davis, A.P. and L.S. Symington, *The yeast recombinational repair protein Rad59 interacts with Rad52 and stimulates single-strand annealing.* Genetics, 2001. **159**(2): p. 515-25.

25. Sugiyama, T., J.H. New, and S.C. Kowalczykowski, *DNA annealing by RAD52 protein is stimulated by specific interaction with the complex of replication protein A and single-stranded DNA.* Proc Natl Acad Sci U S A, 1998. **95**(11): p. 6049-54.

26. Sugiyama, T. and S.C. Kowalczykowski, *Rad52 protein associates with replication protein A (RPA)-single-stranded DNA to accelerate Rad51-mediated displacement of RPA and presynaptic complex formation.* J Biol Chem, 2002. **277**(35): p. 31663-72.

27. Shinohara, A. and T. Ogawa, *Stimulation by Rad52 of yeast Rad51-mediated recombination.* Nature, 1998. **391**(6665): p. 404-7.

28. New, J.H., et al., *Rad52 protein stimulates DNA strand exchange by Rad51 and replication protein A.* Nature, 1998. **391**(6665): p. 407-10.

29. Sung, P., *Function of yeast Rad52 protein as a mediator between replication protein A and the Rad51 recombinase.* J Biol Chem, 1997. **272**(45): p. 28194-7.

30. New, J.H. and S.C. Kowalczykowski, *Rad52 protein has a second stimulatory role in DNA strand exchange that complements replication protein-A function.* J Biol Chem, 2002. **277**(29): p. 26171-6.

31. Longtine, M.S., et al., *Additional modules for versatile and economical PCR-based gene deletion and modification in Saccharomyces cerevisiae.* Yeast, 1998. **14**(10): p. 953-61.

32. Brachmann, C.B., et al., *Designer deletion strains derived from Saccharomyces cerevisiae S288C: a useful set of strains and plasmids for PCR-mediated gene disruption and other applications.* Yeast, 1998. **14**(2): p. 115-32.

33. Agatep, R., R.D. Kirkpatrick, D.L. Parchaliuk, R.A. Woods, and R.D. Gietz, *Transformation of Sacchromyces cerevisiae by the lithium acetate/single-stranded carrier DNA/polyethylene glycol (LiAc/ss-DNA/PEG ptotocol.* Technical Tips Online (http://tto.trends.com), 1998.

34. Mumberg, D., R. Muller, and M. Funk, *Yeast vectors for the controlled expression of heterologous proteins in different genetic backgrounds.* Gene, 1995. **156**(1): p. 119-22.

35. Adzuma, K., T. Ogawa, and H. Ogawa, *Primary structure of the RAD52 gene in Saccharomyces cerevisiae.* Mol Cell Biol, 1984. **4**(12): p. 2735-44.

36. Cadwell, R.C.J., G.F., *PCR primer- a labratory manual*, C.W.D. Dieffenbach, G. S., Editor. 1995. p. 583-589.

37. Church, G.M. and W. Gilbert, *Genomic sequencing.* Proc Natl Acad Sci U S A, 1984. **81**(7): p. 1991-5.

38. Mortensen, U.H., et al., *A molecular genetic dissection of the evolutionarily conserved N terminus of yeast Rad52.* Genetics, 2002. **161**(2): p. 549-62.

39. Lea, D.E., Coulson, C. A., *The distribution in the numbers of mutants in bacterial populations.* Journal of genetics, 1949. **49**: p. 264-285.

40. Bai, Y., A.P. Davis, and L.S. Symington, *A novel allele of RAD52 that causes severe DNA repair and recombination deficiencies only in the absence of RAD51 or RAD59.* Genetics, 1999. **153**(3): p. 1117-30.

41. Ira, G. and J.E. Haber, *Characterization of RAD51-independent break-induced replication that acts preferentially with short homologous sequences.* Mol Cell Biol, 2002. **22**(18): p. 6384-92.

42. Smith, J. and R. Rothstein, *A mutation in the gene encoding the Saccharomyces cerevisiae single-stranded DNA-binding protein Rfa1 stimulates a RAD52-*

independent pathway for direct-repeat recombination. Mol Cell Biol, 1995. **15**(3): p. 1632-41.

43. Smith, J. and R. Rothstein, *An allele of RFA1 suppresses RAD52-dependent double-strand break repair in Saccharomyces cerevisiae.* Genetics, 1999. **151**(2): p. 447-58.

44. Griffith, J.D., et al., *Mammalian telomeres end in a large duplex loop.* Cell, 1999. **97**(4): p. 503-14.

45. Munoz-Jordan, J.L., et al., *t-loops at trypanosome telomeres.* Embo J, 2001. **20**(3): p. 579-88.

46. Li, B. and A.J. Lustig, *A novel mechanism for telomere size control in Saccharomyces cerevisiae.* Genes Dev, 1996. **10**(11): p. 1310-26.

47. de Bruin, D., et al., *Telomere looping permits gene activation by a downstream UAS in yeast.* Nature, 2001. **409**(6816): p. 109-13.

48. de Bruin, D., et al., *Telomere folding is required for the stable maintenance of telomere position effects in yeast.* Mol Cell Biol, 2000. **20**(21): p. 7991-8000.

49. Grunstein, M., *Molecular model for telomeric heterochromatin in yeast.* Curr Opin Cell Biol, 1997. **9**(3): p. 383-7.

50. Wang, R.C., A. Smogorzewska, and T. de Lange, *Homologous recombination generates T-loop-sized deletions at human telomeres.* Cell, 2004. **119**(3): p. 355-68.

51. Bai, Y. and L.S. Symington, *A Rad52 homolog is required for RAD51-independent mitotic recombination in Saccharomyces cerevisiae.* Genes Dev, 1996. **10**(16): p. 2025-37.

52. Davis, A.P. and L.S. Symington, *The Rad52-Rad59 complex interacts with Rad51 and replication protein A.* DNA Repair (Amst), 2003. **2**(10): p. 1127-34.